

MECHANISMS OF CXL017: TARGETING DRUG RESISTANT CANCER

A DISSERTATION  
SUBMITTED TO THE FACULTY OF  
UNIVERSITY OF MINNESOTA  
BY

DAVID LEE LAMPI HERMANSON

IN PARTIAL FULFILLMENT OF THE REQUIREMENTS  
FOR THE DEGREE OF  
DOCTOR OF PHILOSOPHY

Dr. CHENGGUO XING, ADVISER

AUGUST 2012

© DAVID LEE LAMPI HERMANSON 2012

## **Acknowledgements**

First, I would like to thank my family and friends. They have helped push me to pursue graduate education and I would not have completed my Ph.D. without their continued support. I would like to extend special thanks to my parents for instilling in me so many of the qualities that have been invaluable in pursuing research. A special thanks is also due to my wife, whose contributions to my life cannot be totaled.

My most sincere thanks is owed to my research adviser, Dr. Chengguo Xing. Over the past five years, he has helped to guide me through many tough situations in my research, and I am thankful for his patience and helpful thoughts. He has been a wonderful adviser, always providing continuous encouragement and advice.

Colleagues belonging to the department as well as other programs have been very much appreciated as well. I have received a lot of guidance, suggestions, and help from people working in multiple departments, and without their help would not have been able to accomplish everything I did. I would like to especially thank other lab members whom I have closely worked with: Sonia Das, Sadiya Addo, Nick Bleeker, Balasubramanian Srinivasan, Bo Zhou, Aridoss Gopalakrishnan, Ahmad Shaik, Jinling Zhang, and Yunfang Li. You have all made an impact and helped to contribute to this dissertation.

I would also like to thank the faculty members, especially those from the Department of Medicinal Chemistry for all the knowledge you have helped to pass down. I would like to especially thank my committee members Dr. Hanna, Dr. Wagner, and Dr. Distefano for all their feedback and suggestions. I would especially like to acknowledge Dr. Hanna who has written several reference letters on my behalf.

## DEDICATION

This thesis is dedicated to  
**Katie Marie Lampi Hermanson**  
for all of her loving support.

## Abstract

Drug resistance represents a major challenge in the treatment of cancer, and agents with the capacity to overcome drug resistance are urgently needed. One of the most common pathways leading to multidrug resistance is through the overexpression of anti-apoptotic Bcl-2 family proteins. Previous work had identified sHA 14-1 as a lead compound with the ability to overcome drug resistance induced by overexpression of Bcl-2 proteins. In the current work, this compound was further characterized to inhibit the protein SERCA, a calcium pump located on the endoplasmic reticulum, and to overcome drug resistance in multiple cell lines. Further work led to the discovery of CXL017, a sHA 14-1 analog with improved potency and an  $IC_{50}$  value of  $\sim 2 \mu M$  in the multidrug resistant acute myeloid leukemia cell line HL60/MX2. This cell line is mitoxantrone resistant with cross-resistance to doxorubicin and etoposide; all three agents are topoisomerase II inhibitors. The new lead compound was then characterized in 9 pairs of drug resistant leukemia cell lines developed from exposure to standard therapies. CXL017 overcame the drug resistance in each cell line tested, revealing the compound's ability to widely overcome drug resistance. Chronic exposure of HL60/MX2 cells to CXL017 failed to result in the development of resistance to the compound and caused re-sensitization of the cell line to standard therapies. The new cell line, HL60/MX2/CXL017, was then studied along with HL60/MX2 cells in order to characterize the mechanism(s) of resistance in HL60/MX2 cells as well as the changes leading to re-sensitization. These efforts revealed that downregulation of topoisomerase II $\beta$  in HL60/MX2 cells leads to slight resistance to mitoxantrone, but not to etoposide or

doxorubicin. Rather, it is the overexpression of Mcl-1 observed in HL60/MX2 cells relative to HL60 cells that confers multidrug resistance. In HL60/MX2/CXL017 cells, topoisomerase II $\beta$  levels are restored to the levels observed in HL60 cells along with a reduction of Mcl-1 compared to HL60/MX2 cells, leading to the re-sensitization. Overall, data from this work reveals that CXL017 has the potential to overcome drug resistance induced by various treatments, and elucidates the mechanisms leading to drug resistance in HL60/MX2 cells.

## Table of Contents

<b>Acknowledgements .....</b>	<b>i</b>
<b>Dedication .....</b>	<b>ii</b>
<b>Abstract.....</b>	<b>iii</b>
<b>Table of Contents .....</b>	<b>v</b>
<b>List of Tables .....</b>	<b>ix</b>
<b>List of Figures.....</b>	<b>x</b>
<b>List of Abbreviations .....</b>	<b>xiii</b>
<b>CHAPTER 1: Drug resistance in malignancies .....</b>	<b>1</b>
<b>1.1 Cancer and drug resistance .....</b>	<b>1</b>
<b>1.2 General Function of Bcl-2 Family Proteins.....</b>	<b>2</b>
<b>1.3 Calcium signaling and regulation.....</b>	<b>6</b>
<b>1.4 Bcl-2 family proteins in drug resistant AML .....</b>	<b>8</b>
<b>1.5 Anti-apoptotic Bcl-2 protein inhibitors.....</b>	<b>9</b>
<b>1.6 Development of sHA 14-1 .....</b>	<b>12</b>
<b>CHAPTER 2: sHA 14-1 disrupts calcium homeostasis.....</b>	<b>15</b>
<b>2.1 Introduction.....</b>	<b>15</b>
<b>2.2 Results and Discussion.....</b>	<b>16</b>
<b>2.2.1 Measuring cytosolic calcium increases in Jurkat and NALM-6 cells         following treatment with sHA 14-1 .....</b>	<b>16</b>
<b>2.2.2 Protection of Cell by EGTA-AM.....</b>	<b>19</b>
<b>2.2.3 sHA 14-1 causes ER Stress.....</b>	<b>21</b>

2.2.4 sHA 14-1 causes calcium release via SERCA and not IP3R .....	23
2.2.5 Screening of sHA 14-1 analogs in NALM-6 Cells .....	29
2.3 Conclusion .....	31
2.4 Materials and Methods.....	32
2.4.1 Cell Culture .....	32
2.4.2 Cell Viability while chelating calcium.....	32
2.4.3 Measuring cytosolic calcium .....	33
2.4.4 Competition of sHA 14-1 and thapsigargin in Jurkat Cells.....	33
2.4.5 Measurement of SERCA enzymatic inhibition (Performed by Dr. Michelangeli) .....	33
2.4.6 Western blotting for ATF4 (Performed by Dr. Lebien).....	34
CHAPTER 3: Targeting Drug Resistant Cancer.....	35
3.1 Introduction.....	35
3.2 Results and Discussion.....	38
3.2.1 Cytotoxicity evaluation of drug resistant cell lines .....	38
3.2.2 sHA14-1 and analogs overcome drug resistance.....	40
3.2.3 Characterization of HL60/MX2 and CEM/C2.....	45
3.2.4 CXL017 overcomes drug resistance in multiple cell lines.....	50
3.2.5 NCI-60 Testing .....	60
3.2.6 <i>In vivo</i> targeting of drug resistance .....	62
3.3 Conclusion .....	64
3.4 Experimental Procedures.....	65



3.4.1 Cell Cultures.....	65
3.4.2 Cytotoxicity measurements.....	65
3.4.3 Western blotting.....	66
3.4.4 ER calcium measurements.....	67
3.4.5 <i>In vivo</i> evaluation of CXL017 (Performed by Dr. Xing).....	67
<b>CHAPTER 4: CXL017 Mechanism of Action.....</b>	<b>69</b>
4.1 Introduction.....	69
4.2 Results and Discussion.....	70
4.2.1 SERCA inhibition of CXL017 in HL60 and HL60/MX2 cell lines.....	70
4.2.2 Knockdown of SERCA2, SERCA3, Bcl-2, and Mcl-1 in HL60/MX2 cells.	75
4.2.3 Photoaffinity probe labeling of proteins studies.....	81
4.3 Conclusion.....	90
4.4 Experimental Procedures.....	91
4.4.1 Cell Cultures.....	91
4.4.2 <i>In vitro</i> SERCA Inhibition (Nick Bleeker).....	91
4.4.3 ER Calcium Release.....	92
4.4.4 Transduction of HL60/MX2 Cells.....	92
4.4.5 Western Blotting.....	93
4.4.6 Cytotoxicity of CXL037 in HL60 and HL60/MX2 Cells.....	94
4.4.7 Probe Labeling.....	94
<b>CHAPTER 5: Re-sensitization of HL60/MX2 Cells.....</b>	<b>96</b>
5.1 Introduction.....	96

<b>5.2 Results and Discussion.....</b>	<b>97</b>
<b>5.2.1 Long-term exposure of HL60 and HL60/MX2 cells to CXL017 .....</b>	<b>97</b>
<b>5.2.2 Characterization of CXL017 treated cell lines.....</b>	<b>103</b>
<b>5.2.3 Gene expression profiling of SERCA2 (<i>ATP2A2</i>), SERCA3 (<i>ATP2A3</i>), Bcl-2 (<i>BCL2</i>), Bcl-X<sub>L</sub> (<i>BCL2L1</i>), and Mcl-1 (<i>MCL1</i>).....</b>	<b>106</b>
<b>5.2.4 Mcl-1 protein stability .....</b>	<b>109</b>
<b>5.2.5 RNA sequencing.....</b>	<b>113</b>
<b>5.2.6 Topoisomerase II <math>\beta</math> knockdown.....</b>	<b>118</b>
<b>5.2.7 Evaluating Mcl-1 for its contribution to mitoxantrone induced drug resistance.....</b>	<b>122</b>
<b>5.3 Conclusion .....</b>	<b>127</b>
<b>5.4 Experimental Procedures.....</b>	<b>128</b>
<b>5.4.1 Cell Cultures.....</b>	<b>128</b>
<b>5.4.2 Development of Drug Resistant cell lines (Performed by Dr. Sonia Das). 128</b>	<b>128</b>
<b>5.4.3 Evaluation of Cytotoxicity.....</b>	<b>128</b>
<b>5.4.4 Western Blotting .....</b>	<b>129</b>
<b>5.4.5 RNA isolation and qRT-PCR.....</b>	<b>130</b>
<b>5.4.6 RNA sequencing.....</b>	<b>131</b>
<b>5.4.7 Knockdown of topoisomerase II <math>\beta</math>.....</b>	<b>131</b>
<b>5.4.8 Transient transfection of HL60 and HL60/MX2 cells .....</b>	<b>132</b>
<b>6. References.....</b>	<b>133</b>

## List of Tables

<b>Table 3.1: Cytotoxicity of standard therapies in HL60, HL60/MX2, CCRF-CEM, and CEM/C2 cell lines .....</b>	<b>39</b>
<b>Table 3.2 Cytotoxic evaluation of CXL017, ABT-737, isatin-<math>\beta</math>-thiosemicarbazone, and Thapsigargin in drug resistant cell lines .....</b>	<b>59</b>
<b>Table 3.3 Cytotoxicity of CXL017 in <math>\mu</math>M across a panel of 60 cancer cell lines from NCI .....</b>	<b>61</b>
<b>Table 5.1 48 hour IC<sub>50</sub> values of various compounds in cells exposed to CXL017 or Ara-C for 6 months .....</b>	<b>101</b>
<b>Table 5.2 48 hour IC<sub>50</sub> values of various compounds exposed to CXL017 for between 2 and 6 months and cells grown without selective pressure for 2 months (NT cells) .....</b>	<b>102</b>
<b>Table 5.3 qRT-PCR fold change of mRNA in HL60 and HL60/MX2/CXL017/NT cells relative to HL60/MX2 cells .....</b>	<b>108</b>
<b>Table 5.4 48 hour IC<sub>50</sub> values of various compounds in <i>TOP2B</i> knockdown cell lines .....</b>	<b>121</b>

## List of Figures

<b>Figure 1.1 Structures of therapies for AML.....</b>	<b>2</b>
<b>Figure 1.2 Bcl-2 Family Members .....</b>	<b>3</b>
<b>Figure 1.3 Structure of the SERCA inhibitor Thapsigargin .....</b>	<b>7</b>
<b>Figure 1.4 Structures of Bcl-2 small molecule inhibitors .....</b>	<b>11</b>
<b>Figure 1.5 Proposed decomposition of HA 14-1.....</b>	<b>13</b>
<b>Figure 1.6 Structure of sHA 14-1.....</b>	<b>14</b>
<b>Figure 2.1: Cytosolic calcium measurements using Fura-2 .....</b>	<b>18</b>
<b>Figure 2.2: Protection of NALM-6 cells through chelation of internal calcium .....</b>	<b>20</b>
<b>Figure 2.3: ER stress induction by sHA 14-1 .....</b>	<b>22</b>
<b>Figure 2.4: Role of Inositol trisphosphate receptor (IP3R) in sHA 14-1 induced cytotoxicity and calcium release .....</b>	<b>25</b>
<b>Figure 2.5: Competition between sHA 14-1 and Thapsigargin .....</b>	<b>27</b>
<b>Figure 2.6: Inhibition of SERCA 2B by sHA 14-1 and Thapsigargin.....</b>	<b>28</b>
<b>Figure 2.7: Calcium release of CXL analogs measured in NALM-6 cells .....</b>	<b>30</b>
<b>Figure 3.1 Structures of sHA14-1 and analogs tested in HL60, HL60/MX2, CCRF- CEM, and CEM/C2 cell lines.....</b>	<b>37</b>
<b>Figure 3.2 Cytotoxicity of ABT-737 in HL60, HL60/MX2, CCRF-CEM, and CEM/C2 cells.....</b>	<b>42</b>
<b>Figure 3.3 Cytotoxicity of sHA14-1 and analogs in HL60, HL60/MX2, CEM-CCRF, and CEM/C2.....</b>	<b>43</b>

<b>Figure 3.4 Cytotoxicity of thapsigargin in HL60, HL60/MX2, CCRF-CEM, and CEM/C2 cells.....</b>	<b>44</b>
<b>Figure 3.5 Western blotting of anti-apoptotic Bcl-2 family proteins in CCRF-CEM, CEM/C2, HL60, and HL60/MX2 cell lines.....</b>	<b>46</b>
<b>Figure 3.6 Characterization of CCRF-CEM, CEM/C2, HL60, and HL60/MX2 cell lines for ER calcium content and SERCA protein levels .....</b>	<b>49</b>
<b>Figure 3.7 Characterization of drug resistance in HL60, HL60/DNR, HL60/ADR, and HL60/DOX against standard therapies and protein levels.....</b>	<b>52</b>
<b>Figure 3.8 Characterization of drug resistance in CCRF-CEM, CEM/VM1-5, and CEM/VLB100 against standard therapies and protein levels .....</b>	<b>54</b>
<b>Figure 3.9 Characterization of drug resistance in K562, K562/DOX, and K562/HHT300 against standard therapies and protein levels.....</b>	<b>56</b>
<b>Figure 3.10 <i>In vivo</i> treatment of SCID mice with 100mg/kg CXL017 .....</b>	<b>63</b>
<b>Figure 4.1 SERCA1a inhibition by CXL017 and sHA 14-1 .....</b>	<b>72</b>
<b>Figure 4.2 ER calcium release of CXL017 and sHA 14-1 in HL60 and HL60/MX2 Cells .....</b>	<b>74</b>
<b>Figure 4.3 Western Blotting of transduced HL60/MX2 cell lines .....</b>	<b>77</b>
<b>Figure 4.4 Cytotoxicity of CXL017, thapsigargin, and mitoxantrone in HL60/MX2 transduced cell lines.....</b>	<b>80</b>
<b>Figure 4.5 Structure of probe molecule, CXL037 .....</b>	<b>82</b>
<b>Figure 4.6 Probe labeling of target proteins.....</b>	<b>82</b>
<b>Figure 4.7 CXL037 labeling of proteins visualized using in-gel imaging .....</b>	<b>84</b>

<b>Figure 4.8 Cytotoxicity of CXL037 in HL60 and HL60/MX2 Cells.....</b>	<b>86</b>
<b>Figure 4.9 Labeling of purified Bcl-2 protein with CXL037.....</b>	<b>88</b>
<b>Figure 4.10 Labeling of possible target proteins in HL60/MX2 cells with CXL037 A and B .....</b>	<b>89</b>
<b>Figure 5.1 Evaluating acquired drug resistance in HL60/MX2 cells .....</b>	<b>99</b>
<b>Figure 5.2 Assessing drug resistance to CXL017 treated cells.....</b>	<b>100</b>
<b>Figure 5.3 Western blotting of CXL017 treated HL60/MX2 cell lines .....</b>	<b>105</b>
<b>Figure 5.4 Half-life analysis of Mcl-1 in HL60, HL60/MX2, and HL60/MX2/CXL017/NT cells .....</b>	<b>110</b>
<b>Figure 5.5 Mcl-1 accumulation in HL60, HL60/MX2, and HL60/MX2/CXL017/NT cells .....</b>	<b>112</b>
<b>Figure 5.6 Venn diagram of the number of genes differentially expressed in HL60, HL60/MX2/CXL017-6 and HL60/MX2/CXL017/NT cells compared to HL60/MX2 cells.....</b>	<b>115</b>
<b>Figure 5.7 Comparison of gene fold changes between HL60 and HL60/MX2 cells in RNAseq data with qRT-PCR data .....</b>	<b>115</b>
<b>Figure 5.8 qRT-PCR results for <i>TOP2B</i> expression in HL60 and HL60/MX2/CXL017/NT cells compared to HL60/MX2 cells .....</b>	<b>117</b>
<b>Figure 5.9 qRT-PCR data of <i>TOP2B</i> knockdown cells .....</b>	<b>119</b>
<b>Figure 5.10 Cytotoxicity of mitoxantrone in <i>TOP2B</i> knockdown cell lines.....</b>	<b>121</b>
<b>Figure 5.11 Mcl-1 transient knockdown in HL60 and HL60/MX2 cells.....</b>	<b>124</b>
<b>Figure 5.12 Overexpression of Mcl-1 in HL60 cells.....</b>	<b>126</b>

## List of Abbreviations

ALL	Acute lymphoblastic leukemia
AML	Acute myeloid leukemia
Ara-C	Cytarabine
ATF-4	Activating transcription factor 4
AUC	Area under the curve
BCA	Bicinchoninic acid
Bcl-2	B-cell lymphoma-2
BH	Bcl-2 homology
BSA	Bovine serum albumin
CHX	Cycloheximide
CML	Chronic myeloid leukemia
DMSO	Dimethylsulfoxide
Dox	Doxorubicin
EGTA	Ethylene glycol tetraacetic acid
ER	Endoplasmic reticulum
FBS	Fetal bovine serum
FPKM	Fragments per kilobase of exon per million fragments mapped
Fura2-AM	Fura2-acetoxymethyl
HRP	Horse raddish peroxidase
IP3R	Inositol triphosphate receptor
MDR	Multidrug resistance

MOMP	Mitochondrial outer membrane permeabilization
MX	Mitoxantrone
ORF	Open reading frame
PBS	Phosphate buffered saline
P-gp	P-glycoprotein
PVDF	Polyvinylene difluoride
qRT-PCR	Quantitative reverse transcriptase polymerase chain reaction
RNAi	RNA interference
RNAseq	RNA sequencing
ROS	Reactive oxygen species
SD	Standard deviation
SDS-PAGE	Sodium dodecyl sulfate polyacrylamide gel electrophoresis
SEM	Standard error from the mean
SERCA	Sarco-endoplasmic reticulum calcium ATPase
shRNA	Small hairpin loop RNA
siRNA	Small interfering RNA
TBST	Tris buffered saline TWEEN-20
TG	Thapsigargin
Topo II $\beta$	Topoisomerase II $\beta$
UPR	Unfolded protein response



## CHAPTER 1

### 1. Drug resistance in malignancies

#### 1.1 Cancer and drug resistance

Cancer is a disease characterized by uncontrolled growth of abnormal cells in the body. Cancer can be characterized by 6 hallmarks that cells must acquire in order to become malignant. These hallmarks include sustaining proliferative signaling, evading growth suppressors, activating invasion and metastasis, enabling replicative immortality, inducing angiogenesis, and resisting cell death.<sup>1</sup> As humans are exposed to carcinogens, cancer causing agents, every day from the environment, food, cigarettes, and multiple other sources, cells acquire these traits in a multistep process resulting from DNA damage.

Acute myeloid leukemia (AML) is a cancer of the hematopoietic stem cells, and it is the most common acute leukemia that affects adults. In AML, immature leukemic cells accumulate in the bone marrow and other organs where they affect the production of normal blood cells causing anemia, fatal infections, or bleeding. In 2012, it is estimated that 10,200 people will die of AML, while 13,780 will be diagnosed (SEER data). Incidence rate greatly increases with age with a median age of 66 years old. The cancer progresses very quickly and is fatal in weeks to months if untreated.<sup>2</sup>

Considerable effort has gone into designing therapies to treat cancer; however, there is still no cure for cancer to date. Treatment for AML includes high doses of cytarabine (Ara-C), an antimetabolic agent, and an anthracycline, such as doxorubicin, or an anthracenedione, such as mitoxantrone. Doxorubicin and mitoxantrone, as well as

etoposide, are topoisomerase II inhibitors (Figure 1.1).<sup>3</sup> Patients with AML show an initial response rate of 60-80%, but most patients suffer relapse and die within 2 years of remission.<sup>4</sup> Moreover, nearly 70% of relapsed AML is associated with multidrug resistance (MDR).<sup>2</sup> Therefore, therapies must be developed that can effectively treat drug resistance.

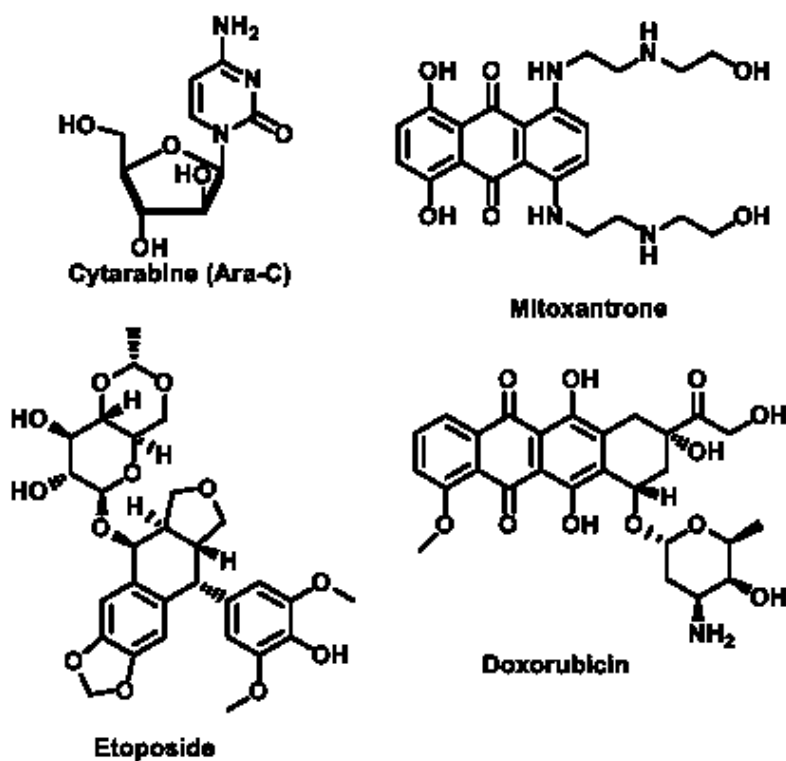


**Figure 1.1 Structures of therapies for AML**

## 1.2 General Function of Bcl-2 Family Proteins

Bcl-2 family proteins are important regulators of apoptosis, a form of programmed cell death. The Bcl-2 protein was the first member of the family identified and is a proto-oncogene involved in the t(14;18) chromosomal translocation observed in low grade B-cell lymphomas.<sup>5,6</sup> The protein family has continued to grow and, currently, there are at least 25 protein members in the Bcl-2 family.<sup>7</sup> These proteins can be split

into two different categories; the anti-apoptotic and pro-apoptotic proteins. These two groups have opposing functions and exist in a delicate balance that maintains normal cellular homeostasis.<sup>8</sup>

There are 7 proteins within the anti-apoptotic group of Bcl-2 family proteins, which include Bcl-2, Bcl-X<sub>L</sub>, Mcl-1, Bcl-W, Bfl-1, Bcl-B, and A1. As the name suggests, these proteins are responsible for inhibiting apoptosis. These proteins all contain four conserved Bcl-2 homology (BH) domains, termed BH1-BH4, as well as a transmembrane (TM) domain (Figure 1.2). The remaining Bcl-2 family proteins are considered pro-apoptotic and can be divided into two sub-groups including the multi-domain proteins, comprised of the BH1-BH3 and TM domains, and the BH3-only proteins. The two most well studied proteins of the multi-domain pro-apoptotic proteins are Bax and Bak, while BH3-only domain proteins include Bad, Bid, NOXA, Bim, and PUMA. As their name would suggest, the pro-apoptotic proteins promote apoptosis.

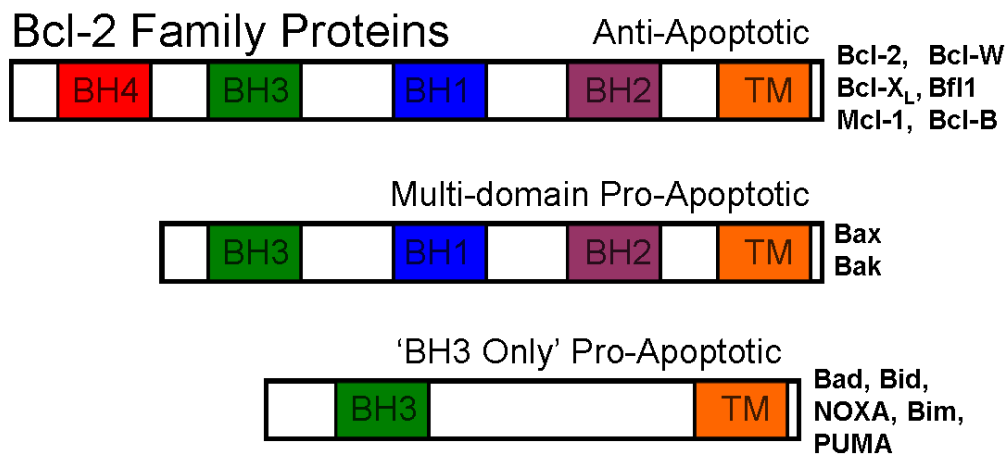


**Figure 1.2 Bcl-2 Family Members**

Each BH domain plays an important role in the function of various Bcl-2 family proteins. The transmembrane region, at the C-termini, controls the protein's localization

and insertion into the mitochondrial membrane, nuclear envelope, or endoplasmic reticulum (ER) membrane.<sup>9-12</sup> The BH1 and BH2 domains are important for ion channel formation and essential for anti-apoptotic proteins to heterodimerize with the pro-apoptotic proteins.<sup>13</sup> The BH3 domain is conserved in all of the Bcl-2 family proteins and is also important for heterodimerization, where it binds into a hydrophobic cleft created by the BH1, BH2, and BH3 domains. Finally, the BH4 domain is conserved only in the anti-apoptotic proteins and is crucial for their function, whereby loss of this domain greatly limits their anti-apoptotic function or even switches their function to pro-apoptotic.<sup>14, 15</sup> The BH4 domain is not involved in interactions with other Bcl-2 family proteins, but is most likely involved in protein-protein interactions with proteins outside the family.<sup>13</sup>

The various expression patterns of the BH domains in the Bcl-2 family proteins, suggest a model for how they operate inside the cell to carry out their function. While several models have been suggested, there are multiple common features.<sup>16</sup> It is generally thought that on the mitochondrial membrane multi-domain pro-apoptotic proteins, Bax and Bak, are sequestered by the anti-apoptotic proteins, Bcl-2, Mcl-1, or Bcl-X<sub>L</sub>. Upon death signals, BH3-only proteins can bind to the anti-apoptotic members and free Bax and Bak. In a second model, the BH3-only proteins can also bind directly to Bax or Bak in order to activate them and cause oligomerization. Once freed, Bax/Bak can homo-oligomerize, which results in pore formation and causes mitochondrial outer membrane permeabilization (MOMP). This leads to cytochrome c release and subsequently apoptosis.<sup>17</sup>

Outside of the mitochondrial membrane, Bcl-2 proteins also localize to the ER where they have been thought to regulate calcium signaling as another way of controlling apoptosis.<sup>18</sup> Bax and Bak have both been shown to increase calcium levels in the ER. They also enhance calcium release from the ER and calcium uptake into the mitochondria resulting in apoptosis.<sup>19</sup> Bcl-2, on the other hand, is able to diminish the release of calcium.<sup>20</sup> The mechanisms surrounding the way Bcl-2 family proteins affect calcium levels are still under investigation, but there have been several reported interactions of Bcl-2 proteins with ER calcium transporters. Inositol triphosphate receptors (IP3Rs) allow for the flux of calcium ions out of the ER into the cytoplasm. Both Bcl-X<sub>L</sub> and Bax are able to interact with IP3R, affecting calcium signaling.<sup>21, 22</sup> Bcl-2 proteins can also interact with the sarco-endoplasmic reticulum ATPase (SERCA), which cycles calcium from the cytosol back into the ER.<sup>23, 24</sup> In light of the substantial evidence surrounding Bcl-2 proteins regulating calcium signaling at the ER, it is important to keep this function in mind when studying Bcl-2 inhibitors.

Given that the Bcl-2 family of proteins tightly controls the process of apoptosis, it is easy to see how they may contribute to the development of cancer. In normal healthy cells the expression of pro- and anti-apoptotic proteins are in perfect balance. Upon certain signals, the pro-apoptotic proteins become overexpressed in relation to the anti-apoptotic proteins and result in apoptosis. This is normally a healthy process and serves to remove damaged cells. However, when the anti-apoptotic proteins become overexpressed, signaling that would normally result in cell death is overcome, resulting in

resistance to cell death, one of the six hallmarks of cancer. Therefore, targeting the overexpression of Bcl-2 proteins has garnered a lot of attention as a treatment for cancer.

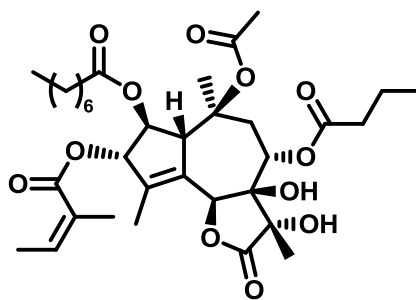
### **1.3 Calcium signaling and regulation**

Given the role of Bcl-2 proteins at the ER, it is important to have an understanding of calcium signaling and the proteins involved. The ER is the cells' main storage organelle for calcium and is the principle site for folding of transmembrane, secretory, and ER-resident proteins. Calcium signaling is highly regulated both spatially and temporally and calcium is an extremely diverse signaling ion, regulating everything from cell proliferation to cell death.<sup>25</sup> Sustained calcium release from the ER leads to uptake of calcium by the mitochondria and the induction of apoptosis through mitochondrial membrane depolarization and cytochrome c release.<sup>26, 27</sup>

As already alluded to, there are two proteins on the ER membrane that maintain calcium homeostasis. The main ion channel that allows the efflux of calcium ions out of the ER into the cytoplasm is IP3R. This process simply requires activation of the receptor as there is a strong concentration gradient of calcium across the ER membrane. Resting levels of calcium concentration are typically 100 nM in the cytosol and high micromolar in ER. As already described, Bcl-2 proteins can interact with IP3R to effect the release of calcium. Conversely, SERCA maintains the concentration gradient by an ATP-dependent transport of calcium from the cytosol into the ER. There are three isoforms of SERCA with differential expression in various tissues. SERCA1 is expressed in only fast-twitch muscle fibers, SERCA2a is expressed mainly in cardiac muscle, SERCA2b is expressed ubiquitously, and SERCA3 is expressed in non-muscle

cells and mainly in blood cells.<sup>28</sup> The isoforms retain high homology, but have slightly different turnover rates and affinities for calcium. SERCA1 and SERCA2a are nearly indistinguishable, while SERCA2b has a slightly lower turnover rate for both calcium transport and ATP hydrolysis.<sup>29</sup> Lastly, SERCA3 displays a reduced affinity for calcium. Therefore, either pharmacological activation of IP3R or inhibition of SERCA can cause calcium release from the ER, resulting in the induction of ER stress and/or apoptosis.

Thapsigargin was identified as a potent SERCA inhibitor in 1991 and is the most widely used inhibitor of SERCA (Figure 1.3).<sup>30</sup> The compound has nanomolar potency against all three isoforms of SERCA, and it is also one of the most specific inhibitors of SERCA.<sup>31</sup> Therefore, thapsigargin is a perfect tool for studying calcium release from the ER and is the gold standard for SERCA inhibition. However, the therapeutic potential of thapsigargin is greatly limited due to its inability to selectively target malignant cells and its high toxicity. However, recent efforts have been made to synthesize an inactive thapsigargin prodrug activated in prostate cancer by prostate-specific antigen providing a way to direct thapsigargin to cancer cells.<sup>32-34</sup>



Thapsigargin (TG)

**Figure 1.3 Structure of the SERCA inhibitor Thapsigargin**

Besides ER calcium release causing apoptosis via mitochondrial uptake and subsequent release of cytochrome c, the emptying of ER calcium stores by SERCA inhibitors can induce ER stress. ER stress induces the unfolded protein response (UPR) pathway, which lowers the unfolded protein load in the ER. There are three arms to UPR that are controlled by three transmembrane proteins that serve as sensors, ATF6, IRE1, and PERK.<sup>35</sup> Upon activation any of the three proteins can initiate a response meant to bring protein folding back into homeostasis. However, if the UPR continues to persist, the pathway progresses to promote apoptosis.<sup>36</sup> This process leads to PERK activation of activating transcription factor-4 (ATF4), which causes the upregulation of the transcription factor CHOP preventing anti-apoptotic Bcl-2 expression.<sup>37</sup>

In summary, calcium signaling is a complex signaling network originating in the ER that can result in apoptosis under sustained release. Apoptosis can occur through mitochondrial uptake of calcium or through the induction of the UPR. SERCA inhibition results in calcium release from the ER and can both activate the UPR and induce apoptosis. Thapsigargin is the most widely used inhibitor of SERCA and can activate ATF4 resulting in cell death.<sup>38</sup> Finally, all of these processes can be affected by the Bcl-2 family of proteins creating a dynamic role for Bcl-2 family proteins at the ER.

#### **1.4 Bcl-2 family proteins in drug resistant AML**

Another feature commonly conveyed by the overexpression of anti-apoptotic Bcl-2 proteins is drug resistance.<sup>39</sup> Overexpression of the *BCL2* gene family is commonly observed in AML as well as in resistance to chemotherapy.<sup>40</sup> High levels of Bcl-2 have been shown to be associated with drug resistance in AML,<sup>41, 42</sup> while higher levels of Bax



are associated with positive outcomes in AML.<sup>43</sup> Furthermore, the ratio of Bax/Bcl-2 is also indicative of patient survival. The higher the Bax/Bcl-2 ratio is the better the rate of complete remission as well as longer overall survival.<sup>44</sup> These studies have revealed an important role of Bcl-2 in relation to drug resistance in AML; however, more recently several lines of evidence have emerged, implicating another anti-apoptotic Bcl-2 protein, Mcl-1, as well. Glaser *et al*, recently found that Mcl-1 is essential for the sustained survival of AML, but Bcl-2 and Bcl-X<sub>L</sub> played only minor roles.<sup>45</sup>

Mcl-1 is a unique anti-apoptotic family member whose expression is heavily regulated in cells. It has a high turnover rate with a half-life of 2-4 hours in most cell lines.<sup>46</sup> Mcl-1 is regulated both transcriptionally and translationally by a number of pathways.<sup>47</sup> Several E3 ubiquitin ligases, including MULE,<sup>48</sup>  $\beta$ -TrCP,<sup>49</sup> and FBW7,<sup>50</sup> can cause poly-ubiquitination of Mcl-1, resulting in protein degradation by the proteasome. Mcl-1 can also be deubiquitinated by USP9X, which prevents its proteasomal degradation.<sup>51</sup> In addition, Mcl-1 can also be phosphorylated by GSK3 $\beta$ ,<sup>52</sup> resulting in decreased protein stability, or by ERK1/2,<sup>53</sup> which increases protein stability. Given the number of ways Mcl-1 is regulated, it is no surprise that abnormal regulation of Mcl-1 can result in adverse effects.

### **1.5 Anti-apoptotic Bcl-2 protein inhibitors**

Several therapeutic approaches have been undertaken aimed at targeting the overexpression of anti-apoptotic Bcl-2 proteins. One of the earliest approaches was Bcl-2 antisense oligonucleotides. The growth and survival of the human leukemia cell line 697 was inhibited by antisense oligodeoxynucleotides in a dose-dependent manner.<sup>54</sup>

Further studies demonstrated that antisense oligonucleotides were effective in AML as well as enhanced the effect of various chemotherapeutics.<sup>55</sup> These studies eventually led to the development of G3139, or Genasense, which showed potent activity in resistant AML cell lines and enhanced the cytotoxicity of other agents.<sup>56</sup> Genasense was eventually moved into clinical trials, but due to limited efficacy has not been approved as a current therapy.<sup>57</sup> In addition to antisense approaches, antibodies directed against Bcl-2<sup>58</sup> and BH3 mimicking peptide approaches have been attempted with limited success.<sup>59-</sup>  
62

Perhaps the most promising approach to targeting Bcl-2 proteins has come in the way of small molecule inhibitors (Figure 1.4). Several small molecule inhibitors have been discovered that disrupt the interaction between pro- and anti-apoptotic Bcl-2 proteins by binding in the BH3 binding domain pocket. One of the first Bcl-1 inhibitors was HA 14-1, which was identified in a virtual screen.<sup>63</sup> HA 14-1 demonstrated selective cytotoxicity against malignant cells overexpressing Bcl-2 as well as the ability to overcome drug resistance.<sup>64-66</sup> In addition, HA 14-1 also sensitized multiple cancer lines to a wide range of therapies.<sup>67-69</sup> These features seemed to validate the use of small molecule inhibitors for the development of therapies directed towards anti-apoptotic Bcl-2 proteins.

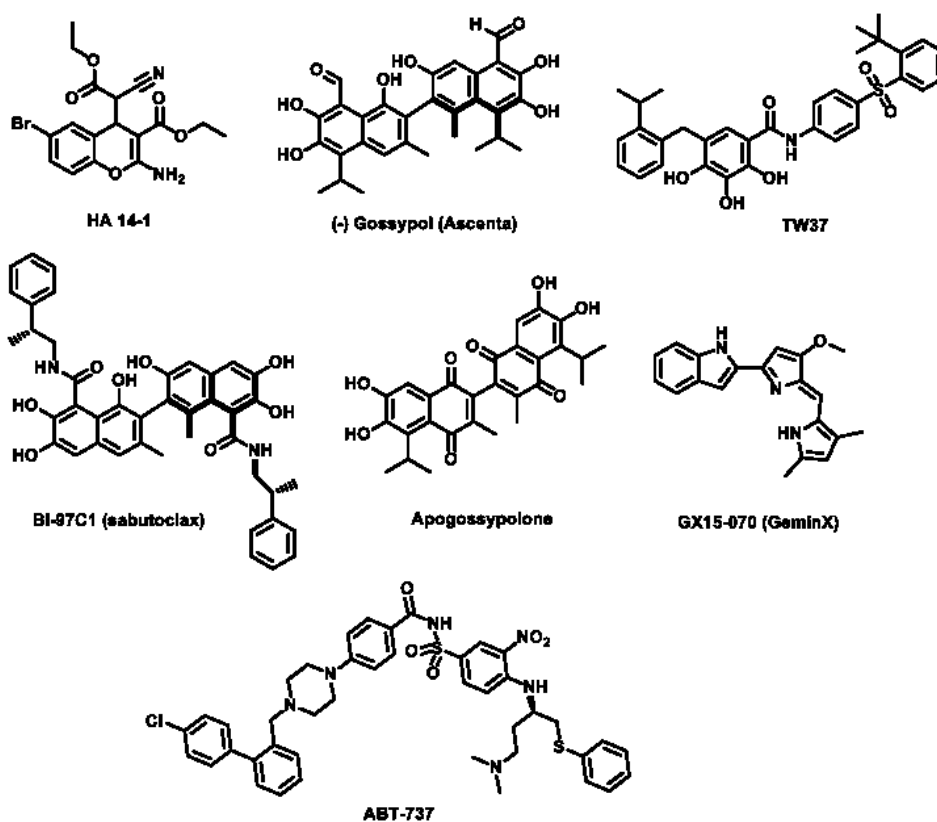


**Figure 1.4 Structures of Bcl-2 small molecule inhibitors**

Other early Bcl-2 inhibitors include (-) gossypol, which showed submicromolar affinity to both Bcl-2 and Mcl-1.<sup>70</sup> Three synthetic derivatives of gossypol have since been tested including, TW-37,<sup>71</sup> apogossypolone,<sup>72</sup> and BI-97C1.<sup>73</sup> These compounds are all pan Bcl-2 inhibitors with micromolar potency and are still currently being evaluated in preclinical studies.<sup>74-76</sup> Obatoclox is another small molecule inhibitor of Bcl-2 and Mcl-1 and has been shown to be effective against the AML cell line OCI-AML3.<sup>77</sup> Obatoclox has entered phase I clinical trials in adults for refractory AML, among other hematological cancers, with encouraging results.<sup>78</sup>

Finally, ABT-737 is yet another small molecule inhibitor identified in an NMR-based screening method. It has high binding affinity to both Bcl-2 and Bcl-X<sub>L</sub> with

dissociation constants ( $K_D$ ) in the nanomolar range;<sup>79</sup> however, ABT-737 lacks binding affinity to Mcl-1. With respect to AML, ABT-737 demonstrates activity in various AML cell lines, but suffers from resistance due to the overexpression of Mcl-1.<sup>77, 80</sup> Given that Mcl-1 overexpression is common in AML, especially in drug-resistant AML, ABT-737 is greatly limited as a potential therapeutic.

### **1.6 Development of sHA 14-1**

Given the promising features already described for HA 14-1, further studies have been carried out by our laboratory. Since limited information was known about HA 14-1, a limited number of compounds were synthesized to evaluate structural modifications.<sup>81</sup> However, shortly after those studies it was discovered that HA 14-1 was unstable in standard cell culture conditions.<sup>82</sup> In these studies, it was revealed that HA 14-1 decomposed rapidly in media with a half-life of 15 minutes. It was further shown that the potency was reduced by 60-fold when HA 14-1 was pre-incubated in media for 24 hours prior to cytotoxicity studies. Decomposition resulted in the production of reactive oxygen species (ROS), which may be responsible for its activity. Importantly, the decomposition pathway was established in this study and none of the products were cytotoxic (Figure 1.5).

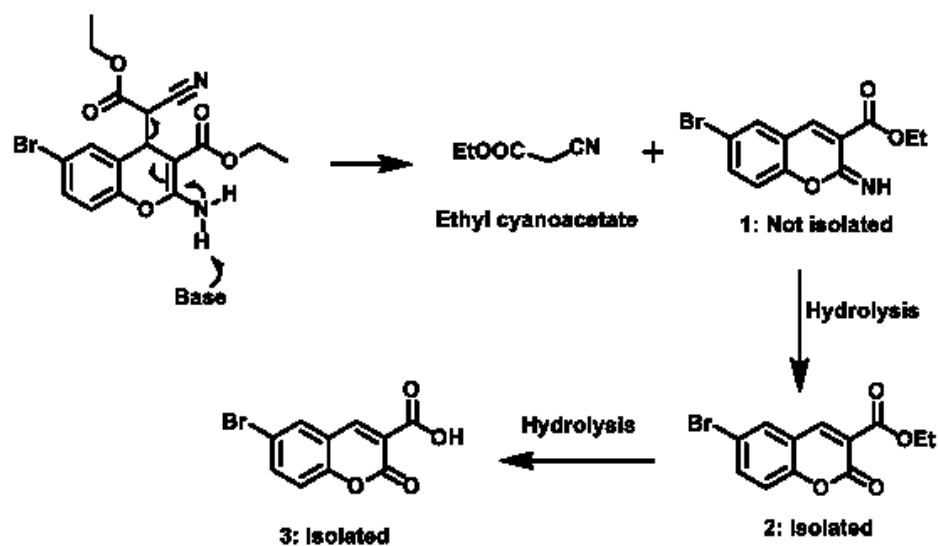


**Figure 1.5 Proposed decomposition of HA 14-1**

With the decomposition pathway known, an effort was made to stabilize HA 14-1. The culmination of those efforts resulted in sHA 14-1, standing for stabile HA 14-1 (Figure 1.6).<sup>83</sup> sHA 14-1 was studied for competitive binding to Bcl-2 and Bcl-X<sub>L</sub> where it demonstrated better binding to both proteins than HA 14-1. The new compound was also tested for stability in culture medium, which resulted in less than a two-fold decrease in activity when pre-incubated in culture medium for 24 hours prior to cytotoxicity studies. Moreover, sHA 14-1 did not induce ROS, but still overcame drug resistance induced by the overexpression of Bcl-2 and Bcl-X<sub>L</sub> in Jurkat cells. Finally, sHA 14-1 was also able to synergize with multiple standard therapies. These results summarize the findings related to sHA 14-1 prior to my research, which was to establish a mechanism of action of sHA 14-1 and its related analogs.

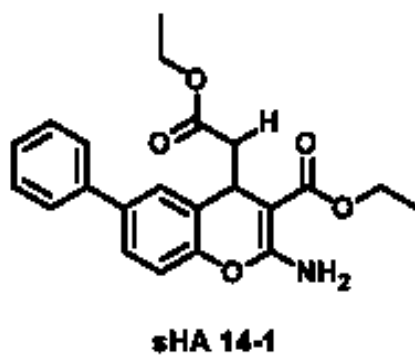


Figure 1.6 Structure of sHA 14-1

## CHAPTER 2\*

### 2. sHA 14-1 disrupts calcium homeostasis

#### 2.1 Introduction

Investigation of sHA 14-1's mechanism of action began by characterizing its impacts on calcium flux. As noted in chapter one, Bcl-2 family proteins can localize to the endoplasmic reticulum (ER) membrane and interact with key calcium regulating proteins controlling apoptosis. Disruption of calcium signaling is one possible mechanism of action for sHA 14-1. Calcium release was measured in Jurkat, an immortalized T lymphocyte cell line, and NALM-6 cells, a pre-B leukemia cell line. Treatment with sHA 14-1 resulted in an increase in cytosolic calcium levels in both cell lines. This observation prompted further studies to elucidate the role cytosolic calcium increase may play in the cytotoxicity of sHA14-1. Upon sustained calcium release, mitochondrial membrane depolarization occurs, leading to the release of cytochrome c and subsequent cell death. Cell permeable calcium chelators are able to effectively lower increases in cytosolic calcium by binding to the excess calcium. Therefore, we sought to use calcium chelators to try and protect against sHA 14-1 induced cell death. A second study was conducted to determine the cellular target leading to calcium release. The two major proteins investigated were SERCA, the ATPase pump responsible for maintaining the concentration gradient across the ER membrane, and IP3R, the major ion channel allowing for calcium flow out of the ER. Finally, several structurally similar analogs of

---

\* Parts of this chapter have been reproduced with permission from Hermanson, David et al. Dual Mechanisms of sHA 14-1 in Inducing Cell Death through Endoplasmic Reticulum and Mitochondria. *Mol Pharmacol.* **2009.** 76, 667-678. Copyright 2009.

sHA 14-1 had been synthesized and were tested for their ability to release calcium in NALM-6 cells.

## **2.2 Results and Discussion**

### **2.2.1 Measuring cytosolic calcium increases in Jurkat and NALM-6 cells**

#### **following treatment with sHA 14-1**

sHA14-1 was tested in Jurkat and NALM-6 cells for its ability to induce cytosolic calcium increases. Increased cytosolic calcium levels were detected by treating cells with a cell permeable fluorescent calcium chelator known as Fura2-acetoxymethyl ester (Fura2-AM). Once Fura2-AM enters the cell, the ester is cleaved and Fura2 becomes trapped in the cytosol. Fura2 is a ratiometric indicator dye that upon calcium binding, undergoes a change in fluorescence intensity at 340 and 380 nm excitation.<sup>84</sup> The intracellular calcium levels are then calculated taking the ratio of fluorescent intensities from the two wavelengths. As cytosolic calcium levels rise, so does the ratio. By using the ratio to evaluate calcium levels, effects of uneven dye loading, photobleaching, and dye leakage are minimized. It was found that sHA 14-1 caused a rapid and dose dependent increase in cytosolic calcium in both cell lines tested (Figure 2.1 A&B). Since extra-cellular calcium was chelated by EGTA in this experiment, this suggested that sHA 14-1 was able to rapidly enter cells and cause calcium release from within the cell. It was hypothesized that the increase in cytosolic calcium was a result of ER calcium release. In order to confirm calcium release was originating from the ER, thapsigargin was employed. Thapsigargin is a SERCA inhibitor known to cause calcium release specifically from the ER.<sup>30</sup> If the cytosolic increase induced by sHA 14-1 was



caused by ER calcium release, the addition of thapsigargin following sHA 14-1 treatment should not result in a further increase of cytosolic calcium. Thapsigargin was first tested as a single agent and produced a rapid increase in cytosolic calcium levels followed by a return to baseline levels within 10 minutes from the point of addition (Figure 2.1 C&D). The fall of calcium back to baseline levels is likely due to calcium leaving the cell and being chelated extracellularly. Addition of thapsigargin following treatment by sHA 14-1 confirmed that sHA 14-1 was causing calcium release from the ER (Figure 2.1 A&B), as indicated by the lack of increased calcium release upon thapsigargin addition. Lastly, an inactive analog of sHA14-1 was also tested. This analog resulted in no detectable increase of cytosolic calcium, suggesting that calcium release from the ER may play a role in the cytotoxic mechanism of sHA14-1.

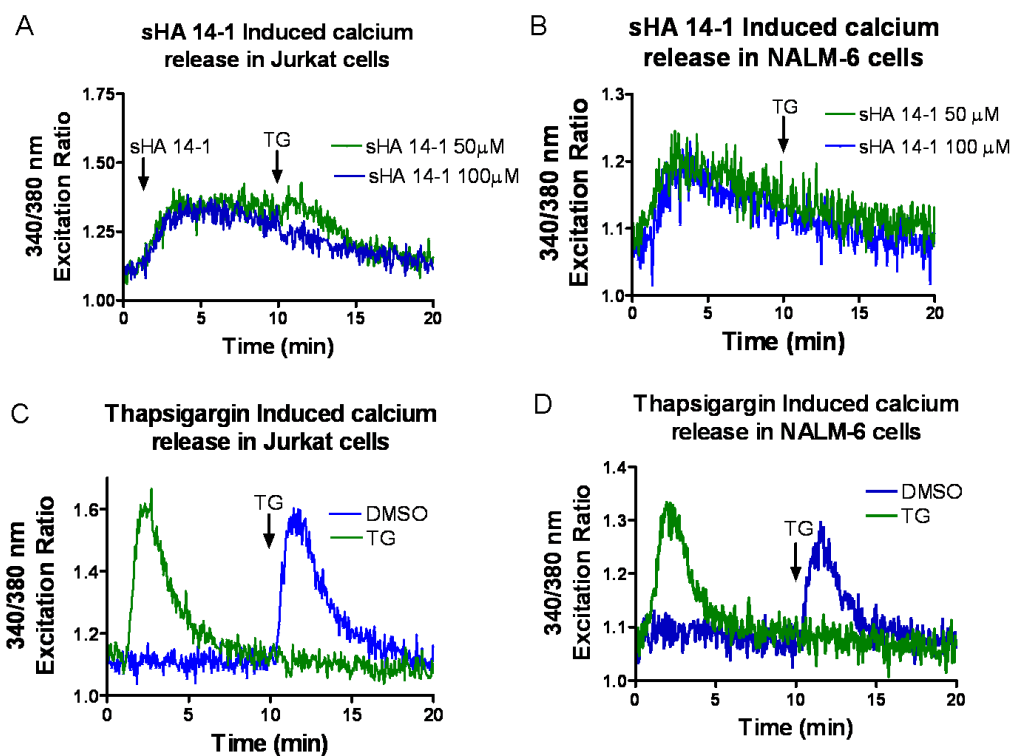


**Figure 2.1: Cytosolic calcium measurements using Fura-2.** After cells were loaded with Fura2-AM, they were added to a cuvette and mixed with media containing EGTA, in order to chelate extracellular calcium, immediately prior to measurements. Readings were obtained by alternating the excitation wavelength from 340 to 380 nm and measuring emission at 510nm for 1 minute prior to addition of compound. A&B) 50 or 100 μM sHA 14-1 was added to the cuvette and readings continued for 9 minutes before the addition of 2 μM thapsigargin (TG). C&D) Either 15 μL of DMSO (Blue line) or 2 μM of thapsigargin (green line) was added one minute after readings were started. Then 2μM of thapsigargin was added again at 10 minutes. Calcium increases were monitored by taking the ratio of fluorescent intensities at 340 and 380 nm. Each curve is representative of at least 3 independent experiments. TG represents thapsigargin.

### 2.2.2 Protection of Cell by EGTA-AM

Given that sHA 14-1 rapidly causes ER calcium release and a rise in cytosolic calcium, it was hypothesized that chelating intracellular calcium would have a protective effect against the compound. To that end, NALM-6 cells were treated simultaneously with the cell permeable acetoxymethyl EGTA, a calcium chelator, and sHA 14-1. Cytotoxicity of sHA 14-1 was measured in the presence of 5  $\mu$ M EGTA-AM. A significant decrease in the amount of cell death caused by sHA 14-1 in NALM-6 cells (Figure 2.2), suggested that cytosolic calcium increase does play a partial role in the mechanism of action. There are multiple potential reasons the protective effect of EGTA is not more dramatic. First, chelating of intracellular calcium can be toxic to cells limiting the amount of EGTA that can be used to 5  $\mu$ M. Since concentrations of calcium in the ER can reach into the mM range,<sup>85</sup> it is possible that 5  $\mu$ M EGTA is not sufficient to fully buffer the rise in calcium. Secondly, EGTA is also better for short-term buffering of calcium, limiting the protective effect over 24 hrs. Lastly, the emptying of ER calcium stores can cause cell death due to ER stress and an accumulation of misfolded proteins.<sup>86</sup>

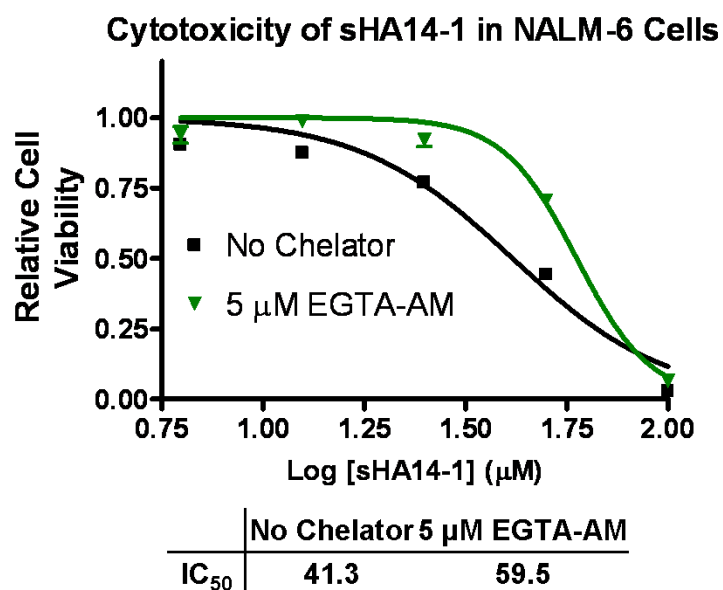


**Figure 2.2: Protection of NALM-6 cells through chelation of internal calcium.** NALM-6 cells were treated with sHA 14-1 or 5 µM EGTA-AM plus sHA 14-1 simultaneously. Cell viability was measured after 24 hours. Data is representative at least 2 independent trials.

### **2.2.3 sHA 14-1 causes ER Stress**

The potential of sHA 14-1 to induce ER stress was investigated due to its ability to elicit calcium release, which can activate the ER stress pathway. Activating transcription factor 4 (ATF4) is an ER stress related protein that is upregulated due to ER stress induction.<sup>87</sup> Western blotting was used to monitor protein levels of ATF4 following treatment by sHA 14-1 or thapsigargin. Using 50  $\mu\text{M}$  of sHA 14-1 in NALM-6 cells led to increased protein levels of ATF4 within 1 hr with continued induction up to 2 hrs (Figure 2.3 A). Cells treated with thapsigargin also displayed an increase in ATF4 after 2 hours of treatment. Performing a dose dependent study of sHA 14-1 using the 2 hr time-point, induction of ATF4 was observed at both the 50 and 100  $\mu\text{M}$  concentrations (Figure 2.3 B). These results indicated that sHA 14-1 activates the ER stress pathway, likely due to the lowering of ER calcium levels. These data further explain why chelation of intracellular calcium by EGTA was ineffective at producing a greater protective effect. Additionally, these data suggest a second mechanism of apoptosis induced by the treatment of sHA 14-1 linked to calcium release from the ER.

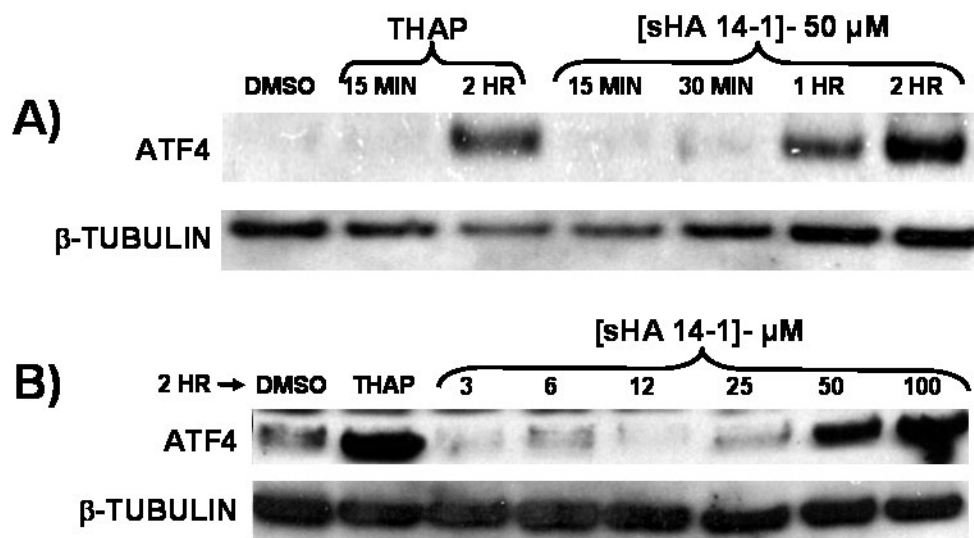


**Figure 2.3: ER stress induction by sHA 14-1.** A) NALM-6 cells were treated with thapsigargin (THAP) or sHA 14-1 for the indicated time points. B) NALM-6 cells were treated for 2 hours with various concentrations of sHA 14-1. Thapsigargin was used as a control and loading levels were assessed using  $\beta$ -tubulin. Results are representative of 2 independent experiments.

#### **2.2.4 sHA 14-1 causes calcium release via SERCA and not IP3R**

Once it was established that sHA 14-1 causes calcium release from the ER the mechanism of calcium release was investigated. As previously mentioned, the two main protein families that regulate calcium levels in the ER are SERCA and IP3R. The former is responsible for uptake of calcium into the ER, and the later is responsible for release of calcium. Therefore, it could be envisioned that sHA 14-1 induces calcium release through inhibition of SERCA. Alternatively, IP3R could be activated in the presence of sHA 14-1 allowing for calcium ions to flow out at a greater rate than they are returned to the ER.

In order to address whether activation of IP3R was responsible, an IP3R knockout cell line was obtained, DT-40 IP3R K.O, an avian derived B-cell line with stable knockout of IP3R. This cell line was tested against sHA14-1 in a cytotoxicity assay and compared to the corresponding wild type cell line, DT-40 W.T. If sHA 14-1 induced calcium release through IP3R, the DT-40 IP3R K.O cells were expected to be resistant to treatment since it was already established that calcium release plays a role in sHA 14-1's cytotoxicity. However, the DT-40 IP3R K.O cells showed no resistance to sHA14-1 relative to DT-40 W.T cells (Figure 2.4 A), which suggests sHA 14-1 is not acting through IP3R. The DT-40 cells were also tested against a standard compound, doxorubicin, to ensure the knock-out line was not hypersensitive to standard therapies (Figure 2.4 B). In order to determine if IP3R knockout affected the ER calcium content or ER calcium release of either cell line, they were tested using thapsigargin and sHA 14-1. It was observed that both cell lines showed little difference in calcium release profiles

regardless of the compound tested (Figure 2.4 C&D). While it was expected that treatment with thapsigargin would result in the same calcium release profile, these results suggested that sHA 14-1 was not causing calcium release from the ER through IP3R. If sHA 14-1 was causing activation of IP3R, the DT-40 IP3R K.O cell line would have been unaffected by treatment with sHA 14-1. This indicated that sHA 14-1 is likely inhibiting SERCA, causing calcium release.



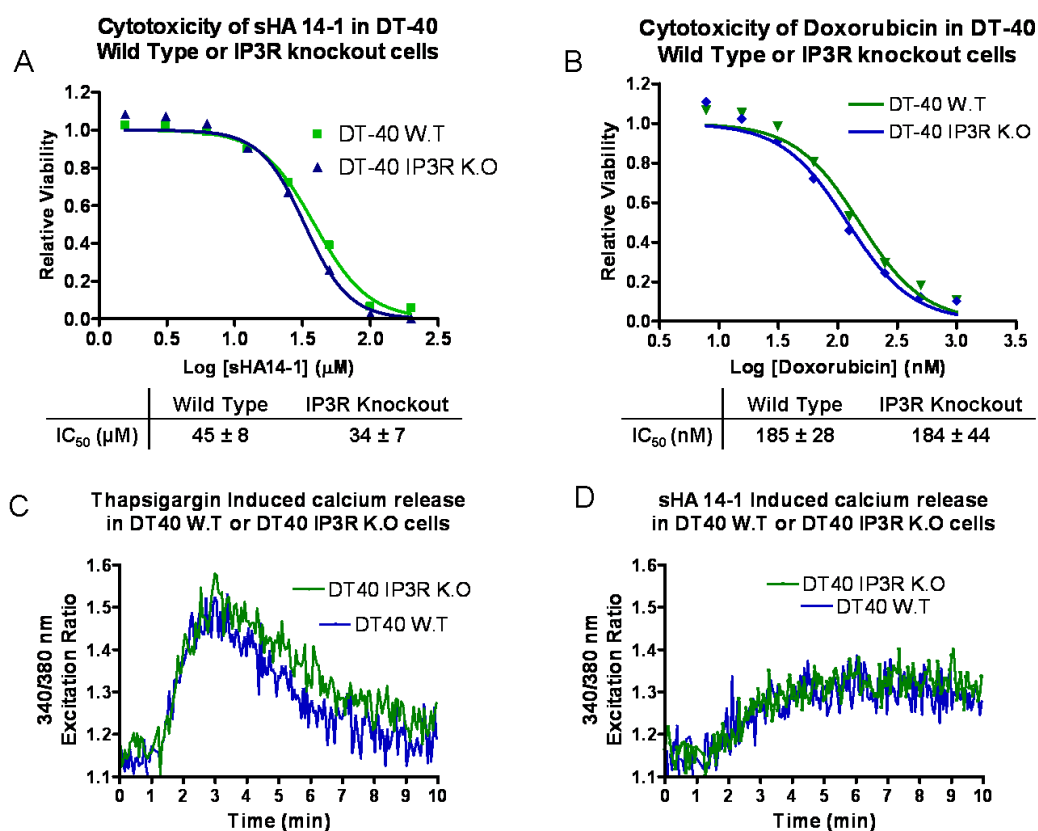


**Figure 2.4: Role of Inositol triphosphate receptor (IP3R) in sHA 14-1 induced cytotoxicity and calcium release.** Cytotoxicity of DT-40 IP3R knockout and DT-40 wild type cell lines was performed using A) sHA 14-1 or B) doxorubicin. ER calcium release was measured using C) thapsigargin or D) sHA 14-1 in DT-40 cells. Data are representative of at least three independent experiments with IC<sub>50</sub> ± S.D.

Given the results from the IP3R studies, SERCA was evaluated as a possible target of sHA 14-1. It was observed that sHA 14-1 resulted in a much lower level of calcium release than thapsigargin treatment, especially when extracellular calcium was not chelated (Figure 2.5 Blue vs. Green curves). Therefore, if both compounds inhibit SERCA, they may compete for binding and the extent of calcium release should vary depending on the ratio of sHA 14-1 to thapsigargin. When sHA 14-1 is in greater excess, the amount of calcium released will be reduced compared to thapsigargin alone. As the concentration of sHA 14-1 is lowered, thapsigargin will bind a greater portion of SERCA and increased calcium release will be observed. Initially, the lowest concentration of thapsigargin eliciting a full calcium response in Jurkat cells was established. Once this was determined, the concentration of thapsigargin was fixed while the concentration of sHA 14-1 was varied. Results showed the expected dose-dependent shift in calcium release. As the concentration of sHA 14-1 was lowered, more calcium release was observed (Figure 2.5). This data suggested that sHA 14-1 had the same cellular target as thapsigargin, namely SERCA. In order to confirm sHA 14-1 inhibited SERCA, sHA14-1 was tested in a coupled enzymatic assay against SERCA2B where it was confirmed sHA 14-1 inhibited SERCA with an  $IC_{50}$  value of approximately 35  $\mu$ M (Figure 2.6). These experiments identified SERCA the target of sHA 14-1 calcium release.

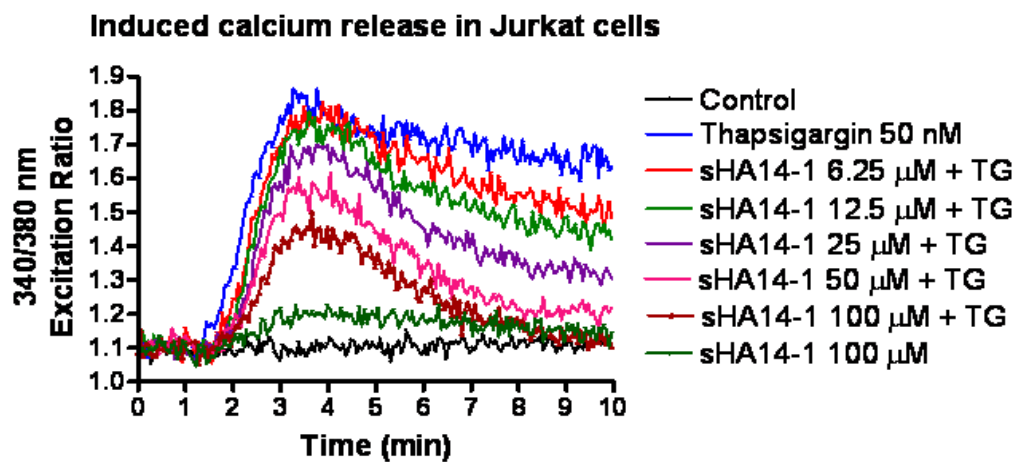


**Figure 2.5: Competition between sHA 14-1 and Thapsigargin.** Calcium release was measured using Fura-2 in Jurkat cells. Readings were obtained by alternating the excitation wavelength between 340 and 380 nm while taking the emission at 510 nm. This data is representative of two independent experiments.

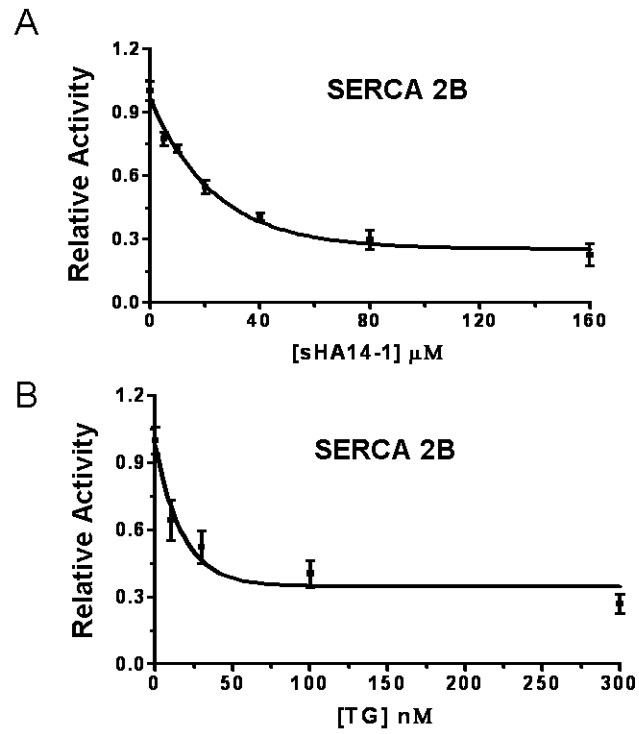
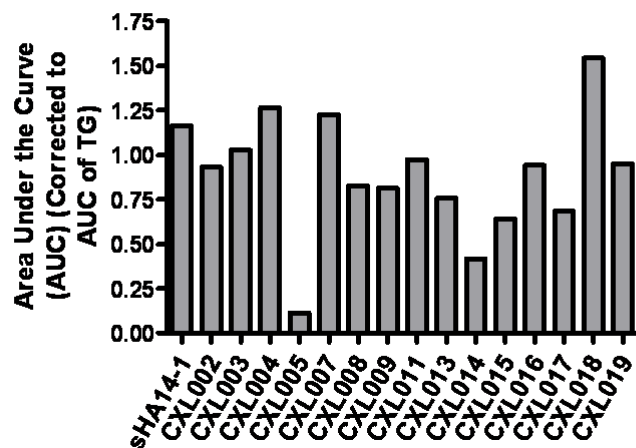


**Figure 2.6: Inhibition of SERCA 2B by sHA 14-1 and Thapsigargin.** A coupled enzyme assay was used to measure SERCA 2B inhibition by A) sHA 14-1 or B) thapsigargin (TG).

### 2.2.5 Screening of sHA 14-1 analogs in NALM-6 Cells

Several additional analogs of sHA 14-1 had been synthesized, so all of the analogs were screened in NALM-6 cells for their ability to cause calcium release. The area under the curve (AUC) was determined for each compound at a single concentration and was used to compare each the analogs. In order to compare the data from different days, thapsigargin was used as a control since it causes complete emptying of the ER. The AUC of each compound was then corrected for the AUC of thapsigargin taken on the same day. In control experiments meant to test each compound for fluorescent interference, it was discovered CXL006, CXL010, and CXL012 all contained significant fluorescence at the wavelengths being used, so were excluded from the analysis. Screening revealed a significant number of analogs caused similar levels of calcium release in relation to sHA 14-1 (Figure 2.7 A); however, there were several compounds to note. The *tert*-butyl phenyl substituted analog, CXL005, caused almost no increase in calcium, yet had a comparable IC<sub>50</sub> value to sHA 14-1 (Figure 2.7 B). On the other hand, the compound with the greatest level of calcium increase was CXL018, which is significantly more potent than sHA 14-1 (Figure 2.7 A & B). Finally, the compound with the highest potency, CXL017, induced similar calcium release compared to sHA 14-1. Overall, the results from this experiment showed little correlation between the calcium release in NALM-6 cells and the cytotoxicity of individual compounds. This indicates that the effects of sHA 14-1 and its analogs have on calcium are likely not the only cytotoxic mechanism and that the contribution calcium perturbation plays in the mechanism of action is likely to vary significantly among the analogs.

**A Calcium Release measured in NALM-6 Cells**



**B**

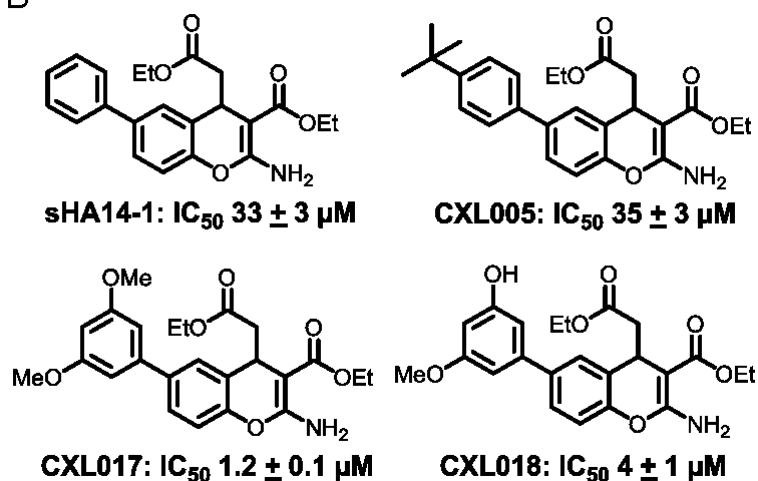


**Figure 2.7: Calcium release of CXL analogs measured in NALM-6 cells.** A) sHA 14-1 analogs were tested in NALM-6 cells for their ability to induce calcium release at 50  $\mu M$ . The area under the curve was calculated and corrected to the AUC of thapsigargin (TG). B) Structures and corresponding  $IC_{50}$  values of select analogs. All  $IC_{50}$  values were determined in triplicate.

## 2.3 Conclusion

In the present studies, sHA 14-1 was shown to induce ER calcium release through inhibition of SERCA. Since calcium signaling can regulate a wide variety of cellular activities, including cell death through apoptosis, it was demonstrated that chelating intracellular calcium with EGTA had a protective effect compared to cells treated with sHA 14-1 alone. This evidence led to an attempt to find the cellular target of sHA 14-1 responsible for calcium release. Two key ER calcium regulating proteins, IP3R and SERCA, were evaluated. IP3R knock-out cells failed to show any resistance to sHA 14-1 and had no detectable difference in calcium release caused by sHA 14-1; therefore, it was concluded that IP3R was unlikely to be the target leading to calcium release. In a competitive assay between the SERCA inhibitor thapsigargin and sHA 14-1, it was discovered SERCA inhibition was likely the cause of the calcium release. sHA 14-1 treatment also caused the activation of ER stress, indicated by the induction of ATF4, likely through the lowering of ER calcium content causing the accumulation of misfolded proteins. Finally, several addition analogs of sHA 14-1 were tested in NALM-6 cells for their ability to induce calcium release. Many of the analogs displayed similar levels of calcium release when compared to sHA 14-1; however, the extent of calcium release did not correlate with cytotoxicity values. This suggested that while sHA 14-1 inhibits SERCA and calcium release does play a role in the mechanism of action of sHA 14-1, these features cannot fully account for the compound's cytotoxicity. In the next chapter, investigation of sHA 14-1, CXL005, CXL017, and CXL018 will be discussed in relation to targeting drug resistance.

## **2.4 Materials and Methods**

### **2.4.1 Cell Culture**

JURKAT cell line was obtained from the ATCC. The human B-lineage acute lymphoblastic leukemia (ALL) cell line NALM-6 was originally established at the University of Minnesota. All human leukemic cell lines were maintained in RPMI-1640 (+) L-Glutamine supplemented with 10% fetal bovine serum and 1% penicillin/streptomycin. The chicken DT-40 B lymphoma cell line and IP<sub>3</sub>R *null* DT-40 cell line were kindly provided by Dr. Chi Li (University of Louisville, Louisville, KY). Both DT-40 cell lines were cultured in RPMI-1640 (+) L-Glutamine supplemented with 1% chicken serum, and 1% penicillin/streptomycin. All cell lines were incubated at 37 °C with 5 % CO<sub>2</sub> in air atmosphere.

### **2.4.2 Cell Viability while chelating calcium**

NALM-6 cells were plated at a density of  $1 \times 10^4$  cells/well in a 96-well plate. Test compounds were added at varying concentrations in 1% DMSO and cells treated with medium containing 1% DMSO served as a control. For protection studies, 5 μM of EGTA-AM was added 1 hour prior to the addition of compound. This allowed for cleavage of the ester and release of free EGTA. After a 24-h treatment with sHA 14-1, relative cell viability in each well was determined using the CellTiter-Blue Cell Viability Assay from Promega (Madison, WI). The IC<sub>50</sub> of each compound was determined by fitting the relative viability of the cells to the drug concentration, using a dose-response model in Prism program from GraphPad Software, Inc. (San Diego, CA).



### **2.4.3 Measuring cytosolic calcium**

Cells at a density of  $1 \times 10^6$  cells/mL were incubated in medium containing 5  $\mu$ M Fura-2AM and 2.5 mM probenecid at room temperature for 30 min. in the dark. The cells were then washed once with cold PBS and re-suspended to a concentration of  $2 \times 10^6$  cells/mL in medium containing 2.5 mM probenecid. To a cuvette with 735  $\mu$ L media containing 100 mM EGTA and 2.5 mM probenecid was added 750  $\mu$ L of the cell suspension. By using 100 mM EGTA, the cell medium contained negligible amounts of free calcium; therefore, the cells had no extracellular calcium source. Readings were obtained for 1 min to set the baseline. After 1 min, 15  $\mu$ L of DMSO containing compound was added, and the readings were continued for another 9 min. Readings were obtained on a dual wavelength fluorometer (Cary Eclipse, Varian, Palo Alto, CA) with excitation wavelengths alternating between 340 and 380 nm and an emission wavelength of 510 nm. Fura-2AM was from Invitrogen (Carlsbad, CA). Thapsigargin was obtained from Acros Organics (Geel, Belgium). EGTA-AM was from VWR Scientific (Batavia, IL).

### **2.4.4 Competition of sHA 14-1 and thapsigargin in Jurkat Cells**

This experiment followed the same general procedure as “measuring cytosolic calcium”, except that extracellular calcium was not chelated by EGTA in this assay. For competition studies, thapsigargin and sHA 14-1 were mixed before adding them to the cell solutions.

### **2.4.5 Measurement of SERCA enzymatic inhibition (Performed by Dr. Michelangeli)**

Pig brain microsome  $\text{Ca}^{2+}$  ATPase<sup>88</sup> was used as a source of SERCA2B, and enzymatic activity measured using a phosphate liberation assay as previously described.<sup>89</sup>

#### **2.4.6 Western blotting for ATF4 (Performed by Dr. Lebien)**

Western blotting was conducted using standard chemiluminescent techniques.<sup>90</sup> Briefly, cells were treated with either thapsigargin or SHA 14-1 for the indicated time points. Cells were then lysed, separated by SDS-PAGE, transferred to membranes and probed with primary antibody. Following a 2-4 h incubation in primary antibody at room temperature the blots were washed, and secondary staining was accomplished using the corresponding IgG conjugated to horseradish peroxidase. Protein loading was assessed using anti-beta tubulin. The anti-activating transcription factor-4 (ATF4) antibody was from Santa Cruz Biotechnology, Inc. (Santa Cruz, CA) and was used at a final dilution of 1:500.

## CHAPTER 3\*

### 3. Targeting Drug Resistant Cancer

#### 3.1 Introduction

Drug resistance is a major obstacle in the treatment of cancer, and compounds that target drug resistance can be valuable in the clinic and as tools to study the mechanisms of drug resistance. It has been reported that targeting anti-apoptotic Bcl-2 family proteins, such as Bcl-2, Bcl-X<sub>L</sub>, or Mcl-1, may be an effective way to overcome drug resistance, as they are commonly overexpressed in resistant cells. Since sHA 14-1 was developed based on the reported Bcl-2 inhibitor HA14-1, it was hypothesized that sHA 14-1 may overcome drug resistance. In fact sHA 14-1 has been previously shown to overcome drug resistance induced by overexpression of Bcl-2 proteins in Jurkat cells.<sup>91</sup> Overexpression of the anti-apoptotic proteins induced multidrug resistance to cisplatin, doxorubicin, thioguanine, and taxol; however, no resistance was observed when these cell lines were treated with sHA 14-1.

In order to further study sHA14-1's ability to overcome resistance, several cell lines that acquired multidrug resistance to standard therapies through treatment, rather than genetic overexpression of anti-apoptotic Bcl-2 proteins, were obtained and studied. Resistance developed naturally to therapies should provide a better representation of drug resistance as well as a better system for testing sHA 14-1. The first set of cell lines

---

\* Parts of this chapter have been reproduced with permission from {Das, S. G. et al. Structure-activity relationship (SAR) study of ethyl 2-amino-6-(3,5-dimethoxyphenyl)-4-(2-ethoxy-2-oxoethyl)-4H-chromene-3-carboxylate (CXL017) and its analogs. **2011**. *54*, 5937-5948}. Copyright {2011} American Chemical Society and from {Gopaladrishnan, A. et al. Structure-activity relationship (SAR) study of ethyl 2-amino-6-(3,5-dimethoxyphenyl)-4-(2-ethoxy-2-oxoethyl)-4H-chromene-3-carboxylate (CXL017) and the potential of the lead against multidrug resistance in cancer treatment. **2012**. *55*, 5566-5581}. Copyright {2012} American Chemical Society.

included HL60, an acute promyelocytic leukemia (AML) cell line, and HL60/MX2, a mitoxantrone resistant cell line with 35-fold less sensitivity to mitoxantrone. This cell line displayed atypical multidrug resistance and was reported to lack overexpression of the efflux pump P-glycoprotein.<sup>92</sup> Resistance was reported to result from altered topoisomerase II $\beta$  activity, the target of mitoxantrone, with lowered levels of topoisomerase II alpha and beta.<sup>93</sup> Also obtained were CCRF-CEM, a human T cell leukemia cell line, and CEM/C2, a camptothecin resistant cell line that is ~970 fold less sensitive to camptothecin than CCRF-CEM parent cells. The CEM/C2 cells also displayed atypical multidrug resistance and had a unique mutation resulting in altered topoisomerase I activity, the cellular target of camptothecin.<sup>94,95</sup>

In this chapter, sHA 14-1 and three analogs will be explored in HL60, HL60/MX2, CCRF-CEM, and CEM/C2 cells for their ability to overcome multidrug resistance. These analogs were chosen based on potency and ability to induce calcium release. sHA 14-1 was the lead molecule with a IC<sub>50</sub> value of 33  $\mu$ M and showed significant calcium release in NALM-6 cells as described in the previous chapter (Figure 2.7). CXL005 contained a *tert*-butyl substitution on the phenyl ring and induced almost no calcium release, but maintained similar activity compared to sHA 14-1 with an IC<sub>50</sub> value of 35  $\mu$ M. The final two analogs were CXL017 and CXL018. CXL018 was chosen based on its ability to cause the greatest level of calcium release and improved potency with an IC<sub>50</sub> of 4  $\mu$ M. This analog contained a hydroxyl group at the 3 position and a methoxy group at the 5 position of the substituted phenyl ring of sHA 14-1.

Finally, CXL017 was a di-methoxy substitution at the 3 and 5 positions of the phenyl ring and demonstrated the highest potency with an  $IC_{50}$  value of 1  $\mu$ M (Figure 3.1).

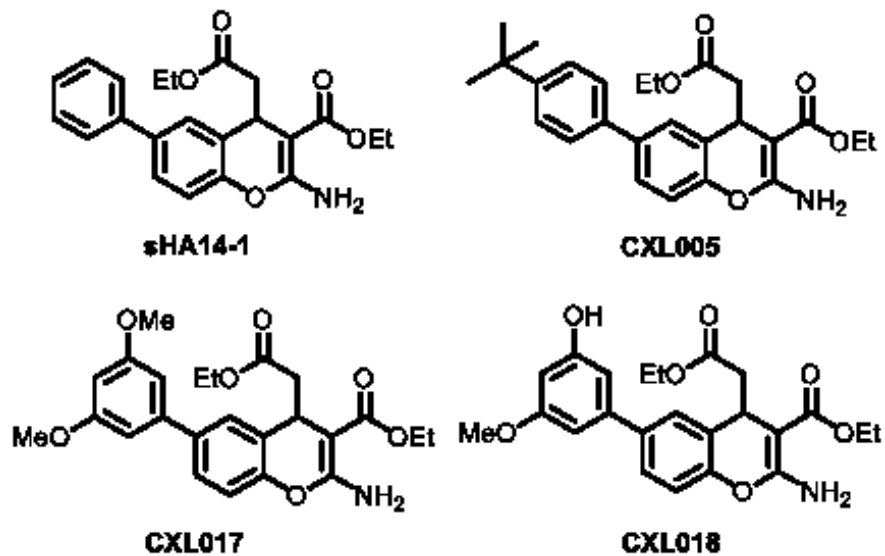


Figure 3.1 Structures of sHA14-1 and analogs tested in HL60, HL60/MX2, CCRF-CEM, and CEM/C2 cell lines

## **3.2 Results and Discussion**

### **3.2.1 Cytotoxicity evaluation of drug resistant cell lines**

HL60, HL60/MX2, CCRF-CEM, and CEM/C2 cell lines were obtained through ATCC and tested for multidrug resistance (Table 3.1). Several standard therapies were used including three topoisomerase II inhibitors, mitoxantrone, etoposide, and doxorubicin, an antimetabolic agent, cytarabine, and an antimicrotubule agent, vincristine. In addition, camptothecin was used in the CEM/C2 cells. HL60/MX2 cells demonstrated cross-resistance to all three topoisomerase II inhibitors, but failed to show any resistance to vincristine or cytarabine. In fact, the HL60/MX2 cells proved to be collaterally sensitive, a rare phenomenon when a resistant cell line shows increased sensitivity to other therapies, to cytarabine. CEM/C2 cells were confirmed to be resistant to camptothecin and were cross-resistant to all three topoisomerase II inhibitors as well as cytarabine, but no resistant was observed to vincristine. These results confirmed that HL60/MX2 and CEM/C2 cells were in fact multidrug resistant cell lines.

**Table 3.1: Cytotoxicity of standard therapies in HL60, HL60/MX2, CCRF-CEM, and CEM/C2 cell lines**

	HL60 IC <sub>50</sub>	HL60/MX2 IC <sub>50</sub>	Fold Resistance	CCRF-CEM IC <sub>50</sub>	CEM/C2 IC <sub>50</sub>	Fold Resistance
Mitoxantrone (μM)	0.055	1.3	24	0.036	0.108	3
Etoposide (μM)	1.6	14.4	9	0.24	0.60	2.5
Doxorubicin (μM)	0.14	0.742	5	0.46	3.1	6.7
Cytarabine (μM)	4	1.6	0.4	0.006	0.25	4.1
Vincristine (nM)	0.06	0.06	1	0.59	0.59	1

IC<sub>50</sub>s are representative of two independent experiments. Fold Resistance is (Parent/Resistant cell line).

### **3.2.2 sHA14-1 and analogs overcome drug resistance**

After confirming multidrug resistance in both HL60/MX2 and CEM/C2 cells, sHA14-1, CXL005, CXL017, and CXL018 (Figure 3.1) were evaluated for their cytotoxicity in each of the four cell lines. In addition ABT-737, a known Bcl-2 inhibitor, was tested in the cell lines for comparison with sHA 14-1 and its analogs. HL60/MX2 cells showed a slight resistance to ABT-737 while CEM/C2 cells showed a slight increase in sensitivity (Figure 3.2 A&B). Strikingly, neither HL60/MX2 nor CEM/C2 cells were resistant to sHA14-1 and its analogs. In fact, CEM/C2 cells were almost 2-fold more sensitive to sHA 14-1, CXL017, and CXL018 in comparison to CCRF-CEM cells, while CXL005 was equipotent in the two cell lines (Figure 3.3A). Collateral sensitivity was also observed in HL60/MX2 cells (Figure 3.3B). The extent of selectivity for sHA 14-1 and its analogs appeared to correlate with calcium release (Figure 2.7). CXL005 was least selective and caused the lowest amount of calcium release, while CXL018 was the most selective compound and was shown to cause the greatest level of calcium release as reported in the previous chapter (Figure 2.7). However, while the level of collateral sensitivity in HL60/MX2 cells appeared to depend on calcium release, the cytotoxic potency of individual compounds seemed to be independent of calcium release. In comparing the effects between HL60/MX2 and CEM/C2 cells, the data suggest that causing calcium release from the ER may lead to selectivity towards HL60/MX2 cells, but not in CEM/C2 cells relative to their respective parental cell lines. This was supported by the cytotoxicity of thapsigargin in both resistant cell lines (Figure 3.4 A&B). HL60/MX2 cells were >450 times more sensitive to thapsigargin compared to



HL60 cells, while CEM/C2 cells were slightly resistant to thapsigargin. Taken together, these results suggest targeting calcium release may be an effective strategy to overcome drug resistance and in some cases selectively target drug resistant cancer.

The results also suggest that sHA14-1, CXL005, CXL017, and CXL018 have a unique profile compared to known Bcl-2 and SERCA inhibitors. While the selectivity towards resistant cell lines correlates well with calcium release and what was observed with thapsigargin treatment, the overall potency of the sHA 14-1 and its analogs did not correlate with calcium release data. This indicates that analogs of sHA14-1 induce cell death through a mechanism independent of calcium release, as well, possibly through inhibiting Bcl-2 family proteins. In the HL60/MX2 cell line, CXL017 has an advantage over ABT-737 because the HL60/MX2 cell line displays collateral sensitivity to CXL017 and slight resistance to ABT-737. On the other hand, in CEM/C2 cells CXL017 retains two fold selectivity, similar to ABT-737, while the cell line is less sensitive to thapsigargin compared to CCRF/CEM.

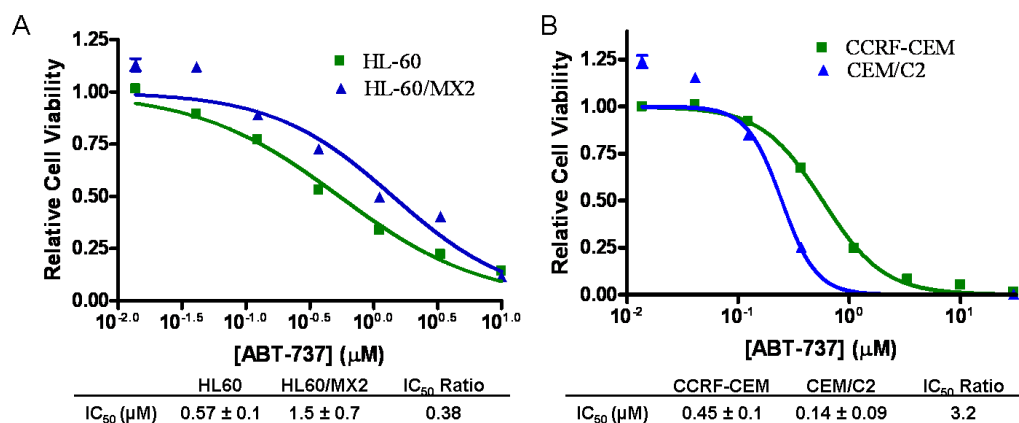


**Figure 3.2 Cytotoxicity of ABT-737 in HL60, HL60/MX2, CCRF-CEM, and CEM/C2 cells.** 48 hour cytotoxicity of given compounds in A) HL60 and HL60/MX2 cells and in B) CEM-CCRF and CEM/C2 cells. Curves are representative of at least duplicate data while IC<sub>50</sub> values are mean ± SEM. These values compare well with experiments performed by other members of the lab whose data are not included in the IC<sub>50</sub> determination.

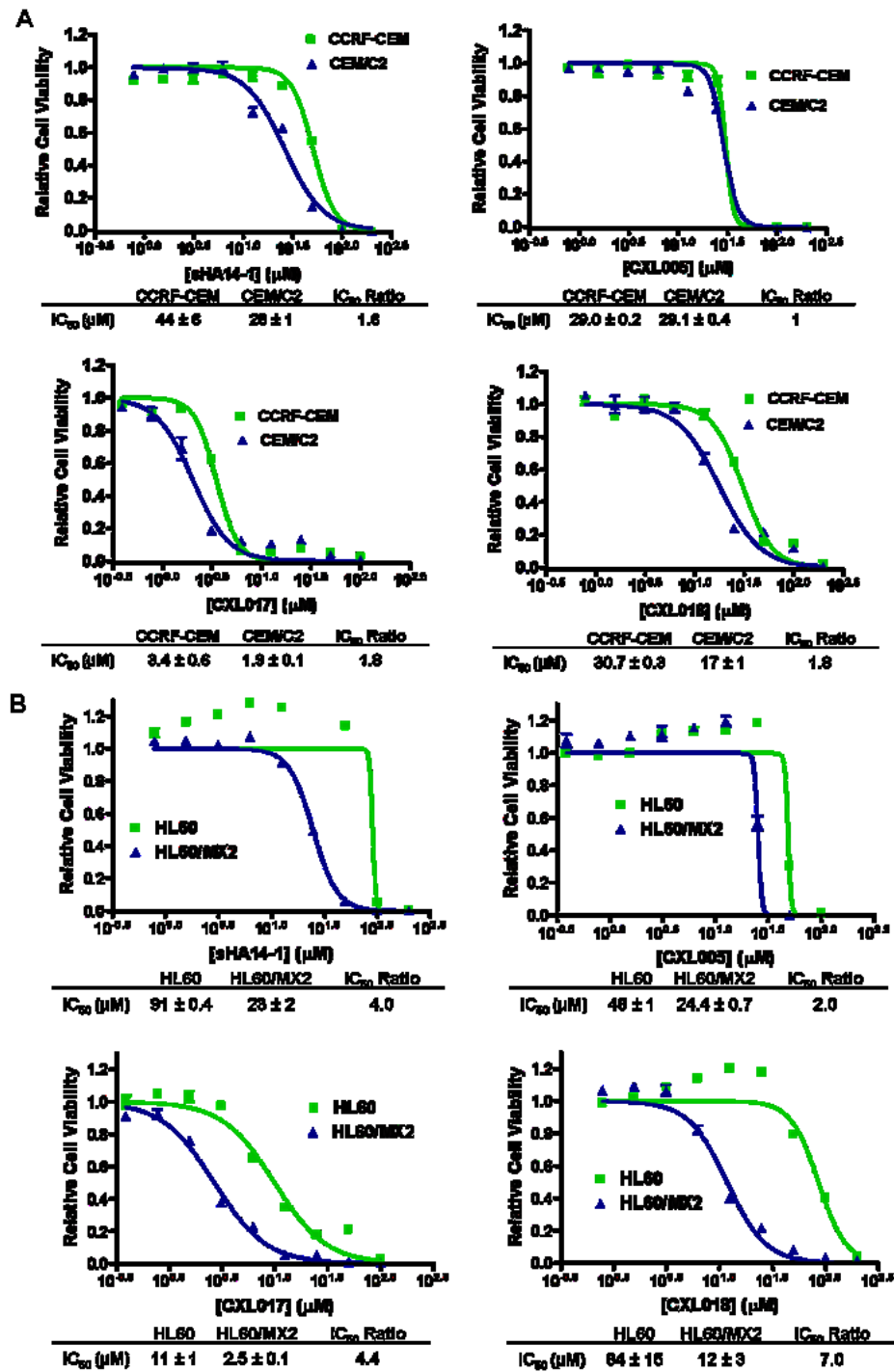
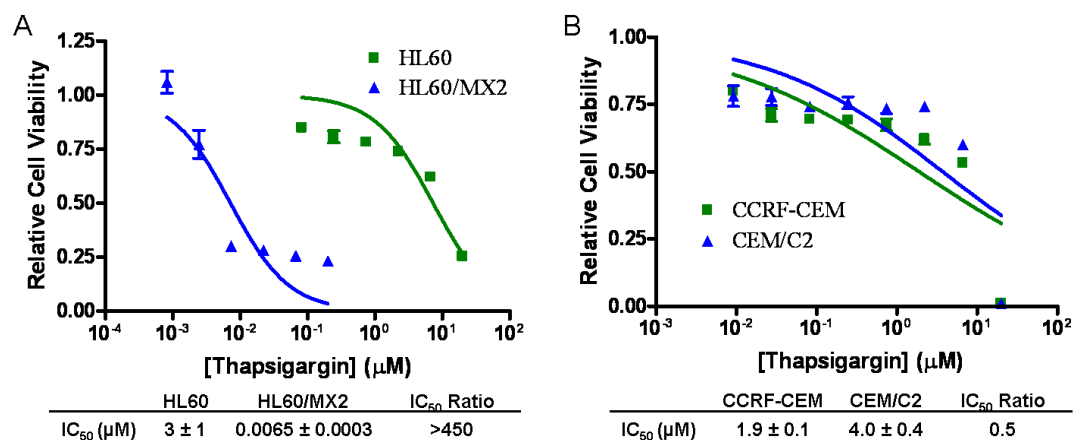


Figure 3.3 Cytotoxicity of sHA14-1 and analogs in HL60, HL60/MX2, CEM-CCRF, and CEM/C2: 48 hour cytotoxicity of given compounds in A) CEM-CCRF and CEM/C2 cells and in B) HL60 and HL60/MX2 cells. Curves are representative of at least duplicate data while IC<sub>50</sub> values are mean ± SD.



**Figure 3.4 Cytotoxicity of thapsigargin in HL60, HL60/MX2, CCRF-CEM, and CEM/C2 cells.** 48 hour cytotoxicity of given compounds in A) HL60 and HL60/MX2 cells and in B) CEM-CCRF and CEM/C2 cells. Curves are representative of at least duplicate data while IC<sub>50</sub> values are mean ± SD. These values compare well with experiments performed by other members of the lab whose data are not included in the IC<sub>50</sub> determination.

### **3.2.3 Characterization of HL60/MX2 and CEM/C2**

In order to characterize the mechanism for the selective cytotoxicity observed with sHA 14-1, CXL005, CXL017, and CXL018, both resistant cell lines were characterized for their levels of Bcl-2 family proteins and compared against the corresponding parent cell line. Following multiple Western blots, it was revealed that neither drug resistant cell line overexpressed Bcl-2. This was concluded based on multiple repeats that displayed small variations in the level of Bcl-2, but not in a consistent manner. CEM/C2 cells, but not HL60/MX2 cells, had an increase in Bcl-X<sub>L</sub>, and both resistant cell lines overexpressed the anti-apoptotic protein Mcl-1 (Figure 3.5). Increased levels of Mcl-1 have been shown to play a large role in drug resistance in both acute myelogenous leukemia (AML)<sup>96</sup>, HL60/MX2 cells, and acute lymphoblastic leukemia (ALL)<sup>97</sup>, CEM/C2 cells. Therefore, it is possible that the overexpression of Mcl-1 is involved in the observed multidrug resistance in these cell lines.

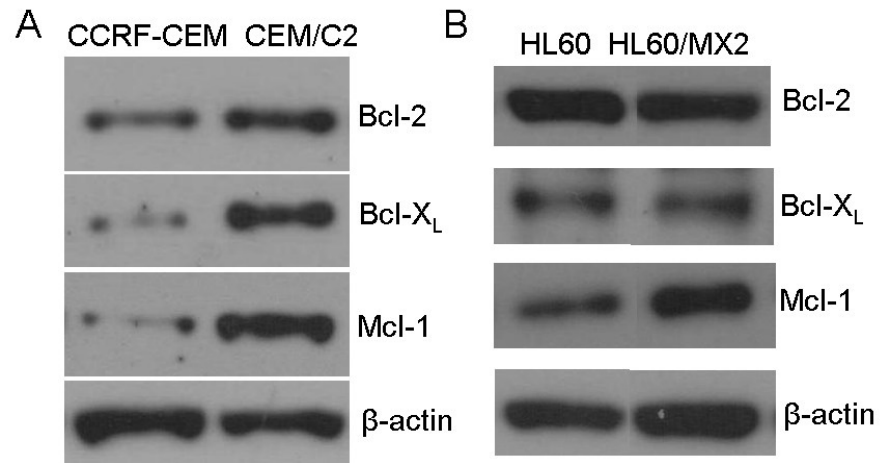


**Figure 3.5 Western blotting of anti-apoptotic Bcl-2 family proteins in CCRF-CEM, CEM/C2, HL60, and HL60/MX2 cell lines.** Results are representative of at least two independent experiments.

Since we hypothesize that the ability to induce calcium release was responsible for the observed selectivity towards HL60/MX2 cells, ER calcium levels were quantified for each cell line. When compared to HL60 cells, HL60/MX2 cells released much higher levels of calcium into the cytoplasm upon treatment with thapsigargin, as measured with Fura-2 (Figure 3.6 B), supporting our hypothesis. On the other hand, CEM/C2 cells released the same amount of calcium as CCRF-CEM cells (Figure 3.6 A). Cytoplasmic calcium increases can result in mitochondrial membrane depolarization leading to the release of cytochrome c and subsequent cell death.<sup>98</sup> Since HL60/MX2 cells have greater calcium release upon thapsigargin treatment, it is likely that the threshold is reached at lower concentrations than in HL60 cells of thapsigargin resulting in the observed selectivity. In the CEM/C2 cells, no selectivity is observed with thapsigargin treatment because the calcium content is the same in both the resistant and parental cell lines.

Protein levels of SERCA 2 and 3 were then measured in order to determine if the cause for increased ER calcium content in HL60/MX2 cells was from an overexpression of SERCA. SERCA isoforms 2 and 3 were chosen to be investigated based on reported tissue distribution. SERCA2b is the major isoform and is found in almost all tissues while SERCA3 is predominantly found in hematological cells.<sup>99</sup> SERCA1, on the other hand, is found primarily in muscle tissue.<sup>28</sup> Results showed that both SERCA 2 and 3 were up-regulated in the HL60/MX2 cell line when relative to HL60 (Figure 3.6 D). Conversely, CEM/C2 cells showed no difference in protein levels in either SERCA2 or SERCA3 (Figure 3.6 C). Since increased levels of SERCA would be expected to result

in raised levels of ER calcium content, these data supported the observations from the calcium release studies.



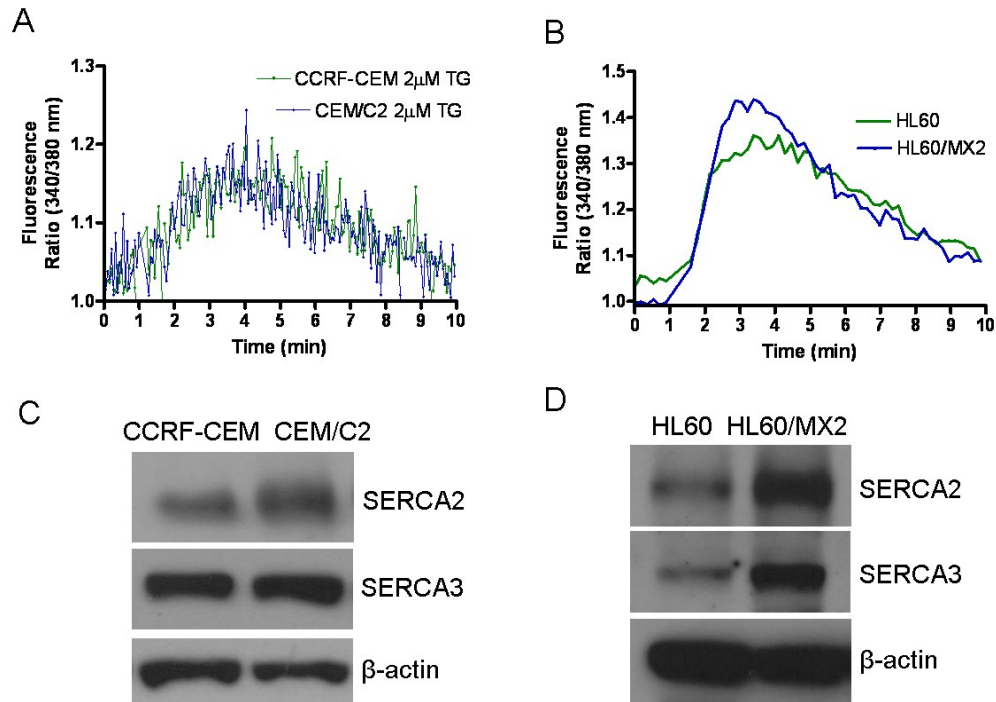


**Figure 3.6 Characterization of CCRF-CEM, CEM/C2, HL60, and HL60/MX2 cell lines for ER calcium content and SERCA protein levels.** ER calcium release induced by 2 $\mu$ M thapsigargin (TG) detected by Fura-2 in A) CCRF-CEM and CEM/C2 cells and B) HL60 and HL60/MX2 cells. Western blotting of SERCA2 and SERCA3 protein levels in A) CCRF-CEM and CEM/C2 cells and B) HL60 and HL60/MX2 cells.  $\beta$ -actin was used as a loading control. Results are representative of at least two independent experiments.

### **3.2.4 CXL017 overcomes drug resistance in multiple cell lines**

Given that CXL017 was the most potent analog and retained the favorable features of sHA 14-1, future studies were conducted using CXL017. In order to evaluate the scope of CXL017's ability to overcome drug resistance, several leukemia cell lines with reported drug resistance were acquired and tested using various therapies for multidrug resistance. Since multiple drug resistant cell lines were obtained with the same parental cell line, while testing the cell lines for multidrug resistance each resistant cell line was compared to the corresponding parent line from which it had been developed.

Other than HL60 and HL60/MX2 there were three other pairs of AML cell lines including HL60/ADR<sup>100</sup>, HL60/DNR<sup>100</sup>, and HL60/DOX<sup>101</sup> resulting from exposure to adriamycin (also known as doxorubicin), daunorubicin, and doxorubicin, respectively, were obtained. It is interesting to note that despite two cell lines being treated with the same compound and the third compound being very similar, they all displayed different profiles of multidrug resistance (Figure 3.7 A). The HL60/ADR cell line was very similar to HL60/MX2 in its profile with cross-resistance to all three topoisomerase II inhibitors and collateral sensitivity to cytarabine. In addition to resistance to the topoisomerase II inhibitors, both the HL60/DNR and HL60/DOX cell lines were cross-resistant to vincristine as well. The only AML line showing resistance to cytarabine was HL60/DOX. These differences in cytotoxicity profiles could arise due to different treatment regimes or to natural variability in the way the cell lines became resistant to the same therapy. Both HL60/ADR and HL60/DNR are reported to overexpress the efflux

pump P-glycoprotein (P-gp),<sup>100</sup> which may account for the resistance to vincristine since it is a well-known P-gp substrate.<sup>102</sup>

Western blotting revealed several differences in protein expression patterns between the three cell lines (Figure 3.7 B). None of the resistant cell lines overexpressed SERCA2, and only HL60/ADR showed a significant overexpression of SERCA3. Amongst anti-apoptotic Bcl-2 family proteins, both the HL60/DNR and HL60/DOX overexpressed Mcl-1. None of the cell lines overexpressed Bcl-X<sub>L</sub>, but the HL60/ADR line showed a reduction in the protein level. Finally, both the HL60/DNR and HL60/ADR lines overexpressed Bcl-2 with the later having a much higher level, while levels of Bcl-2 protein were slightly down-regulated in HL60/DOX cells. These data demonstrate that each resistant cell line varies significantly in its drug sensitivity profile as well as protein expression.

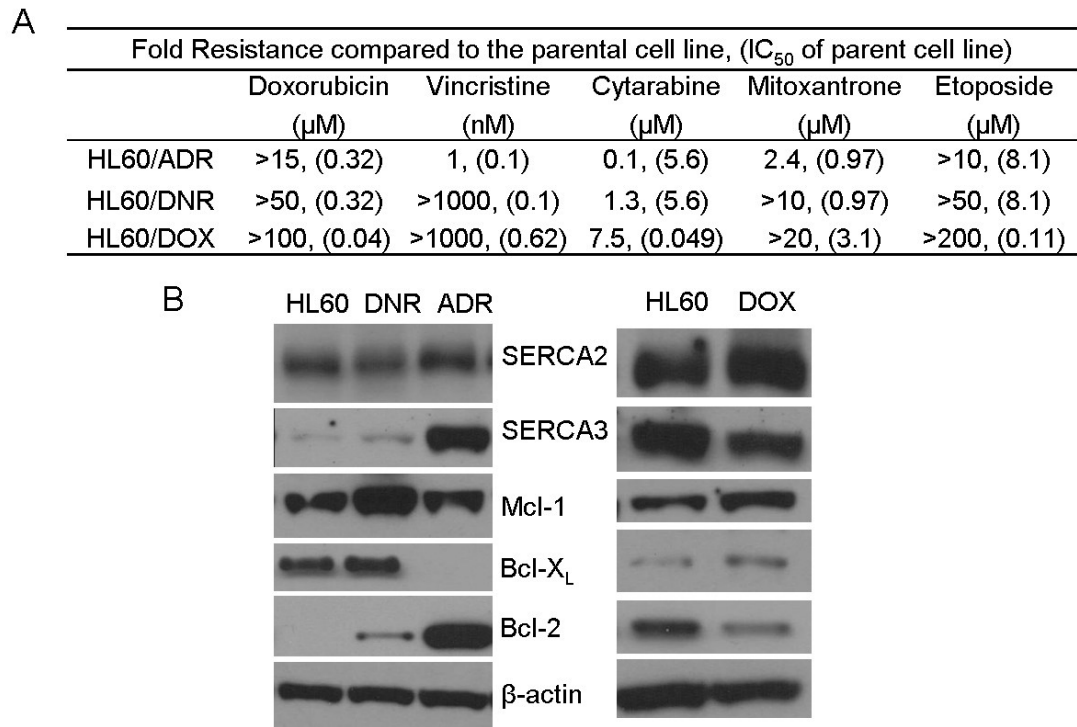


**Figure 3.7 Characterization of drug resistance in HL60, HL60/DNR, HL60/ADR, and HL60/DOX against standard therapies and protein levels.** A) 48 hour cytotoxicity of shown standard therapies in drug resistant cell lines. Data are given as the fold resistance with the  $IC_{50}$  value of the parental line shown in parentheses. B) Western blotting of various proteins in drug resistant cell lines. Data are representative of at least two independent experiments.

In addition to CEM/C2 cells, two other ALL cell lines were obtained, CEM/VM1-5 and CEM/VLB100. The CEM/VM1-5 cells were treated with teniposide, another topoisomerase II inhibitor, and were reported to be >150 fold resistant due to a reduction in topo II activity. CEM/VLB100 cells had been treated with vinblastine, an anti-microtubule agent, and resistance was at least partially the result of overexpression of P-gp.<sup>103</sup> The CEM/VM1-5 line displayed multidrug resistance to other topoisomerase II inhibitors, doxorubicin, etoposide, and mitoxantrone, as well as cytarabine, but was not resistant to vincristine (Figure 3.8 A). The CEM/VLB100 cell line was cross-resistant to the three topoisomerase II inhibitors listed previously as well as vincristine, likely resulting from the overexpression of P-gp, but showed no cross-resistance to cytarabine. Western blotting revealed an increase in SERCA3 expression in the CEM/VLB100 line but no changes in SERCA2 (Figure 3.8 B). Mcl-1 was barely detectable in either the parent or resistant cell lines while Bcl-X<sub>L</sub> expression was lower in both resistant cell lines. No changes in the Bcl-2 protein were observed. As with the AML cell lines, these cell lines demonstrated varied patterns of drug resistance as well as protein expression. These cell lines will continue to aid in evaluating the scope of CXL017's ability to overcome drug resistance in leukemia.

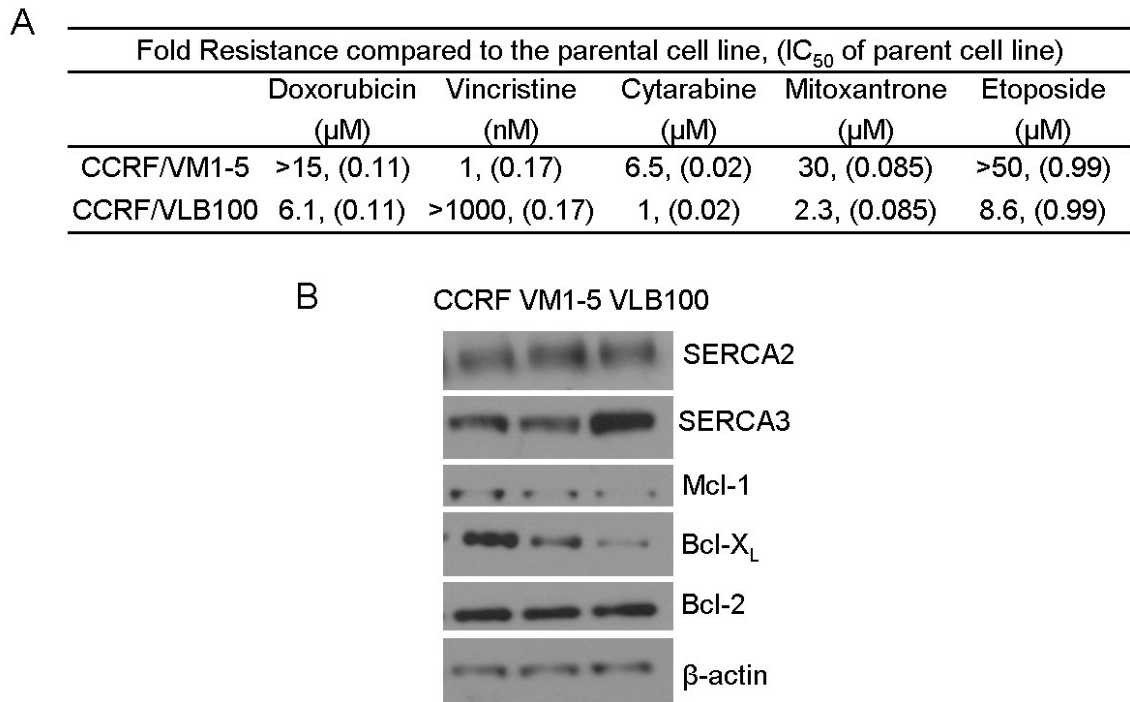


**Figure 3.8 Characterization of drug resistance in CCRF-CEM, CEM/VM1-5, and CEM/VLB100 against standard therapies and protein levels.** A) 48 hour cytotoxicity of shown standard therapies in drug resistant cell lines. Data are given as the fold resistance with the  $IC_{50}$  value of the parental line shown in parentheses. B) Western blotting of various proteins in drug resistant cell lines. Data are representative of at least two independent experiments

Finally, two CML resistant cell lines were characterized and tested for multidrug resistance. These included K562/DOX and K562/HHT300, resulting from treatment with doxorubicin and homoharringtonine, an anti-microtubule agent, respectively. Both of these cell lines were also reported to overexpress P-gp.<sup>104</sup> Both cell lines were found to be cross-resistant to all the therapies evaluated, displaying the greatest extent of multidrug resistance among all the cell lines tested (Figure 3.9 A). Both cell lines had reduced expression of SERCA3 protein and little change in the levels of SERCA2. With respect to the Bcl-2 family proteins, little change was observed with the exception that K562/HHT300 cells overexpressed Bcl-2 while both the parent and K562/DOX cells had undetectable levels (Figure 3.9 B).

A

	Fold Resistance compared to the parental cell line, (IC <sub>50</sub> of parent cell line)				
	Doxorubicin ( $\mu$ M)	Vincristine (nM)	Cytarabine ( $\mu$ M)	Mitoxantrone ( $\mu$ M)	Etoposide ( $\mu$ M)
K562/DOX	>10, (0.44)	>1000, (0.1)	1.5, (14)	5.1, (0.51)	>15, (2.3)
K562/HHT300	>20, (0.44)	>1000, (0.1)	7, (14)	>10, (0.51)	>1000, (2.3)

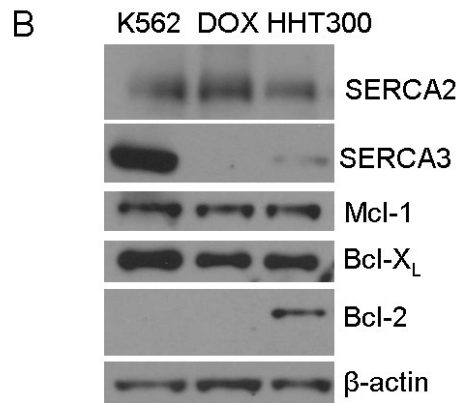


**Figure 3.9 Characterization of drug resistance in K562, K562/DOX, and K562/HHT300 against standard therapies and protein levels.** A) 48 hour cytotoxicity of shown standard therapies in drug resistant cell lines. Data are given as the fold resistance with the IC<sub>50</sub> value of the parental line shown in parentheses. B) Western blotting of various proteins in drug resistant cell lines. Data are representative of at least two independent experiments



This compilation of cell lines has a wide range of drug resistant properties and creates an effective set to test the scope of CXL017's ability to overcome drug resistance. Importantly, several of the cell lines overexpress P-gp and would indicate whether or not CXL017 was a substrate for the efflux pump as well. If CXL017 is a P-gp substrate, it should have a similar resistance pattern to vincristine, a substrate for P-gp. Upon 48 hour treatment with CXL017, none of the resistant cell lines tested revealed cross-resistance (Table 3.2). These results suggest that CXL017 can overcome drug resistance resulting from varied sources. This is an important feature for any compound that is aimed at targeting drug resistance because, as indicated by the panel of drug resistant lines tested herein, there are multiple mechanisms at play in the formation of resistance even to a single therapy. Another important implication is that CXL017 is not a substrate for P-gp as none of the cell lines overexpressing P-gp displayed resistance. However, given the varied levels of protein changes observed in these cell lines, it remains unclear how CXL017 is overcoming drug resistance. There is not a clear trend in either SERCA levels or Bcl-2 family protein changes, suggesting CXL017 may target different pathways depending on the cell line or may target an entirely different protein.

As a comparison to CXL017, cell lines were evaluated with ABT-737 and thapsigargin as well. Also included was isatin- $\beta$ -thiosemicarbazone, a compound reported to selectively target cell lines overexpressing P-gp.<sup>105</sup> Several of the cell lines were slightly cross-resistant to ABT-737 and only CEM/VLB100 was collaterally sensitive (Table 3.2). As expected, cell lines that were reported to overexpress P-gp were found to be collaterally sensitive to isatin- $\beta$ -thiosemicarbazone, while no difference in

potency was observed in cells lacking overexpression of P-gp. Thapsigargin was the most susceptible to cross-resistance with 5 of the 7 cell lines having some resistance, three with greater than 10-fold. Markedly, ABT-737 and thapsigargin suffer from drug resistance at a much higher frequency than CXL017, suggesting these compounds have limited applications for the treatment of drug resistant leukemia.

Fold Resistance compared to the parental cell line, (IC <sub>50</sub> of parent cell line)				
	CXL017 (μM)	ABT-737 (μM)	Isatin (μM)	Thapsigargin (μM)
HL60/ADR	0.4, (12.2)	4.5, (10.5)	0.47, (31)	1.0, (0.078)
HL60/DNR	0.8, (12.2)	4.9, (10.5)	0.64, (31)	>50, (0.078)
HL60/DOX	0.5, (4.5)	19.7, (0.76)	1.0, (6.8)	>50, (0.007)
CCRF/VM1-5	ND	2.2, (1.2)	2.1, (14)	1.0, (0.31)
CCRF/VLB100	0.9, (3.9)	0.3, (1.2)	0.66, (14)	7.7, (0.31)
K562/DOX	1.1, (9.1)	2.7, (35)	0.47, (27)	4.2, (0.17)
K562/HHT300	0.75, (9.1)	2.3, (35)	0.43, (27)	>10, (0.17)

**Table 3.2 Cytotoxic evaluation of CXL017, ABT-737, isatin-β-thiosemicarbazone, and Thapsigargin in drug resistant cell lines.** Data are given as the fold resistance with the IC<sub>50</sub> value of the parental line shown in parentheses. 48 hour cytotoxicity. ND is not determined.

### 3.2.5 NCI-60 Testing

In order to further evaluate CXL017, the compound was submitted to the NCI-60 human tumor cell line anticancer drug screen.<sup>106</sup> The screen was developed in the 1980s and has been used for testing novel compounds in an attempt to identify drug candidates as well as for determining possible molecular targets through comparison to other compounds with known mechanisms. CXL017 was found to have a mean GI<sub>50</sub> value of 1.04  $\mu$ M across the whole panel, which includes leukemia, non-small cell lung, colon, central nervous system, melanoma, ovarian, renal, prostate, and breast cancer cell lines. The highest level of activity for CXL017 was in leukemia, colon cancer, and melanoma, while CXL017 showed the least amount of activity in non-small cell lung cancer and ovarian cancer (Table 3.3). COMPARE is an algorithm used to identify similarities between a database of compounds and a “seed” compound, in this case CXL017. The results from this analysis showed that CXL017 had limited correlation with other agents, again suggesting CXL017 has a unique mechanism.

**Table 3.3 Cytotoxicity of CXL017 in  $\mu\text{M}$  across a panel of 60 cancer cell lines from NCI.**

<b>Panel/cell lines</b>	<b>GI<sub>50</sub> (<math>\mu\text{M}</math>)</b>	<b>Panel/cell lines</b>	<b>GI<sub>50</sub> (<math>\mu\text{M}</math>)</b>
<b>Leukemia</b>		<b>Melanoma</b>	
HL-60(TB)	0.35	UACC-62	0.55
K-562	0.39	M14	0.55
SR	0.45	LOX IMVI	0.72
CCRF-CEM	0.81	SK-MEL-5	0.89
MOLT-4	0.80	SK-MEL-2	1.4
RPMI-8226	1.9	SK-MEL-28	2.6
<b>Non-Small Cell Lung Cancer</b>		UACC-257	12
NCI-H460	0.54	<b>Ovarian Cancer</b>	
NCI-H522	0.62	OVCAR-3	0.32
HOP-62	0.89	NCI/ADR-RES	0.49
A549/ATCC	1.2	IGROV1	0.93
EKVX	1.3	SK-OV-3	1.4
HOP-92	1.4	OVCAR-8	3.8
NCI-H23	2.0	OVCAR-5	4.1
NCI-H322M	4.0	OVCAR-4	5.2
NCI-H226	4.4	<b>Renal Cancer</b>	
<b>Colon Cancer</b>		A498	0.36
HT29	0.39	CAKI-1	0.71
HCT-116	0.42	UO-31	1.4
SW-620	0.49	ACHN	1.5
KM12	0.50	786-0	2.3
HCT-15	0.55	RXF 393	2.5
COLO 205	1.2	SN12C	2.8
HCC-2998	2.5	TK-10	3.4
<b>CNS Cancer</b>		<b>Prostate Cancer</b>	
SF-295	0.48	PC-3	0.83
SF-539	0.49	DU-145	1.5
U251	0.63	<b>Breast Cancer</b>	
SF-268	1.1	HS 578T	0.32
SNB-75	1.3	MCF7	0.45
SNB-19	1.9	MDA-MB-468	0.67
<b>Melanoma</b>		BT-549	0.77
MDA-MB-435	0.27	MDA-MB-231/ATCC	1.5
MALME-3M	0.39	T-47D	3.7

### 3.2.6 *In vivo* targeting of drug resistance

CXL017 was tested in a xenograft mouse model at a dose of 100 mg/kg/day to determine whether it was effective *in vivo*. Mice were subcutaneously injected with HL60 or HL60/MX2 cells in either the left or right flank, respectively. Based on previously determined pharmacokinetic studies, the dose of 100 mg/kg/day was chosen as a safe and tolerable dose with maximum serum concentrations reaching  $\sim 4 \mu\text{M}$ . Once the tumors had grown to a size of  $40 \text{ mm}^3$ , CXL017 was administered by intraperitoneal injection 6 days a week for 3 weeks. Throughout the time course, body weights of the individual mice were closely monitored. There was no effect on the body weight due to treatment with CXL017. The average tumor size was used to measure the effectiveness of CXL017. There was no difference observed in the size of tumors where HL60 cells had been injected when comparing the treated mice with control mice (Figure 3.10 A). However, there was a significant reduction in tumor growth where HL60/MX2 cells had been injected (Figure 3.10 B). This indicates that HL60/MX2 cells are collaterally sensitive towards CXL017 *in vivo* as well. The results also demonstrate that CXL017 can be effective *in vivo*, although at a very high dose. Poor bioavailability is likely the main reason as serum concentrations did not reach a high enough level to reduce HL60 tumor growth.

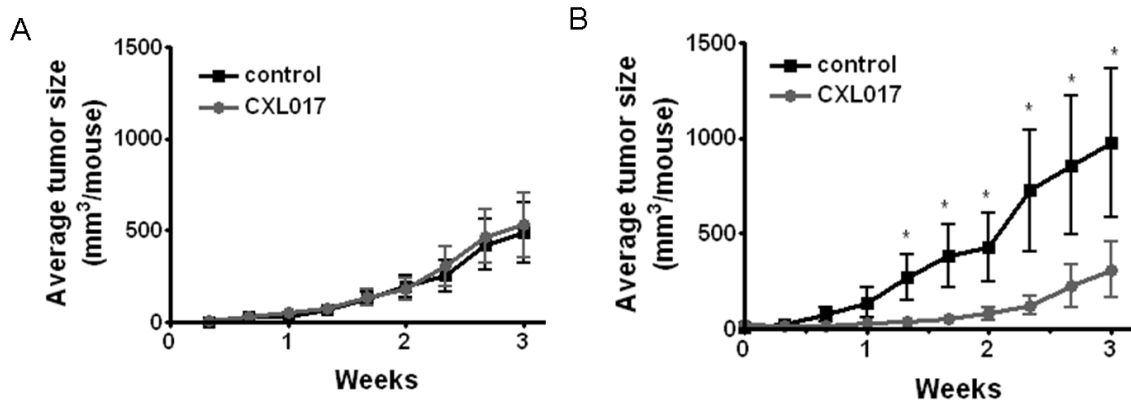


**Figure 3.10** *In vivo* treatment of SCID mice with 100mg/kg CXL017. A) HL60 tumor growth in SCID mice. B) HL60/MX2 tumor growth in SCID mice. \* indicated statistical significance from vehicle control p-value < 0.05

### 3.3 Conclusion

Drug resistance is a major hurdle in the treatment of cancer, and compounds that are able to overcome resistance are of high importance both in the clinic and as tools to elucidate possible new targets and mechanisms to target resistant cells. Initially, two sets of parent and drug resistant lines were characterized for multi-drug resistance. Following testing with several therapies, HL60/MX2 and CEM/C2 cells were subjected to treatment with several analogs of sHA 14-1 as well as thapsigargin and ABT-737. Both HL60/MX2 and CEM/C2 exhibited cross resistance to several topoisomerase II inhibitors. The analogs of sHA 14-1 demonstrated selectivity towards both of the resistant cell lines when compared to the corresponding parent cells. The selectivity in HL60/MX2 cells appeared to correlate with how well each analog caused calcium release. These analogs also performed favorably when compared to thapsigargin and ABT-737. From these studies, a new lead compound emerged, CXL017, with low micromolar potency. This compound remained as selective as sHA 14-1 and was >20-fold more potent. Armed with this new and more potent compound, several other resistant pairs of cell lines were acquired and evaluated against several standard therapies in addition to CXL017, ABT-737, and thapsigargin. None of the evaluated cell lines demonstrated resistance to CXL017, and most of them were collaterally sensitive to CXL017. This suggests that CXL017 could be very useful for the study of drug resistance. Additionally, CXL017's cytotoxicity profile compared favorably to all of the other therapies employed in the testing. Using the NCI-60 drug screen, it was discovered that CXL017 displays good activity across a wide range of cell lines and has a unique



mechanism of action. Finally, it was demonstrated that CXL017 did have *in vivo* activity and was able to target HL60/MX2 tumors more effectively than HL60 within the same mouse. In the next chapter, the mechanism of action for CXL017 will be further explored.

### **3.4 Experimental Procedures**

#### **3.4.1 Cell Cultures**

HL60, HL60/MX2, CCRF-CEM, and CCRF-CEM/C2 were purchased from ATCC. K562, K562/HHT300, K562/DOX, HL60/ADR, and HL60/DNR cell lines were provided by Dr. Tang. HL60 and HL60/DOX cell lines were provided by Dr. Ganapathi. CCRF-CEM, CCRF-CEM/VM-1-5 and CCRF-CEM/VLB100 were provided by Dr. Beck. HL-60 cell line was grown in IMDM Glutamax media supplemented with 20% FBS. All other cell lines were grown in RPMI 1640 purchased from ATCC, supplemented with 10% FBS at 37°C with 5% CO<sub>2</sub> in air atmosphere.

#### **3.4.2 Cytotoxicity measurements**

The *in vitro* cytotoxicity was determined by the compounds ability to inhibit the growth of tumor cells. Measurements were performed using the CellTiter-Blue Cell Viability Assay kit from Promega (Madison, Wisconsin). In brief, the tumor cells were plated in a 96-well plate at a density of  $1 \times 10^4$  cells/well. The cells were treated with a series of 3-fold dilutions of test compounds with final concentrations of 1% DMSO in final volume. Cells treated with 1% DMSO served as controls. Cells were incubated for 48 hours at 37 °C, and the relative viability was measured using CellTiter-Blue. IC<sub>50</sub> values were determined by plotting the relative viability by the log of drug concentration

and fitting to a sigmoidal dose-response (variable slope) model in GraphPad Prism software (San Diego, CA).

### **3.4.3 Western blotting**

Cells were lysed in RIPA buffer (10mM Tris-HCl pH=8.0, 150mM NaCl, 1mM EDTA, 1% Igebal, 0.5% Sodium deoxycholate, and 0.1% Sodium Dodecyl Sulfate) containing 1% protease inhibitor from Sigma (St. Louis, MO). Cells were kept on ice for 20 minutes in lysis buffer after vortexing, and then centrifuged at 17 x g for 15 minutes. The supernatant was collected, and protein concentration was determined by bicinchoninic acid (BCA) assay (Pierce, ThermoScientific, Rockford, IL). Following quantification, 40 µg of total protein was mixed with loading dye and sample reducing agent (NuPAGE, Invitrogen, Carlsbad, CA), boiled for 5 minutes, and separated by gel electrophoresis at 150 V on a NuPAGE 4-12% Bis-Tris Gel (Invitrogen, Carlsbad, CA). Proteins were then transferred at 40 V to a polyvinylidene difluoride (PVDF) membrane from Millipore (Billerica, MA). Membranes were blocked in 5% milk in tris buffered saline TWEEN20 (TBST) for 1 hour at room temperature followed by incubation with primary antibody overnight at 4 °C. Membranes were washed 3 times in TBST for 5 minutes and then incubated in the appropriate HRP conjugated antibody (1:3000) for 3 hours at room temperature. Detection was performed using supersignal chemiluminescence system from Pierce (Rockford, IL). The SERCA2 IID8 (1:200), SERCA3 XL-6 (1:300), Mcl-1 S-19 (1:400), Bcl-X<sub>s/L</sub> S-18 (1:750), antibodies were from Santa Cruz Biotechnology, Inc. (Santa Cruz, CA) and used at the specified dilution. The

anti-Bcl-2 B3170 antibody (1:10,000), the anti- $\beta$ -actin (1:40,000) antibody, and secondary antibodies were from Sigma–Aldrich (St. Louis, MO).

#### **3.4.4 ER calcium measurements**

$1 \times 10^6$  cells/mL were incubated in medium containing 5  $\mu$ M Fura-2AM and 2.5 mM probenecid at room temperature in the dark for 1 h. The cells were washed with cold PBS and re-suspended at  $2 \times 10^6$  cells/mL in medium containing 2.5 mM probenecid. To a cuvette with 735  $\mu$ L media containing 100 mM EGTA and 2.5 mM probenecid was added 750  $\mu$ L of the cell suspension. The cell suspension was mixed by pipetting. The cell media contained a negligible amount of free calcium under this condition. After fluorescent readings were recorded for 1 min, 15  $\mu$ L of DMSO containing thapsigargin was added. Readings were obtained on a dual wavelength fluorometer (Cary Eclipse, Varian, Palo Alto, CA) with excitation wavelengths alternating between 340 and 380 nm and an emission wavelength of 510 nm.

#### **3.4.5 *In vivo* evaluation of CXL017 (Performed by Dr. Xing)**

For *in vivo* anticancer potential evaluation, female athymic nude mice obtained from Harland were maintained in a laminar airflow cabinet under pathogen-free conditions and used at 6 to 12 weeks of age. The protocol for animal experiments was approved by the Institutional Animal Care and Use Committee (IACUC) of the research animal resources facility at the University of Minnesota. Upon arrival, all mice were maintained on standard diet and housed in the pathogen-free animal quarters at the University of Minnesota Cancer Center. After one week of acclimation, HL60 cell ( $5 \times 10^6$  in 0.1 mL PBS:Metrigel (v/v 1:1)) were implanted subcutaneously into the left flank

of each mouse. At the same time, HL60/MX2 cells ( $5 \times 10^6$  in 0.1 mL PBS:Metrigel (v/v 1:1)) were implanted subcutaneously into the right flank of the same mouse. Formation of a bulla indicated a satisfactory injection. Tumors were measured three times a week with a caliper. Tumor volumes were calculated using the following formula:  $\frac{1}{2}(w_1 \times w_2 \times w_2)$  where  $w_1$  is the largest tumor diameter and  $w_2$  is the smallest tumor diameter. When tumors induced by HL60/MX2 reached  $40 \text{ mm}^3$ , mice were randomized into two groups with similar distribution in HL60/MX2 induced tumor size and bodyweight, ten mice each group. Mice in Group 1 were given carrier (PEG400:EtOH (v/v 2:1), 0.1 mL) alone via i.p. injection. Mice in Group 2 were given CXL017 (100 mg/kg of body weight). Treatment was once a day for three weeks. Mice were euthanized with  $\text{CO}_2$ , and tumors removed and weighed.

## CHAPTER 4

### 4. CXL017 Mechanism of Action

#### 4.1 Introduction

CXL017 has been shown to effectively and selectively target drug resistant leukemia cell lines with low micromolar potency, yet the mechanism by which this occurs was still unknown. Nine different multidrug resistant cell lines, with varying mechanisms of resistance, were all sensitive to treatment with CXL017. This property makes CXL017 an ideal candidate for further studies in order to overcome drug resistance. Based on previous knowledge of sHA 14-1 and the reported Bcl-2 inhibitor HA 14-1, several potential mechanisms for how CXL017 overcomes resistance existed. These included, 1) through a mechanism involving SERCA and ER stress similar to sHA 14-1, the parent compound to CXL017, which has been characterized to inhibit SERCA and cause ER stress<sup>107</sup>, 2) targeting of anti-apoptotic Bcl-2 proteins given that CXL017 originally came from the putative Bcl-2 inhibitor HA 14-1, and 3) a combination of the two pathways or an entirely new target yet to be identified. Given the previous data involving the cytotoxic profiles of ABT-737 and thapsigargin, scenario 3 seemed most likely to be true. In the previous chapter, results indicated CXL017 does not have the same selectivity/resistance profile as ABT-737, a well-known and characterized Bcl-2/Bcl-X<sub>L</sub> inhibitor<sup>79</sup>, or as thapsigargin, a very potent SERCA inhibitor<sup>31</sup>. Both of these compounds suffered from drug resistance in multiple cell lines. Nevertheless, SERCA and anti-apoptotic Bcl-2 family protein inhibition have been shown to be viable mechanisms in targeting drug resistance<sup>108, 109</sup>.

In this chapter, the possible mechanism by which CXL017 overcomes drug resistance in HL60/MX2 cells will be explored. HL60/MX2 cells were chosen for further investigation on the basis that they were the most well-defined and well-studied drug resistant cell line in our laboratory. CXL017 will be studied as a SERCA inhibitor and for its ability to cause ER stress. Next, genetic regulation of several possible targets will be undertaken, followed by studies using a probe molecule with the possibility of target identification through covalent modification and detection of target proteins.

## **4.2 Results and Discussion**

### **4.2.1 SERCA inhibition of CXL017 in HL60 and HL60/MX2 cell lines**

The first step towards defining the mechanism of action of CXL017 was to investigate its SERCA inhibition potential. It has previously been shown in chapter 2 that CXL017 caused similar levels of calcium release compared to sHA 14-1 in NALM-6 cells and that sHA 14-1 inhibited SERCA. However, CXL017 had not yet been characterized for its potential to inhibit SERCA. A coupled enzyme assay was used to determine CXL017 has a  $K_i$  value of 17.8  $\mu\text{M}$  with a maximal inhibition of 62% against SERCA1a (Figure 4.1A). Even though SERCA1a is mainly expressed in fast-twitch muscle fiber and has a slightly reduced calcium affinity and higher  $V_{\text{max}}$  compared to SERCA2b, the housekeeping form of SERCA,<sup>28</sup> it is commonly used in enzymatic assays due to ease of purification. The main structural difference between SERCA1a and SERCA2b is the c-terminal extended tail, which accounts for SERCA2b's higher affinity for calcium.<sup>110</sup> SERCA inhibition studies with sHA 14-1 support using SERCA1a as an acceptable model for SERCA2B inhibition, since sHA 14-1 demonstrated similar

inhibitory potential with both isoforms.<sup>107</sup> The results from this *in vitro* assay suggested that CXL017 is a partial SERCA inhibitor with moderate potency. The results also indicated CXL017 and sHA 14-1 have similar SERCA inhibition values (Figure 4.1B). Therefore, SERCA inhibition does not appear to account for the improved potency of CXL017 over sHA 14-1 given their comparable inhibition data and that the  $K_i$  value is well above the  $IC_{50}$  value of 2.5  $\mu$ M in HL60/MX2 cells.

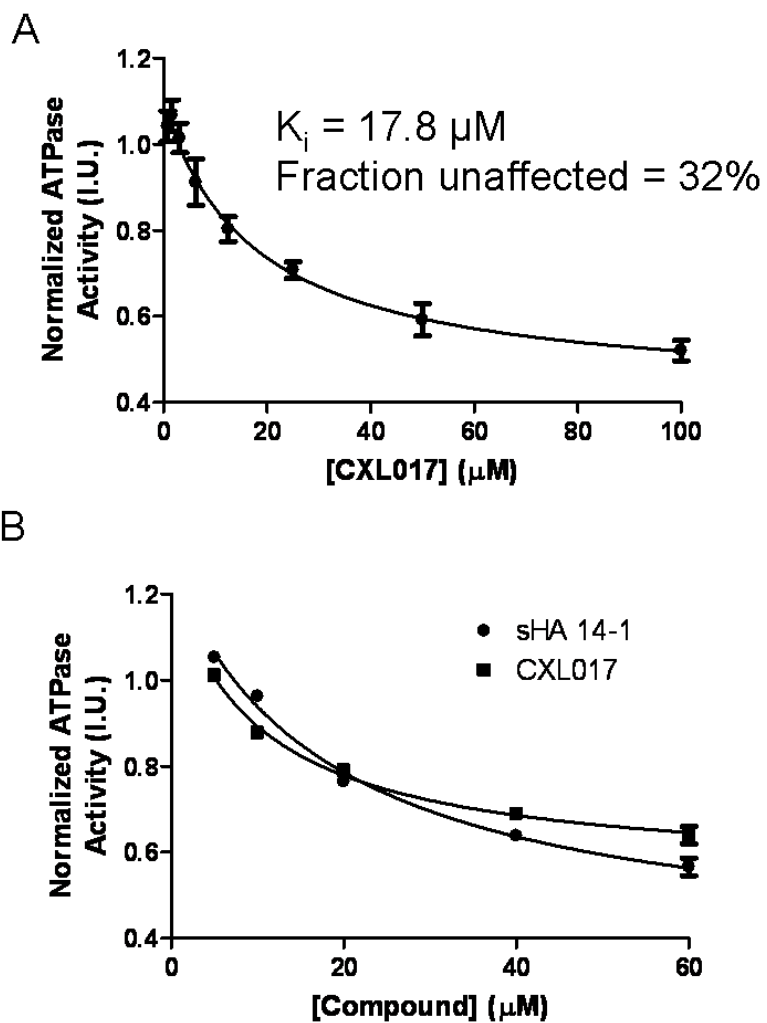


**Figure 4.1** SERCA1a inhibition by CXL017 and sHA 14-1. A) CXL017 inhibition of SERCA1a at a single calcium concentration of 3.981  $\mu\text{M}$  of free calcium. Fraction unaffected represents fractional  $V_{\text{max}}$  at saturating concentrations of CXL017. B) Comparison of CXL017 and sHA 14-1 inhibition in SERCA1a at 3.981  $\mu\text{M}$  free calcium. Curve fitting was done by GraphPad Prism using a partial inhibitory model.



Induction of ER calcium release by CXL017 in HL60 and HL60/MX2 cells was also studied. In both cell lines, sHA 14-1 was more effective in causing calcium release from the ER than CXL017 (Figure 4.2). Given that CXL017 had similar inhibition values against SERCA1a and caused similar calcium release in NALM-6 cells compared to sHA 14-1, it was surprising to observe such a difference in calcium release in HL60 and HL60/MX2 cells. In chapter 3 it was hypothesized that the extent to which a compound was selective towards HL60/MX2 cells correlated to the SERCA inhibition potential of the compound. This hypothesis was supported by the correlation of calcium release levels in NALM-6 cells with compound selectivity as well as the ability of thapsigargin to potently select for HL60/MX2 cells over HL60 cells; however, the current data measuring calcium release in HL60/MX2 cells does not fully support that hypothesis. Since cytotoxicity is measured after a treatment period of 48 hours while calcium release measurements are monitored for only 10 minutes, the possibility that calcium release is important to selectivity cannot be ruled out from this set of experiments, however. The data involving thapsigargin treatment in HL60 and HL60/MX2 cells is still strongly indicative of mechanism involving SERCA inhibition and ER stress in the collateral sensitivity of HL60/MX2 cells towards thapsigargin (Figures 3.3 and 3.4). In addition preliminary cytotoxicity testing with two other known SERCA inhibitors has shown HL60/MX2 cells are also collaterally sensitive to those compounds. Finally, it can be concluded that SERCA inhibition is insufficient in explaining the improved cytotoxicity of CXL017 over sHA 14-1 since they were equipotent SERCA inhibitors.

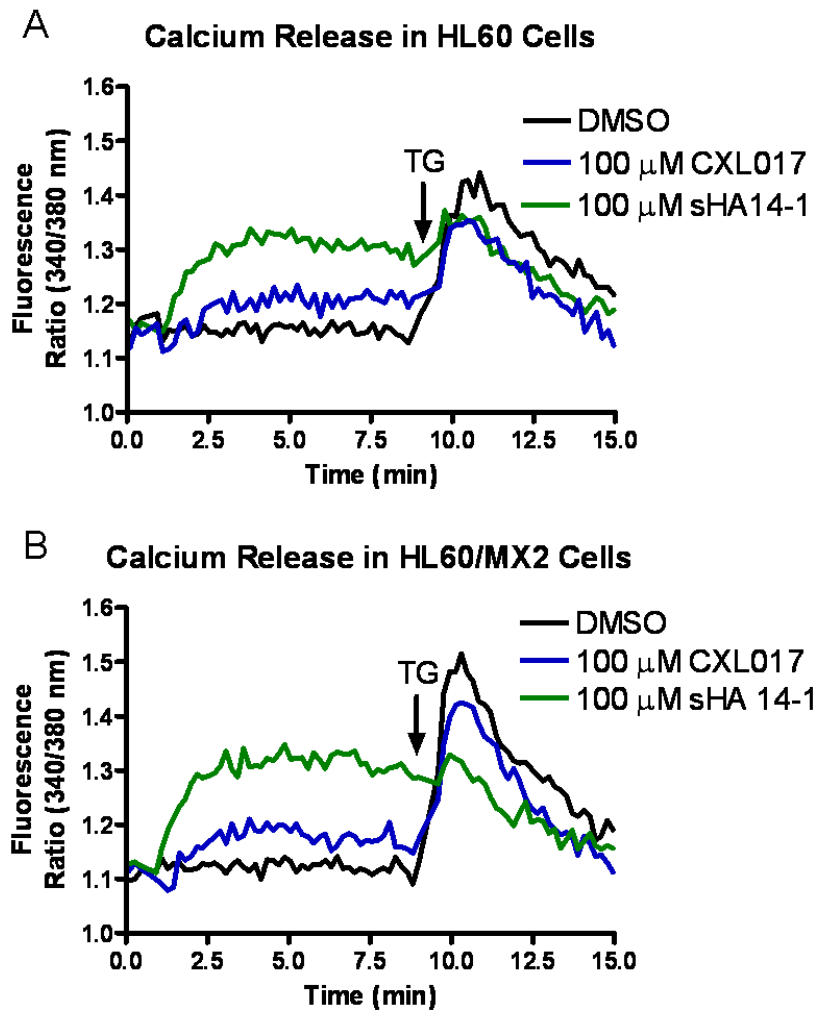


**Figure 4.2 ER calcium release of CXL017 and sHA 14-1 in HL60 and HL60/MX2 Cells.** ER calcium release detected by Fura-2 in A) HL60 cells and B) HL60/MX2 cells. After 1 minute of collecting baseline readings, cells were treated with either DMSO (Black lines), 100  $\mu$ M CXL017 (Blue lines), or 100  $\mu$ M sHA 14-1 (Green lines) for 8 minutes, when thapsigargin (TG) was added to measure the remaining levels of ER calcium. Data is representative of two independent experiments.

#### **4.2.2 Knockdown of SERCA2, SERCA3, Bcl-2, and Mcl-1 in HL60/MX2 cells**

In an effort to resolve the function individual protein changes may have regarding the selectivity of CXL017 and thapsigargin in HL60/MX2 cells, specific protein knockdown was required. Therefore, RNA interference (RNAi) was used to create stable knockdown cell lines that would be studied for changes in sensitivity to CXL017, thapsigargin, or mitoxantrone. Short hairpin RNAs (shRNAs) were transduced into HL60/MX2 cells via lentivirus followed by puromycin selection to develop stably expressing shRNA cells. Once transduced, the shRNA becomes incorporated into the host cells genome, is transcribed, and degrades the mRNA of the target protein, which results in protein reduction. Lentiviruses were purchased containing shRNAs targeting SERCA2, SERCA3, Bcl-2, or Mcl-1. These proteins were chosen on the basis of several previous findings. As demonstrated in chapter 3, both SERCA2 and SERCA3 were greatly overexpressed in HL60/MX2 cells compared to HL60 cells. It was hypothesized that this overexpression led to the increased ER calcium levels in HL60/MX2 cells and resulted in the collateral sensitivity observed towards thapsigargin; therefore knockdown of SERCA2 or SERCA3 in HL60/MX2 cells should result in a lowering of ER calcium and resistance to thapsigargin. Bcl-2 was chosen to knockdown because HA 14-1 was reported as a Bcl-2 antagonist<sup>111</sup>. Finally, Mcl-1 was chosen for knockdown due its overexpression in HL60/MX2 cells. After selecting the cells with puromycin, cells were collected, lysed, and analyzed by Western blot for successful protein knock-down. Successful knockdown of SERCA2, SERCA3, and Bcl-2 was achieved (Figure 4.3),

while knockdown of Mcl-1 was unsuccessful despite the use of several different shRNA constructs from multiple vendors.

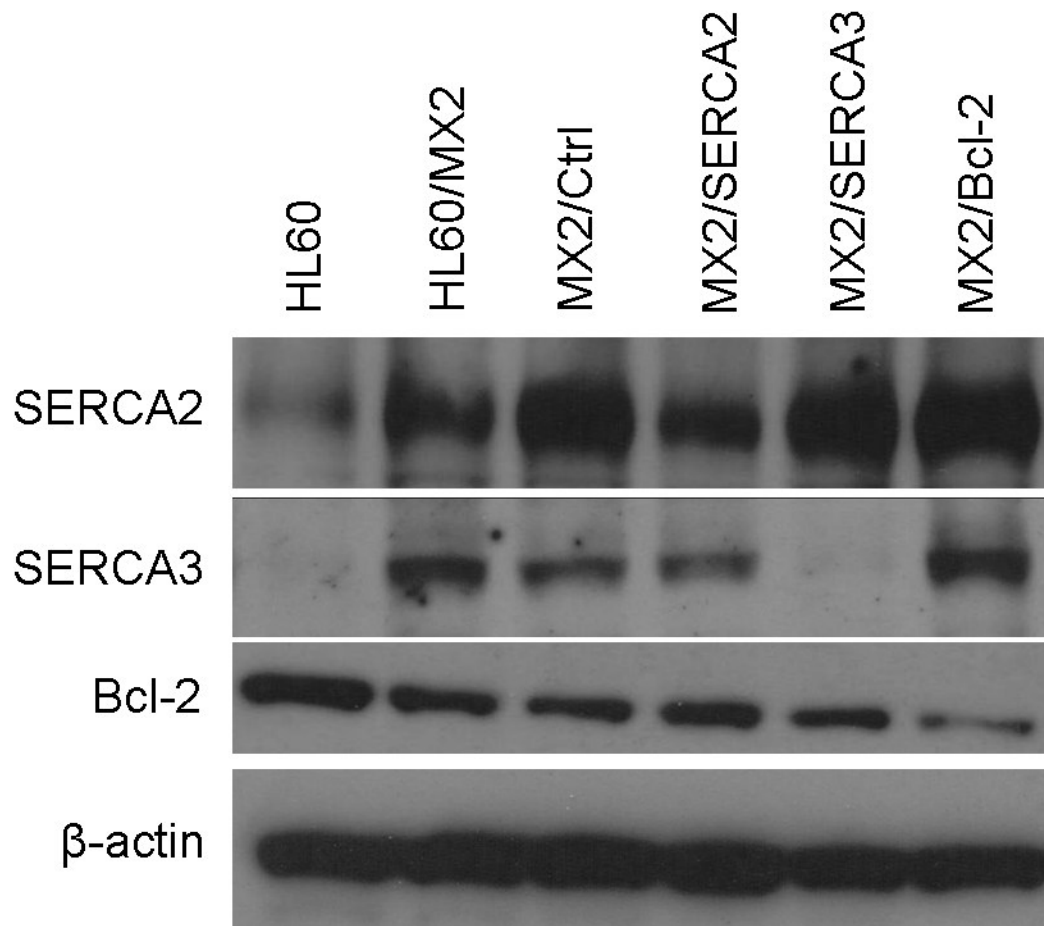


**Figure 4.3 Western Blotting of transduced HL60/MX2 cell lines.** HL60/MX2 cells were stably transduced with shRNA targeted to SERCA2, SERCA3, and Bcl-2. MX2/Ctrl cells were transduced with scrambled shRNA.  $\beta$ -actin was used as a loading control. Western blots are representative of two independent experiments.

Following knockdown, CXL017, thapsigargin, and mitoxantrone were assayed for their cytotoxicity in the modified cell lines. Knockdown of SERCA2 and SERCA3 was predicted to result in acquired resistance of HL60/MX2 cells to CXL017 and thapsigargin, since knockdown of SERCA may lower calcium levels in the ER, while not affecting the cytotoxicity of mitoxantrone. Successful knockdown of Bcl-2 was expected to result in increased sensitivity to all treatments, as Bcl-2 is an anti-apoptotic protein with a general mechanism of action in drug resistance. However, the  $IC_{50}$  values of all three compounds remained unchanged in all of the protein knockdown cell lines. To further evaluate the effects of each compound on the cell lines, several concentrations close to the  $IC_{50}$  value of each compound were evaluated. Any change in drug sensitivity resulting from the knockdown is most likely to be revealed in this range. Again, no changes were observed in relative cell viability (Figure 4.4), indicating that downregulating any one of these proteins individually is not enough to induce drug resistance or sensitivity to any of the agents evaluated. The failure of SERCA2 or SERCA3 individual knockdown to induce resistance could result from the overexpression of the remaining isoform as, upon knockdown of either SERCA2 or SERCA3, the protein levels of the other isoform remain unchanged (Figure 4.3). Another possible explanation is that while the protein was knocked down, calcium levels may not have been lowered. In this case though, HL60/MX2 SERCA2 or SERCA3 knockdown cells may have been more sensitive to thapsigargin as cells would have had difficulty maintaining the higher levels of ER calcium in HL60/MX2 cells. Bcl-2 knockdown effects may have been

limited by other anti-apoptotic Bcl-2 family proteins taking over its role, such as the overexpression of Mcl-1.

The failure to produce stable knockdown of Mcl-1 in HL60/MX2 cells may be due to the importance of Mcl-1 to cell survival. During attempts to knockdown the protein, it was observed that cells transduced with shRNA targeting Mcl-1 compared to scrambled shRNA were less viable even before puromycin selection. It is hypothesized that knockdown of Mcl-1 results in cell death in the HL60/MX2 cell line; therefore, only cells that incorporated the puromycin resistant gene without the Mcl-1 targeted shRNA survived the selection process.

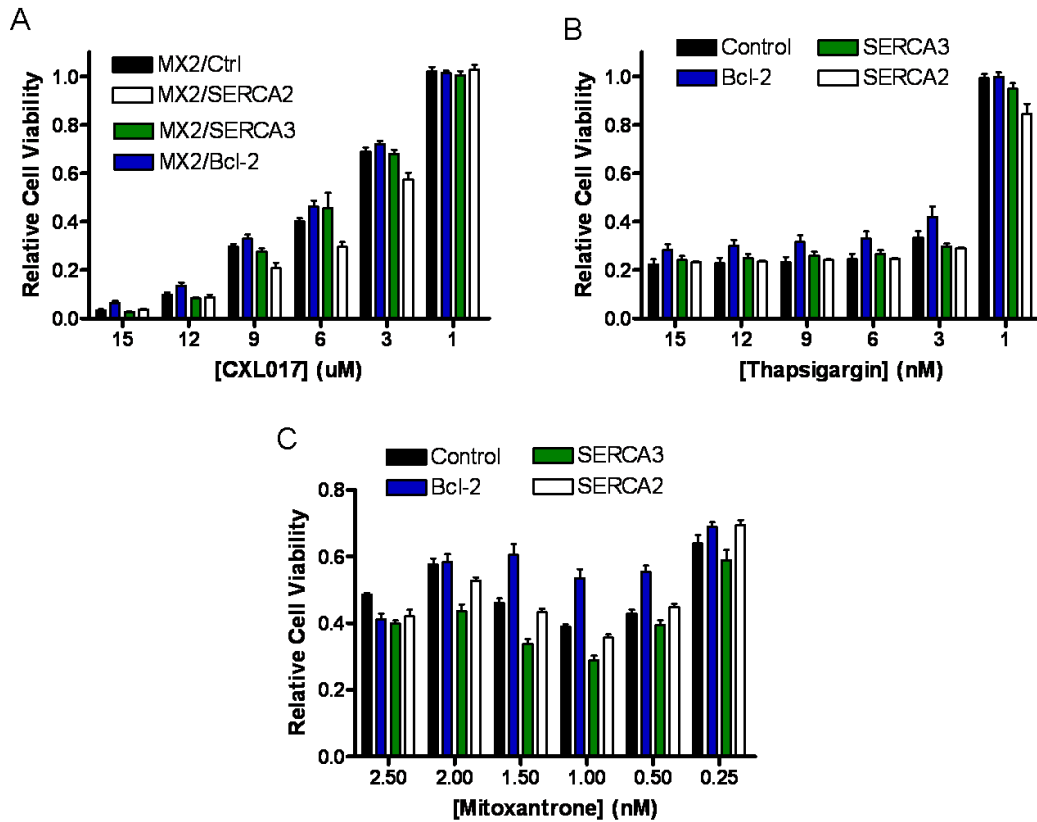


**Figure 4.4 Cytotoxicity of CXL017, thapsigargin, and mitoxantrone in HL60/MX2 transduced cell lines.** 48 hour cytotoxicity of A) CXL017, B) Thapsigargin, and C) Mitoxantrone was measured in stably transduced cells at the shown concentrations. The data shown is the average cell viability across three independent experiments each performed in triplicate.



### 4.2.3 Photoaffinity probe labeling of proteins studies

Photoaffinity protein labeling experiments were also attempted to elucidate possible binding targets of CXL017. Before photoaffinity labeling experiments could begin, a photoreactive analog of CXL017 capable of covalently modifying proteins with specific interactions had to be synthesized. This was achieved by attaching an azide group to the 3' position of the 6-phenyl ring of sHA 14-1 (Figure 4.5). Phenyl azides such as this one can be photoactivated using 366 nm UV light, which results in formation of a reactive nitrene that can undergo hydrogen insertion resulting in covalent modification of target proteins<sup>112</sup>. The ethyl esters of sHA 14-1 were also replaced by propargyl esters in the probe molecule, resulting in CXL037 (Figure 4.5). This substitution allows for “click” chemistry to be performed between the alkyne of the probe and an aliphatic azide.<sup>113</sup> Either Rhodamine-azide or biotin-azide was used as the second substrate for the “click” reaction. Once CXL037 is covalently attached to Rhodamine, labeled proteins can be detected through in-gel fluorescence with an excitation of 532 nm and an emission of 580 nm, while the biotin moiety can be detected using horseradish peroxidase (HRP) conjugated streptavidin following transfer of the labeled proteins to a PVDF membrane (Figure 4.6).

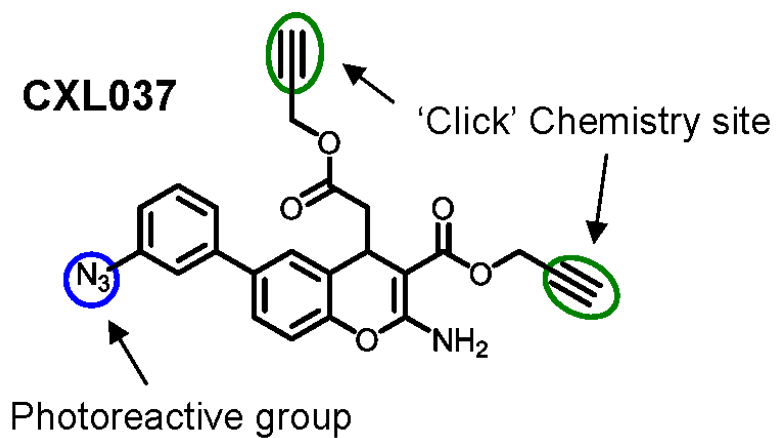


Figure 4.5 Structure of probe molecule, CXL037

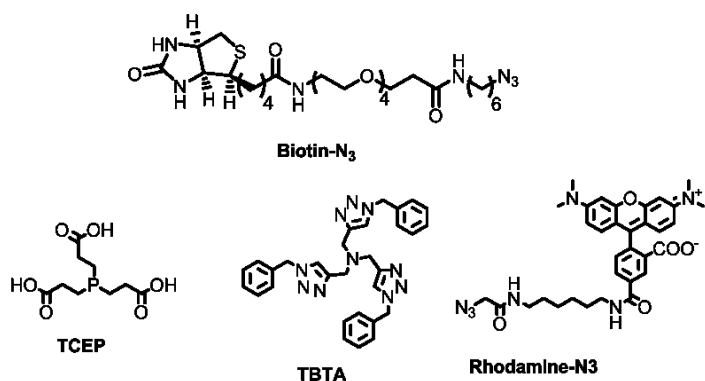
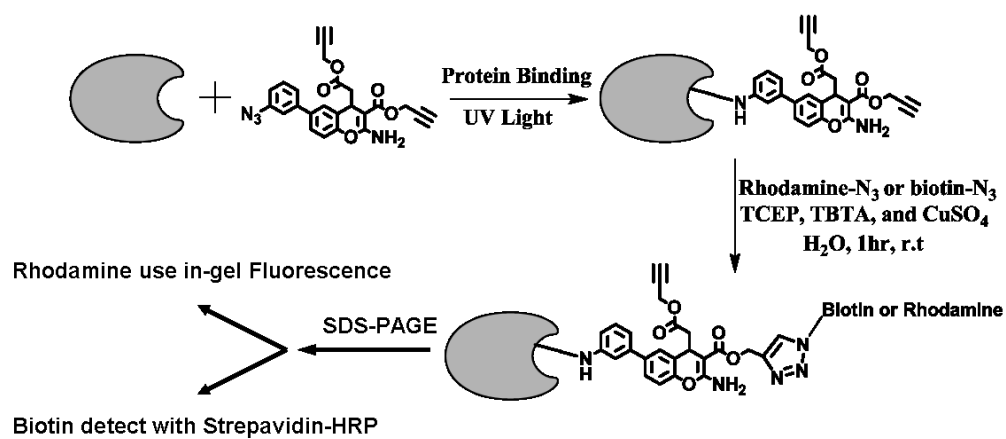
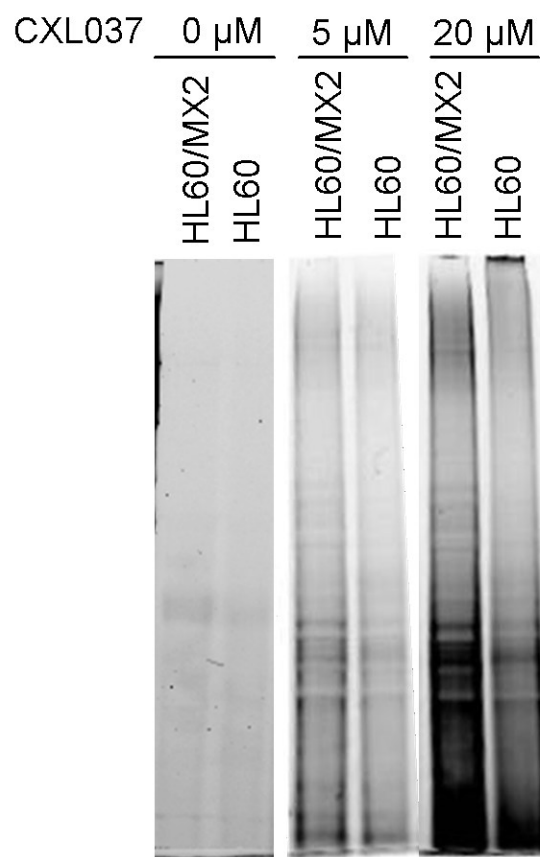


Figure 4.6 Probe labeling of target proteins

After confirming that the probe molecule CXL037 was active with IC<sub>50</sub> values of single digit  $\mu$ M in both HL60 and HL60/MX2 cells by cytotoxicity experiments, protein labeling was performed by mixing CXL037 with 100  $\mu$ g of either HL60/MX2 or HL60 cell lysate. Following photoactivation and “click” chemistry with Rhodamine-azide, treated lysates were separated using gel electrophoresis under reducing conditions. Labeled proteins were identified using in-gel fluorescent imaging. Several bands were detected indicating covalent modification had occurred between several proteins and the probe molecule; however, there were no discernable differences between HL60 and HL60/MX2 treatments (Figure 4.7). This is likely due to the limited selectivity of CXL037. Another limitation to this experiment was the use of in-gel imaging. Very few high molecular weight proteins were observed and it was difficult to get resolution of individual protein bands despite optimization of the amount of Rhodamine-azide used. Therefore, it was necessary to develop a system with better controls that would allow for the identification of likely target proteins of CXL037 as well as an improved imaging technique.



**Figure 4.7 CXL037 labeling of proteins visualized using in-gel imaging.** HL60 and HL60/MX2 cell lysate (100  $\mu$ g) was incubated with 0, 5, or 20  $\mu$ M of CXL037. Following exposure to UV light, “click” chemistry with Rhodamine-azide, and separation via gel electrophoresis, labeled proteins were visualized on the Typhoon 7000 by fluorescence using an excitation of 532 nm and emission of 580 nm.

In order to address the obstacles posed from previous experiments, single enantiomers of CXL037 were used along with a new detection method. It was discovered that the individual enantiomer CXL037B was much more potent than CXL037A. (Figure 4.8) This made CXL037A the ideal control to detect non-specific labeling of highly abundant proteins. Detection of labeled proteins following “click” chemistry with biotin-azide was achieved through the use of HRP-conjugated streptavidin following the transfer of labeled proteins to a membrane. Streptavidin has a very high binding affinity for biotin allowing for very sensitive detection of labeled proteins. Another change from previous experiments was the use of purified proteins in order to simplify the interpretation of the results and allow for optimization.

Once conditions were established that allowed for the labeling of purified SERCA, a known protein target, or Bcl-2, a suspected protein target, cell lysates would be used to discover new proteins CXL037 may interact with. Comparing proteins labeled by CXL037B with those labeled by CXL037A would allow for the determination of specific proteins that may be involved in the mechanism of action as opposed to high abundance proteins that are likely to be non-specifically labeled. When using purified proteins, bovine serum albumin (BSA) was used as a non-specific binding control in order to optimize the amount of CXL037 needed to achieve labeling of target proteins with minimal labeling of non-specific proteins.

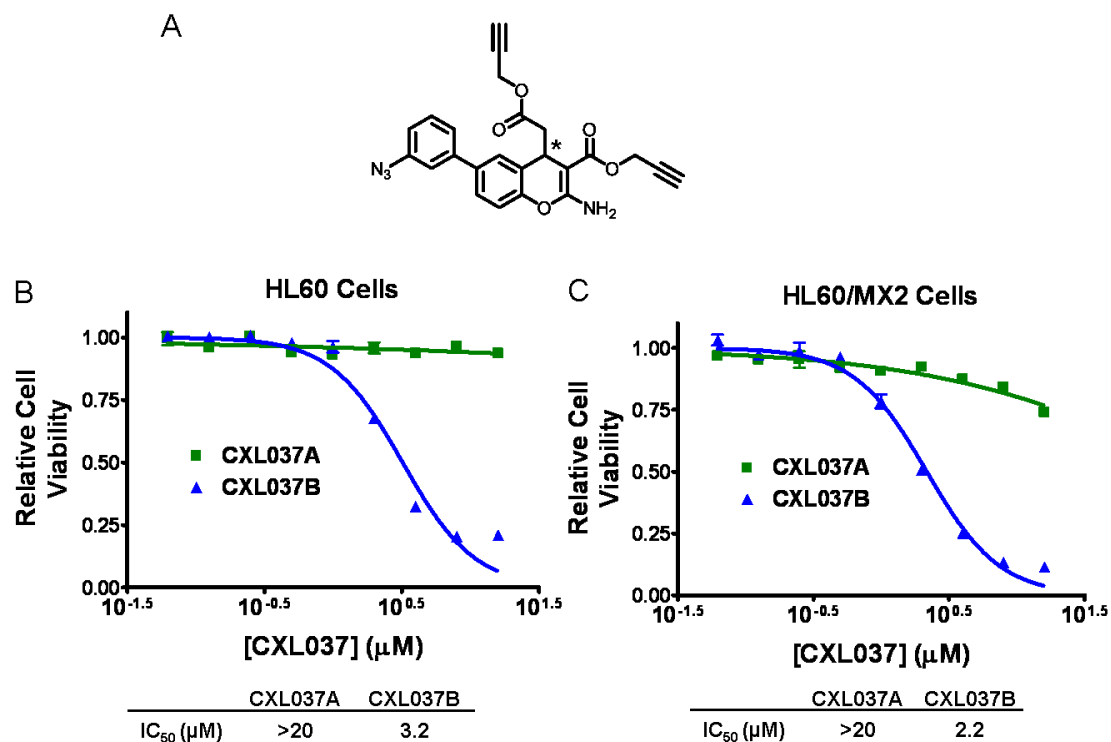


**Figure 4.8 Cytotoxicity of CXL037 in HL60 and HL60/MX2 Cells** A) Structure of CXL037 with stereocenter indicated by \*. Absolute configuration of CXL037A and B yet to be defined. B&C) 48 hour cytotoxicity of CXL037 enantiomers in B) HL60 cells and C) HL60/MX2 Cells. Data is representative of two independent experiments.

Using the new probes and detection method, purified Bcl-2 protein was incubated with CXL037 A or B to determine photoaffinity labeling. In the absence of UV light, almost no Bcl-2 was detected by streptavidin-HRP (Lanes 1-2 of Figure 4.9), indicating CXL037 must be activated by UV light before labeling can occur. Similarly, biotin-azide was also necessary for the detection of Bcl-2 (Figure 4.9, lanes 3-4), which suggests that the streptavidin detection method was specific to biotin labeled proteins. Finally, CXL037 was required to achieve labeling (Figure 4.9, Lane 5), confirming that the biotin-azide could not randomly label proteins. Lanes 6 and 7 of Figure 4.9 show the equal labeling of Bcl-2 by both CXL037 A and CXL037 B even after several rounds of optimization. Non-specific labeling occurred when BSA was used as well (Figure 4.9, Lanes 8-9). This suggests that the photoaffinity group used in CXL037 is probably too reactive resulting in labeling of proteins non-specifically. When HL60/MX2 cells were treated with either CXL037 A or B, multiple bands were observed even in controls without the biotin-azide or without CXL037 A or B (Figure 4.10), which could be due to detection of naturally occurring biotinylated proteins. CXL037 A and B did demonstrate labeling of two proteins (indicated by arrows in Figure 4.10) that do not appear in control lanes. However, the proteins are observed in lysates treated with both CXL037A and CXL037B indicating they may not be important to the mechanism of action. Taken together, the results from the affinity studies suggest further optimization must be carried out; perhaps generating a new analog with a less reactive protein affinity group would result in more specific protein labeling.

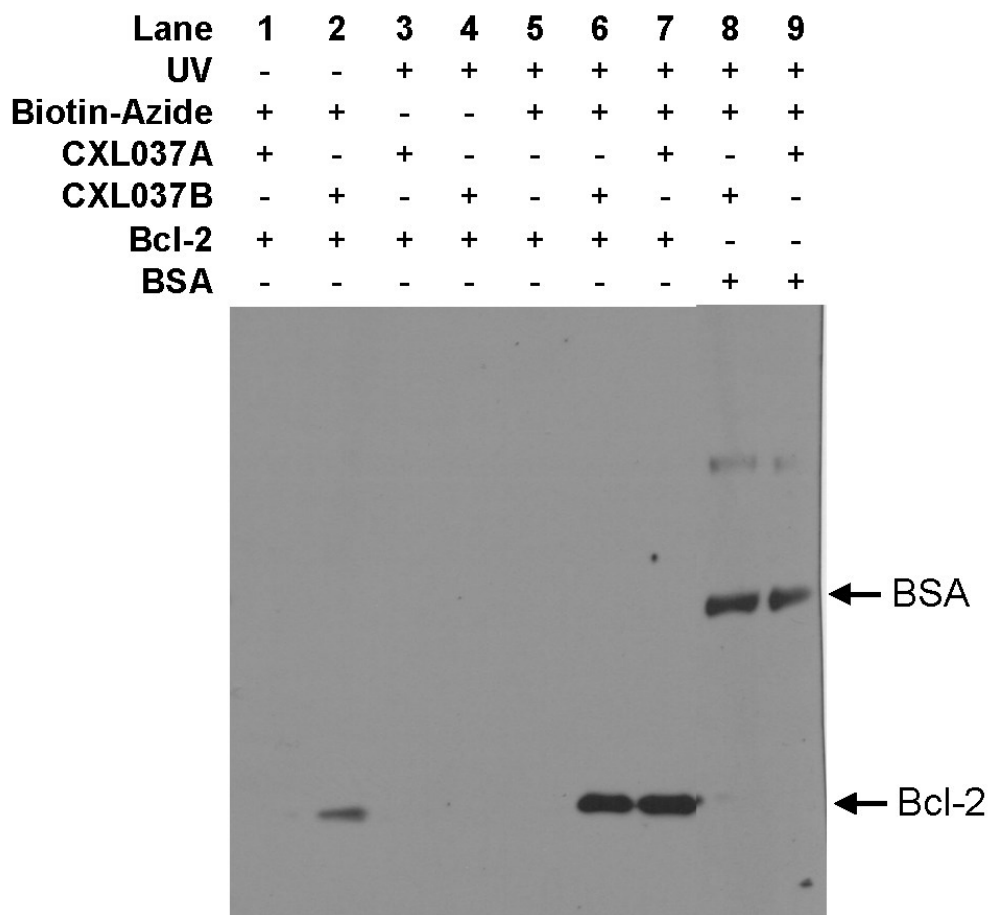


**Figure 4.9 Labeling of purified Bcl-2 protein with CXL037.** Purified Bcl-2 protein was labeled using CXL037 and BSA was used as a non-specific labeling control. Protein was mixed with CXL037, exposed to UV light (366 nm), and “click” chemistry was performed with a biotin-azide. The proteins were then separated via gel electrophoresis, transferred to a membrane, and visualized using streptavidin-HRP by chemiluminescence.



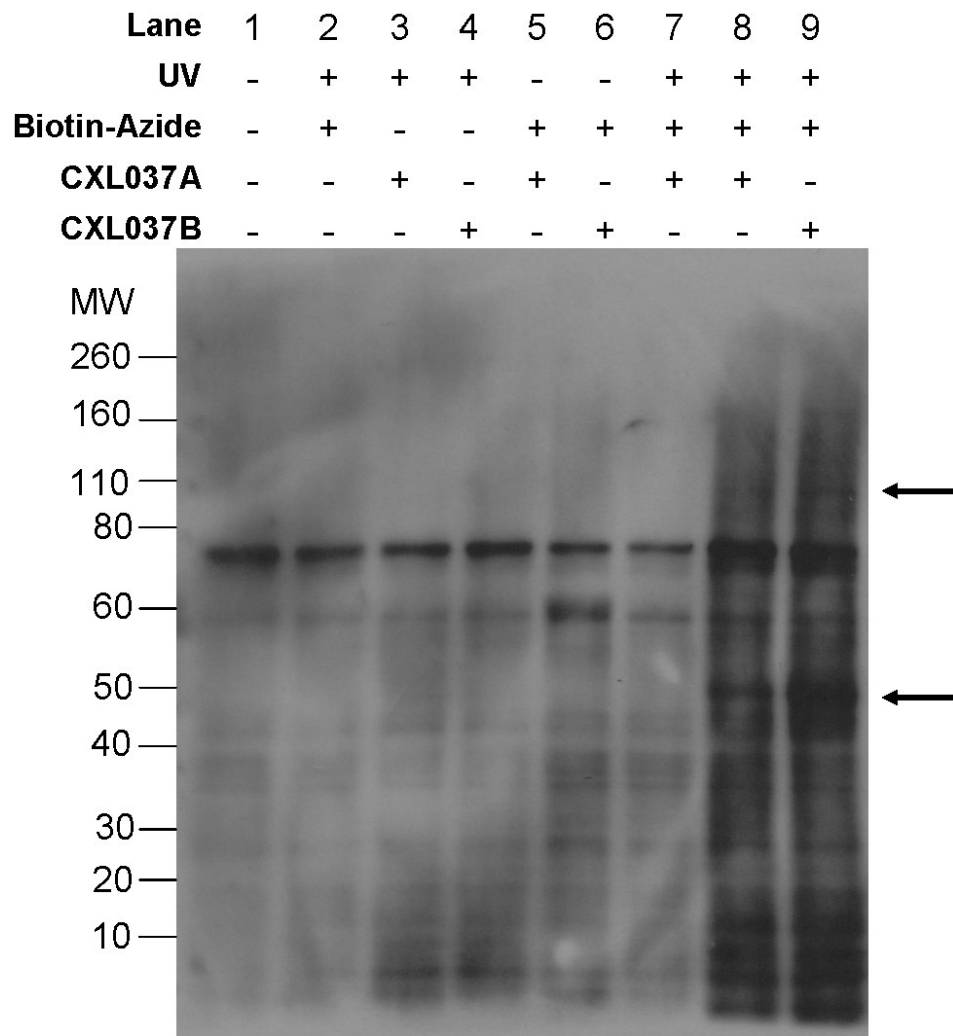


**Figure 4.10 Labeling of possible target proteins in HL60/MX2 cells with CXL037 A and B.** HL60/MX2 cells were treated with CXL037 A or B. Following treatment, cells were lysed and exposed to UV light to allow labeling to occur. “Click” chemistry was then performed using biotin-azide, followed by gel electrophoresis and transfer to a membrane. The labeled proteins were visualized using streptavidin-HRP conjugate.

### 4.3 Conclusion

Elucidating the cellular target(s) of CXL017 may uncover effective mechanisms to treat drug resistant cancer. Given that thapsigargin and sHA 14-1 are SERCA inhibitors and are more potent in HL60/MX2 cells than HL60 cells, this represented a likely mechanism for CXL017's selectivity towards HL60/MX2 cells. In addition, recent evaluation of multiple SERCA inhibitors in HL60 and HL60/MX2 continues to reveal selectivity towards HL60/MX2 cells, supporting the argument that HL60/MX2 cells are more susceptible to targeting of SERCA and ER calcium stores than HL60 cells. However, it had not been confirmed that CXL017 was a SERCA inhibitor *in vitro*. Data revealed that CXL017 was able to inhibit SERCA with similar potency as sHA 14-1, with an IC<sub>50</sub> value of 17.8 μM. Although, calcium release studies showed that sHA 14-1 was more effective in HL60 and HL60/MX2 cells than CXL017. Therefore, it was concluded that SERCA inhibition by CXL017 was unlikely to account for the increased potency relative to sHA 14-1, but may still contribute to the collateral sensitivity of HL60/MX2 cells. In an effort to resolve the individual protein contributions to either drug resistance or collateral sensitivity, knockdown of SERCA2, SERCA3, and Bcl-2 was successfully completed. Transduction of Mcl-1 was unsuccessful, likely due to cell death when Mcl-1 was knocked down. Disappointingly, knockdown produced no change in the sensitivity of the transduced cell lines to CXL017, thapsigargin, or mitoxantrone. Finally an affinity probe, CXL037, was used to try and identify possible binding proteins that may reveal the cellular targets. Conditions for protein labeling and subsequent “click” chemistry were successfully established; however, the non-specific labeling of proteins by CXL037

proved problematic. The reactivity of the aromatic azide used as the photo-reactive group in CXL037 could result in the labeling of proteins non-specifically and requires further synthesis of less reactive probes.

## **4.4 Experimental Procedures**

### **4.4.1 Cell Cultures**

HL60 and HL60/MX2 were purchased from ATCC. The HL-60 cell line was grown in IMDM Glutamax media supplemented with 20% FBS, while HL60/MX2 cells were grown in RPMI 1640 purchased from ATCC, supplemented with 10% FBS at 37°C with 5% CO<sub>2</sub> in air atmosphere.

### **4.4.2 *In vitro* SERCA Inhibition (Nick Bleeker)**

Ca<sup>2+</sup>-dependent ATPase activity was measured using LSR vesicles purified from fast-twitch skeletal muscle of New Zealand white rabbits in a NADH-linked enzyme-coupled microtiter plate assay (200 uL/well) and free calcium was tightly controlled using an EGTA buffering system as previously described.<sup>114, 115</sup> All reactions were conducted at 37 °C in triplicate or duplicate and results are reported as the mean of three independent experiments. ATP hydrolysis was determined as the rate of NADH oxidation, measured from the absorbance at 340 nm using a Molecular Devices SpectraMax Plus (Sunnyvale, CA) spectrophotometer. Compounds were introduced into the assay at their respective concentrations with 1% DMSO in the final assay volume. All data fitting was carried out using GraphPad Prism (San Diego, CA) software.

#### **4.4.3 ER Calcium Release**

$1 \times 10^6$  cells/mL were incubated in medium containing 5  $\mu$ M Fura-2AM and 2.5 mM probenecid at room temperature in the dark for 1 h. The cells were washed with cold PBS and re-suspended at  $2 \times 10^6$  cells/mL in medium containing 2.5 mM probenecid. To a cuvette with 735  $\mu$ L media containing 100 mM EGTA and 2.5 mM probenecid was added 750  $\mu$ L of the cell suspension. The cell suspension was mixed by pipetting. The cell media contained a negligible amount of free calcium under this condition. After fluorescent readings were recorded for 1 min, 15  $\mu$ L of DMSO containing thapsigargin was added. Readings were obtained on a dual wavelength fluorometer (Cary Eclipse, Varian, Palo Alto, CA) with excitation wavelengths alternating between 340 and 380 nm and an emission wavelength of 510 nm.

#### **4.4.4 Transduction of HL60/MX2 Cells**

$1 \times 10^5$  cells in 1 mL of complete media containing 5  $\mu$ g/mL polybrene (Santa Cruz Biotechnology, Santa Cruz, CA) were plated in a 12-well tissue culture plate. Cells were transduced with lentivirus containing either scrambled shRNA or shRNA targeting the gene of interest at a multiplicity of infection (MOI) of 3. The lentivirus was obtained from Santa Cruz Biotechnology, Inc (Santa Cruz, CA). After 8 hours, the cells were centrifuged and re-suspended in 1 mL of fresh media. 48 hours after transduction, cells were selected with 3  $\mu$ g/mL puromycin for a period of 72 hours. Cells were analyzed via Western blot 1-2 weeks after transduction to evaluate protein knockdown.

#### **4.4.5 Western Blotting**

Cells were lysed in RIPA buffer (10mM Tris-HCl pH 8.0, 150mM NaCl, 1mM EDTA, 1% Igebal, 0.5% Sodium deoxycholate, and 0.1% Sodium Dodecyl Sulfate) containing 1% protease inhibitor from Sigma (St. Louis, MO). Cells were kept on ice for 20 minutes in lysis buffer after vortexing, and then centrifuged at 17 x g for 15 minutes. The supernatant was collected, and protein concentration was determined by bicinchoninic acid (BCA) assay (Pierce, ThermoScientific, Rockford, IL). Following quantification, 40 µg of total protein was mixed with loading dye and sample reducing agent (NuPAGE, Invitrogen, Carlsbad, CA), boiled for 5 minutes, and separated by gel electrophoresis at 150 V on a NuPAGE 4-12% Bis-Tris Gel (Invitrogen, Carlsbad, CA). Proteins were then transferred at 40 V to a polyvinylidene difluoride (PVDF) membrane from Millipore (Billerica, MA). Membranes were blocked in 5% milk in tris buffered saline TWEEN20 (TBST) for 1 hour at room temperature followed by incubation with primary antibody overnight at 4 °C. Membranes were washed 3 times in TBST for 5 minutes and then incubated in the appropriate HRP conjugated antibody (1:3000) for 3 hours at room temperature. Detection was performed using supersignal chemiluminescence system from Pierce (Rockford, IL). The SERCA2 IID8 (1:200), SERCA3 XL-6 (1:300), and Mcl-1 S-19 (1:400) antibodies were from Santa Cruz Biotechnology, Inc. (Santa Cruz, CA) and used at the specified dilution. The anti-Bcl-2 B3170 antibody (1:10,000), the anti-β-actin (1:40,000) antibody, and secondary antibodies were from Sigma–Aldrich (St. Louis, MO).

#### **4.4.6 Cytotoxicity of CXL037 in HL60 and HL60/MX2 Cells**

The *in vitro* cytotoxicity was determined by their ability to inhibit the growth of tumor cells. Measurements were performed using the CellTiter-Blue Cell Viability Assay kit from Promega (Madison, Wisconsin). In brief, the tumor cells were plated in a 96-well plate at a density of  $1 \times 10^4$  cells/well. The cells were treated with a series of 3-fold dilutions of test compounds with final concentrations of 1% DMSO in final volume. Cells treated with 1% DMSO served as controls. Cells were incubated for 48 hours at 37 °C, and the relative viability was measured using CellTiter-Blue. IC<sub>50</sub> values were determined by plotting the relative viability by the log of drug concentration and fitting to a sigmoidal dose-response (variable slope) model in GraphPad Prism software (San Diego, CA).

#### **4.4.7 Probe Labeling**

1 µg of Bcl-2 was added to a pointed bottom 96-well plate in 9 µL phosphate buffered saline (PBS). An equal molar ratio of BSA (2.5 µg) was used as a non-specific control. 1 µL of 10X probe was then added to make the final concentration of probe 250 nM. The plate was then shaken for 1 hour in the dark followed by exposure to 366 nm light for 20 minutes on ice. Next, the “click” reaction was performed by adding in order 1 µL of 14X Rhodamine-azide or biotin azide, TCEP, TBTA, and CuSO<sub>4</sub> to make final concentrations of 100 µM, 1 mM, 200 µM, and 1 mM, respectively. The click reaction was allowed to proceed for 1 hr at room temperature in the dark. Following “click” reaction, proteins were mixed with loading dye and sample reducing agent (NuPAGE, Invitrogen, Carlsbad, CA), boiled for 5 minutes, and separated by gel electrophoresis at

150 V on a NuPAGE 4-12% Bis-Tris Gel (Invitrogen, Carlsbad, CA). In-gel imaging was performed using the Typhoon FLA 7000 (GE Healthcare Life Sciences, Pittsburgh, PA) with excitation of 532 nm and emission of 580 nm. For samples treated with biotin-azide, proteins were then transferred at 40 V to a polyvinylidene difluoride (PVDF) membrane from Millipore (Billerica, MA). The membrane was then blocked with 1% BSA in PBS with 0.05% TWEEN 20 at room temperature for 1 hour and washed two times for 5 minutes each using PBS with 0.05% TWEEN 20. Membranes were then incubated with streptavidin-HRP polymer conjugate from Sigma (St. Louis, MO) diluted 1:10,000 in PBS with 0.05% TWEEN 20 at room temperature for 1 hour. After washing two times again, detection was performed using supersignal chemiluminescence system from Pierce (Rockford, IL).

## CHAPTER 5

### 5. Re-sensitization of HL60/MX2 Cells

#### 5.1 Introduction

Despite the advancement in chemotherapeutics, drug resistance is still one of the largest obstacles in the treatment of cancer. CXL017 has already been demonstrated to selectively target drug resistant cell lines, including HL60/MX2 (mitoxantrone resistant), both *in vitro* and *in vivo*. In addition, none of the other drug resistant cell lines, with various modes of attaining resistance, displayed resistance to CXL017.<sup>116</sup> This feature was unique to CXL017 compared to several other compounds, which all suffered from drug resistance in at least one cell line tested. This makes CXL017 an intriguing candidate for the treatment of drug resistant malignancies. The question remained, however, whether cancer cells could acquire resistance to CXL017. Cancer cells are rapidly dividing and prone to errors in replication allowing for drug resistance to be acquired quickly through modification of a target by either under or over expressing certain proteins. Therefore, the possibility of acquired drug resistance in HL60 and HL60/MX2 cells upon prolonged sub-lethal exposure to CXL017 was explored.

After six months of exposure to CXL017, it was discovered that the HL60/MX2 cells failed to develop stable resistance to CXL017 and had become re-sensitized to several treatments, including mitoxantrone. This led to further studies in attempts to elucidate the mechanisms by which the re-sensitization occurred. Western blotting was used to evaluate the levels of the key proteins that have been investigated in earlier chapters including Mcl-1, SERCA 2 and 3, Bcl-2, Bcl-X<sub>L</sub>, along with various other pro-



apoptotic Bcl-2 family members, while RNA sequencing (RNAseq) was used to get a sense of the overall global changes occurring in each cell line. These experiments will be the main focus of this chapter, as well as regulation of Mcl-1 and topoisomerase II $\beta$  (topo IIB), the cellular target of mitoxantrone.

## **5.2 Results and Discussion**

### **5.2.1 Long-term exposure of HL60 and HL60/MX2 cells to CXL017**

The goal of this experiment was to determine if either HL60 or HL60/MX2 cells would develop resistance to CXL017 upon chronic exposure. Cells were cultured in the presence of CXL017 or cytarabine (Ara-C), the primary therapy for AML, for a period of six months. Negative control cells cultured in the presence of DMSO alone were also maintained, while Ara-c was used as a positive control to monitor the development of drug resistance to a primary therapy. The concentration of the respective compounds was increased over the treatment period depending on cell viability in order to maintain a selective pressure on cells while allowing for some cell survival. Cells were harvested and stored every two months for future evaluation. Two additional treatments with ABT-737, a Bcl-2/Bcl-X<sub>L</sub> inhibitor, and thapsigargin, the SERCA inhibitor, were also performed for a period of three months. Each cell line was re-named according to the following pattern: parent cell line/treatment condition-length of time (i.e HL60/MX2/CXL017-6 stands for HL60/MX2 cells treated with CXL017 for 6 months).

Upon completion of the treatment period the cells were tested for sensitivity to their respective treatments. HL60/MX2 cells treated for three months with either ABT-737 or thapsigargin developed 9-fold or 3-fold resistance, respectively (Figure 5.1 A and

B). In the case of Ara-C treated cells, both HL60 and HL60/MX2 developed well over 250-fold resistance to the therapy within the 6 month treatment period (Figure 5.1 C and D). CXL017 treated HL60 cells, on the other hand, only developed a 1.3-fold resistance, while HL60/MX2/CXL017-6 cells exhibited a 2.3-fold resistance to the compound (Figure 5.2 A and B). In order to evaluate if the resistance observed was stable, HL60/MX2/CXL017-6 and HL60/MX2/Ara-C cells were maintained for another two months in the absence of selective pressure. The new cell lines, termed HL60/MX2/CXL017/NT or HL60/MX2/Ara-C/NT, were then tested with the respective therapies. In Ara-C cells the resistance remained >250-fold, while in the CXL017 treated cell line the resistance was almost completely lost and was reduced to 1.2-fold (Figure 5.2 C and D). These results indicate that both HL60 and HL60/MX2 cells develop strong and stable resistance to Ara-C in the course of six months, and HL60/MX2 cells begin to form resistance to ABT-737 or thapsigargin within three months. However, cells cultured in the presence of CXL017 develop only minimal yet transient resistance. Therefore, it appears that CXL017 remains a promising compound for targeting drug resistance since cancer cells are less likely to acquire drug resistance to the compound.

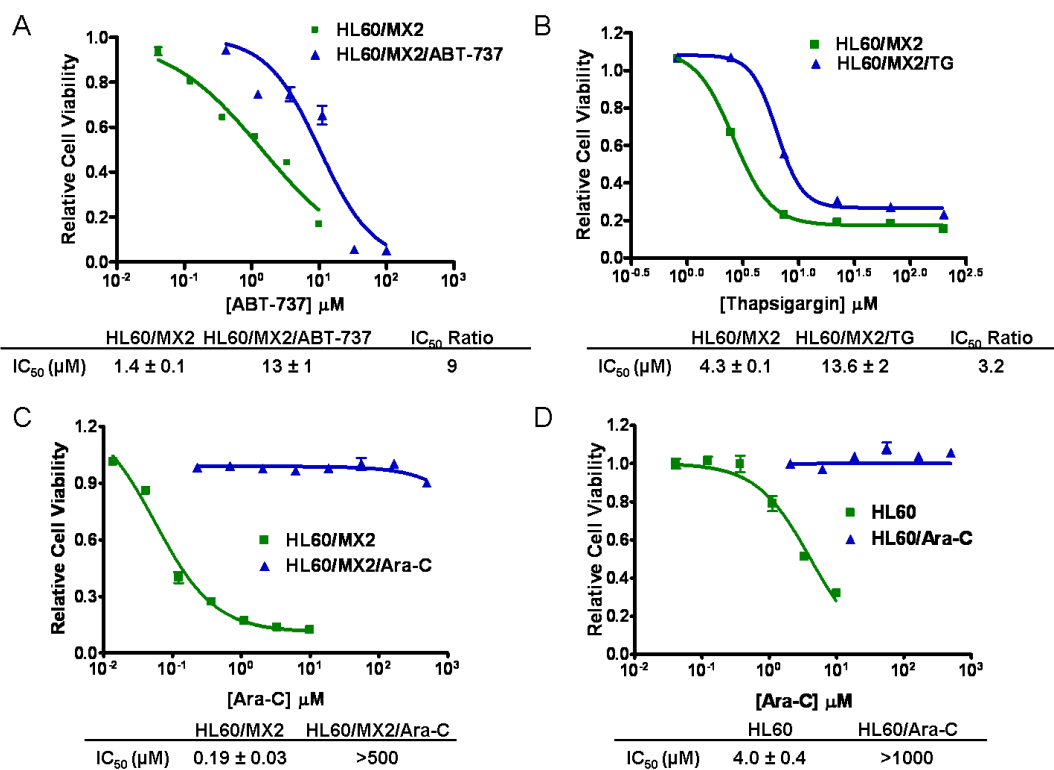


**Figure 5.1 Evaluating acquired drug resistance in HL60/MX2 cells.** Cells were treated with sub-lethal doses of A) ABT-737 or B) thapsigargin (TG) for 3 months followed by 48 hour cytotoxic evaluation with the same compound to assess drug resistance. C) HL60/MX2 cells and D) HL60 cells were treated with sub-lethal doses of cytarabine (Ara-C) for a period of 6 months followed by cytotoxicity to measure drug resistance. Results are representative of two independent experiments.

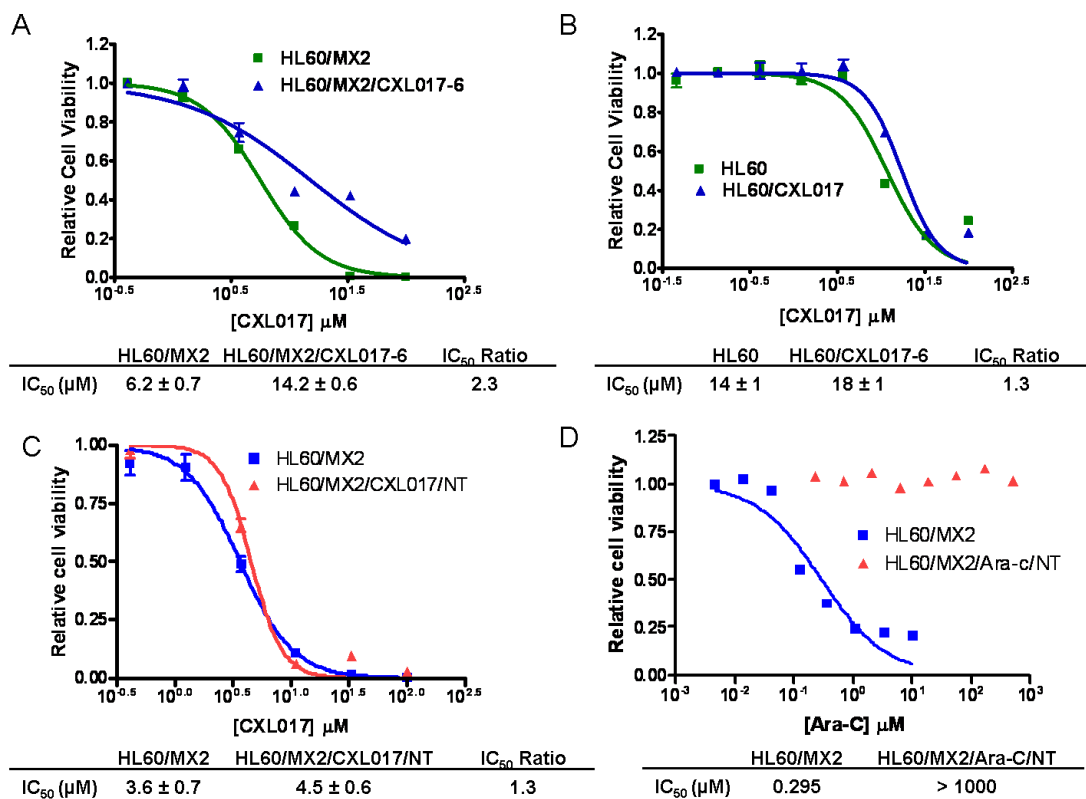


**Figure 5.2 Assessing drug resistance to CXL017 treated cells.** A) HL60/MX2 cell and B) HL60 cells were treated with sub-lethal doses of CXL017 for a period of 6 months followed by 48 hour cytotoxicity experiments. C) HL60/MX2/CXL017-6 cells or D) HL60/MX2/Ara-C cells were allowed to grow without selective pressure for two months followed by cytotoxic evaluation. Curves are representative of at least two independent experiments.

Despite the lack of resistance to CXL017, the cell lines were evaluated with a series of compounds to observe if chronic CXL017 treatment induced any changes favoring drug resistance in the cytotoxicity profile of HL60/MX2 cells. The compounds that were tested include: mitoxantrone (MX), doxorubicin (dox), Ara-C, etoposide, ABT-737, and thapsigargin. Surprisingly, the HL60/MX2/CXL017 showed collateral sensitivity to every compound tested except thapsigargin (Table 5.1). In fact, the HL60/MX2/CXL017-6 cell line was more sensitive than HL60 cells. In the case of thapsigargin, a 30-fold resistance was observed. In comparison, HL60/MX2/Ara-C cells demonstrated cross-resistance to every agent tested to varying degrees, except for CXL017, which was equipotent in HL60/MX2/Ara-C cell and HL60/MX2 cells.

**Table 5.1 48 hour IC<sub>50</sub> values of various compounds in cells exposed to CXL017 or Ara-C for 6 months.**

	HL60	HL60/CXL017	HL60/MX2	HL60/MX2/CXL017-6	HL60/MX2/Ara-C
Mitoxantrone (nM)	16 ± 2	9.0 ± 0.5	724 ± 81	6.5 ± 0.8	1870 ± 400
Doxorubicin (µM)	0.14 ± 0.02	0.137 ± 0.004	1.2 ± 0.3	0.061 ± 0.009	1.8 ± 0.4
Cytarabine (µM)	4.0 ± 0.4	2.1 ± 0.3	0.36 ± 0.09	0.033 ± 0.004	>500
Etoposide (µM)	1.62 ± 0.06	1.3 ± 0.4	14 ± 1	0.360 ± 0.02	19 ± 3
CXL017 (µM)	14 ± 1	18.8 ± 1.2	4.2 ± 0.7	14.2 ± 0.6	3.4 ± 0.4
ABT-737 (µM)	1.4 ± 0.4	1.3 ± 0.2	2.7 ± 0.2	0.232 ± 0.15	8.8 ± 0.5
Thapsigargin (nM)	3000 ± 105	38 ± 3	6.5 ± 0.2	192 ± 9	24 ± 3

Data represented are an average of three independent experiments with SEM. (Performed by Dr. Sonia Das)

The collateral sensitivity that was induced by treatment of CXL017 prompted further investigation into the timing of re-sensitization. Since cells were harvested and stored every two months throughout the treatment period, cytotoxicity was performed for each cell line including 2, 4, and 6 months of CXL017 treatment along with the HL60/MX2/CXL017/NT line (where selective pressure had been removed) (Table 5.2). It was observed that the collateral sensitivity was present in the HL60/MX2/CXL017-4 cells, while not in the 2-month treated cells. The other important observation from this data is that while the weak resistance to CXL017 was lost after removing the selective pressure, the collateral sensitivity is fully retained.

**Table 5.2 48 hour IC<sub>50</sub> values of various compounds exposed to CXL017 for between 2 and 6 months and cells grown without selective pressure for 2 months (NT cells)**

	HL60/MX2	MX2/CXL017-2	MX2/CXL017-4	MX2/CXL017-6	MX2/CXL017/NT
Mitoxantrone (nM)	724 ± 81	1205 ± 70	4 ± 1	6.5 ± 0.8	4.1 ± 0.1
Doxorubicin (µM)	1.2 ± 0.3	2.3 ± 0.7	0.052 ± 0.02	0.061 ± 0.009	0.055 ± 0.007
Cytarabine (µM)	0.36 ± 0.09	2.0 ± 0.7	0.039 ± 0.01	0.033 ± 0.004	0.013 ± 0.007
Etoposide (µM)	14 ± 1	13 ± 2	0.22 ± 0.04	0.360 ± 0.02	0.230 ± 0.02
CXL017 (µM)	4.2 ± 0.7	6.2 ± 0.6	6.6 ± 0.9	14.2 ± 0.6	4.6 ± 0.5
ABT-737 (µM)	2.7 ± 0.2	2.6 ± 0.5	0.5 ± 0.1	0.232 ± 0.15	0.31 ± 0.06
Thapsagargin (nM)	6.5 ± 0.2	9 ± 1	94 ± 29	192 ± 9	14 ± 4

Data represented are an average of three independent experiments with SEM. (Performed

by Dr. Sonia Das)

### 5.2.2 Characterization of CXL017 treated cell lines

Given that CXL017 treated cells showed such a drastic re-sensitization to several standard therapies, the newly created cell lines offered a new way of evaluating drug resistance in HL60/MX2 cells. Therefore, these cell lines were characterized for their Bcl-2 family protein and SERCA protein levels by Western blot. A strong correlation was observed among several protein changes and the collateral sensitivity observed in the CXL017/MX2/CXL017-4 cell line. Amongst the anti-apoptotic Bcl-2 proteins Mcl-1, Bcl-X<sub>L</sub>, and Bcl-2, significant protein changes in Mcl-1 and Bcl-X<sub>L</sub> occurred, while there was only a slight lowering in the levels of Bcl-2. Mcl-1 protein levels were greatly reduced in the HL60/MX2/CXL017-4 cells and continued through both the 6-month treated and HL60/MX2/CXL017/NT cell line (Figure 5.3 B). Opposite to Mcl-1, Bcl-X<sub>L</sub> protein levels were increased beginning at 4-months of treatment and remained raised throughout the remaining time. Since both Mcl-1 and Bcl-X<sub>L</sub> are anti-apoptotic and contribute to drug resistance, the changes in protein levels would appear contradictory. In combination with the cytotoxicity data, these results would suggest that the lowered Mcl-1 protein level likely outweighs the increase in Bcl-X<sub>L</sub> levels in relation to drug sensitivity. Changes in two main pro-apoptotic Bcl-2 family members, Bak and Bax, were also characterized by Western blot. No change in Bak protein was observed, but there was a general lowering of Bax protein in the re-sensitized cells. The reduced levels of Bax were unexpected because, typically, reduced levels of Bax results in resistance.<sup>117</sup>  
<sup>118</sup> Another one of the pro-apoptotic Bcl-2 family members, Noxa, was Western blotted for in HL60/MX2/CXL017-6 and CXL017/NT cells. Noxa is the primary pro-apoptotic

binding partner for Mcl-1.<sup>119</sup> Levels of Noxa were found to be increased in both of the CXL017 treated cell lines compared to either HL60 or HL60/MX2 (Figure 5.3 C). Taken together, this data suggests that in the CXL017 treated cell lines the overexpression of Noxa combined with the lowering of Mcl-1 proteins likely has a greater effect on drug sensitivity than the increase in Bcl-X<sub>L</sub> and reduction in Bax.

Changes in SERCA2 and SERCA3 protein levels were also evaluated. The levels of both proteins were overexpressed starting at 4-months treatment. Whereas Mcl-1 levels were altered towards the protein levels observed in HL60 parent cells, SERCA protein levels continued to increase in the CXL017 treated cell lines. In other words, CXL017 treated cells have higher levels of SERCA than HL60/MX2 cells, which have higher levels than HL60 cells (Figure 5.3 A and B). SERCA protein level changes also correlate well with the onset of thapsigargin resistance in HL60/MX2/CXL017-4 (refer to Table 5.2). However, the HL60/MX2/CXL017/NT cells lose their resistance to thapsigargin while the protein expression of SERCA 2 and 3 remain elevated.



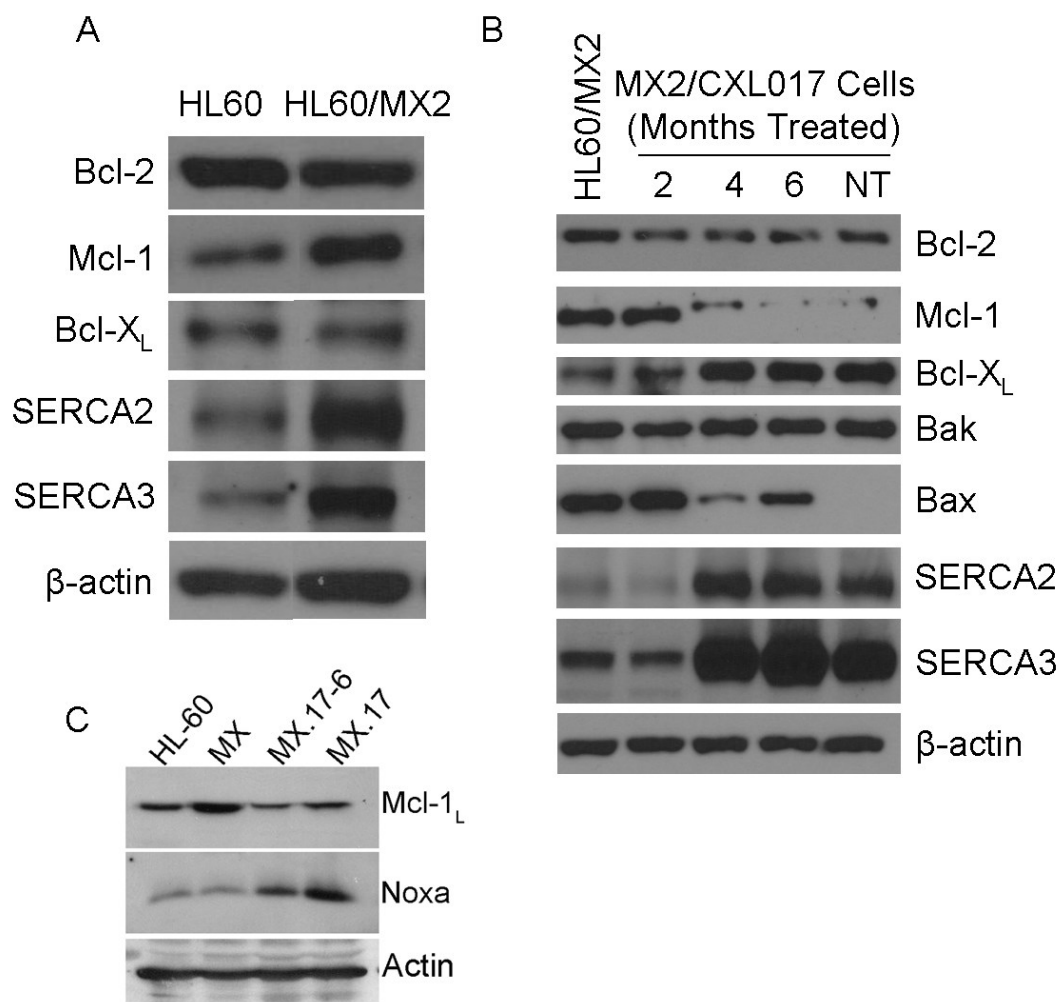


**Figure 5.3 Western blotting of CXL017 treated HL60/MX2 cell lines.** A) Analysis of HL60 and HL60/MX2 cell lysates for various proteins. B) Analysis of CXL017 treated cells for varying time points. C) Analysis of Noxa in CXL017 treated cells. (Performed by Xazmin from Dr. Ameeta Kelekar's lab) Total cell lysates were separated by SDS-PAGE and immunoblotted for various proteins. β-actin was used as a loading control and data are representative of three biological replicates.

### **5.2.3 Gene expression profiling of SERCA2 (*ATP2A2*), SERCA3 (*ATP2A3*), Bcl-2 (*BCL2*), Bcl-X<sub>L</sub> (*BCL2L1*), and Mcl-1 (*MCL1*)**

In order to further explore the cause of the observed protein changes, quantitative reverse transcriptase polymerase chain reaction (qRT-PCR) was used to determine the level of gene expression in HL60, HL60/MX2, and HL60/MX2/CXL017/NT cells. After isolating total RNA from each cell line in triplicate, samples were submitted for analysis. Quantification of each gene revealed several changes in gene expression amongst the cell lines (Table 5.3). Gene expression differences between HL60 and HL60/MX2 cells were only minor for all five genes that were analyzed, where the largest change in expression was only 1.7-fold increase for *ATP2A3*, *SERCA3*, and *MCL1* in HL60/MX2 cells. HL60/MX2 cells overexpress SERCA2, SERCA3, and Mcl-1 proteins compared to HL60 cells, which was supported by the gene expression for all three proteins. However, the extent to which gene expression is altered is relatively minor compared to the protein changes observed and suggests further regulation of these proteins may be occurring in HL60/MX2 cells. Supporting this hypothesis is the fact that similar changes in *BCL2L1*, gene code for Bcl-X<sub>L</sub>, expression are also present, but its protein level is unaltered between HL60 and HL60/MX2 cells.

HL60/MX2/CXL017/NT cells, on the other hand, exhibited expression changes of >2-fold in all three anti-apoptotic Bcl-2 proteins that were analyzed as well as SERCA3 (Table 5.3). While both SERCA2 and SERCA3 proteins are increased in HL60/MX2/CXL017/NT cells compared to HL60/MX2 cells, only the gene expression of SERCA3 was increased with no change in SERCA2. Among the anti-apoptotic Bcl-2

family proteins, *BCL2* was the only gene with lowered expression in the CXL017 treated cell line compared to HL60/MX2, which correlates with the slightly lowered protein levels. *BCL2L1* expression was dramatically increased and supports the results from Western blotting of this protein, which also showed a large increase in the expression of Bcl-X<sub>L</sub> (Figure 5.3 B). Intriguingly, expression of *MCL1* was actually increased 3-fold in HL60/MX2/CXL017/NT cells while protein levels of Mcl-1 were drastically decreased in this cell line. This suggests that there is significant post-transcriptional regulation of Mcl-1. The protein half-life of Mcl-1 is short relative to other anti-apoptotic Bcl-2 proteins and is known to be tightly controlled through phosphorylation and the ubiquitin/proteasome degradation pathway.<sup>47, 52, 53, 120, 121</sup> It is also known that Mcl-1 can be regulated at the translational level.<sup>122</sup> Therefore, given that Mcl-1 protein levels are decreased while *MCL1* expression is increased, there are likely alterations in protein stability or translation in CXL017 treated cells. Overall, the results from the qRT-PCR indicate that changes in gene expression do not always correlate with the changes at the protein level, which should be expected given the number of mechanisms cells have developed to control protein expression. Therefore, when comparing minor changes in gene expression in HL60/MX2 cells to either HL60 or HL60/MX2/CXL017/NT cells, caution must be used.

**Table 5.3 qRT-PCR fold change of mRNA in HL60 and HL60/MX2/CXL017/NT cells relative to HL60/MX2 cells.**

<b>Data represented are gene expression levels relative to HL60/MX2. Data was normalized to the expression level of <math>\beta</math>-actin.</b>		
	<b>HL60</b>	<b>HL60/MX2/ CXL017/NT</b>
<i>BCL2</i> (Bcl-2)	0.9 $\pm$ 0.3	0.35 $\pm$ 0.05
<i>MCL1</i> (Mcl-1)	0.6 $\pm$ 0.3	3.3 $\pm$ 0.3
<i>BCL2L1</i> (Bcl-X <sub>L</sub> )	0.7 $\pm$ 0.4	16 $\pm$ 3
<i>ATP2A2</i> (SERCA2)	0.8 $\pm$ 0.1	0.95 $\pm$ 0.2
<i>ATP2A3</i> (SERCA3)	0.6 $\pm$ 0.2	2.2 $\pm$ 0.6

Data are displayed with gene name in italics and protein name in parentheses. Fold changes are the average of three experiments with SD.

#### 5.2.4 Mcl-1 protein stability

Based on the hypothesis that Mcl-1 was being post-transcriptionally regulated, alterations in the protein half-life of Mcl-1 were measured in HL60, HL60/MX2, and HL60/MX2/CXL017/NT cells. In order to determine the half-life of Mcl-1, cells were treated with cycloheximide (CHX), which is a eukaryotic translation inhibitor<sup>123, 124</sup>, and lysates were made at varying time points. Lysates were then Western blotted for Mcl-1 and densitometry was used to quantify the remaining protein levels at each time point (Figure 5.4 A). The half-life of the protein was then determined by fitting the data to a one phase exponential decay curve. The protein half-life of Mcl-1 in HL60/MX2 cells was found to be the longest at 2.1 hours, while in HL60 cells the half-life was slightly shorter at 1.8 hours. In HL60/MX2/CXL017/NT cells, Mcl-1 had a much shorter half-life, compared to HL60/MX2 cells, of only 1.2 hours (Figure 5.4 B). These data indicate that the lowered Mcl-1 protein levels observed in CXL017 chronically treated cells is at least partially due to a shorter protein half-life.

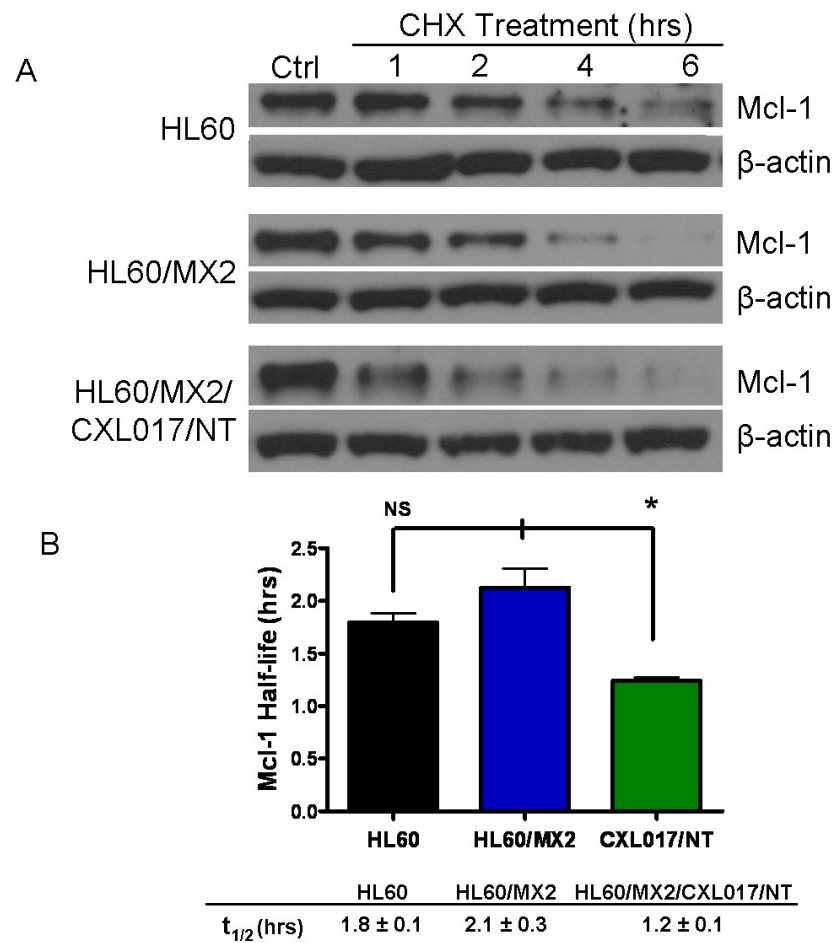


**Figure 5.4 Half-life analysis of Mcl-1 in HL60, HL60/MX2, and HL60/MX2/CXL017/NT cells.** A) Representative Western blots of protein degradation following treatment with 10  $\mu\text{g/mL}$  cycloheximide (CHX), a protein translation inhibitor. Cells were treated with CHX for the given amount of time, collected, lysed, and total lysate was separated via gel electrophoreses. B) Half-life of Mcl-1 in various cell lines determined by using densitometry of Western blots of cells treated with CHX.  $\beta$ -actin was used to correct for loading differences and fitted using GraphPad Prism 4. Half-life determinations are the average of two independent experiments with SD. \* represents  $p < 0.05$ .

While the main Mcl-1 degradation pathway is through the proteasome, there have been reports that Mcl-1 can be degraded in a proteasome independent process as well.<sup>125</sup> Therefore, in order to explore whether the shortened half-life of Mcl-1 was a proteasome dependent process, cells were treated with a proteasome inhibitor, MG-132<sup>126</sup>, for 6 hours followed by Western blotting to monitor the accumulation of Mcl-1 (Figure 5.5 A). Again, densitometry was performed and the fold increase of Mcl-1 relative to non-treated cells was determined. In all three cell lines, the levels of Mcl-1 increased from between 2.6-fold in HL60/MX2 to nearly 6-fold in HL60 and HL60/MX2/CXL017/NT cells (Figure 5.5 B). This confirmed that the proteasome is at least partially responsible for Mcl-1 degradation in these cell lines.

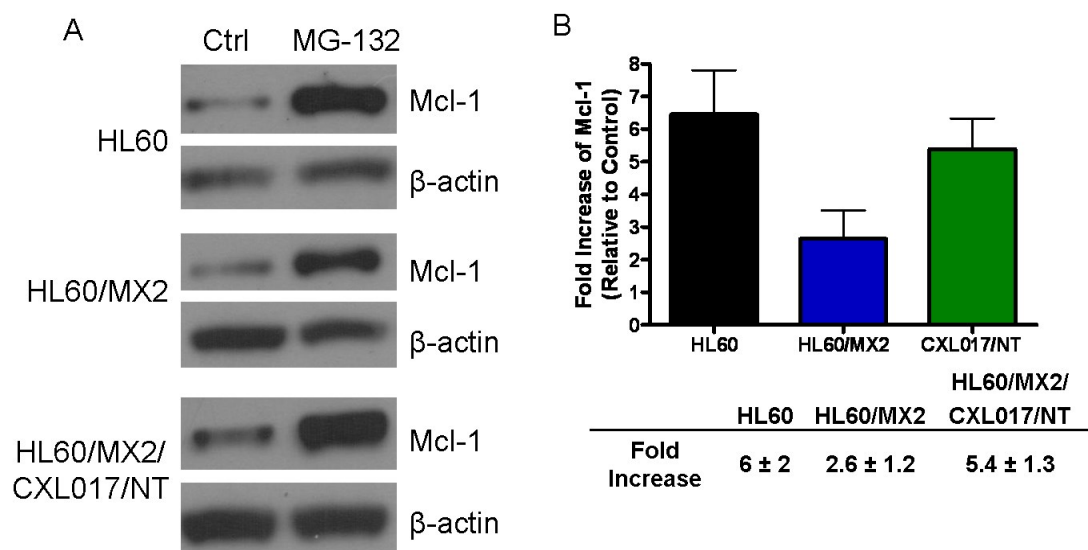


**Figure 5.5 Mcl-1 accumulation in HL60, HL60/MX2, and HL60/MX2/CXL017/NT cells.** A) Western blot of Mcl-1 accumulation in various cell lines after treatment with 10  $\mu$ M MG-132, a proteasome inhibitor. Cells were treated for 6 hours with MG-132, collected, lysed, and proteins were immunoblotted for Mcl-1.  $\beta$ -actin was used as a loading control. B) Fold increase of Mcl-1 relative to untreated controls determined by densitometry of Western blots using  $\beta$ -actin to normalize loading levels. Data are an average of at least two independent experiments with SD.



### 5.2.5 RNA sequencing

RNA sequencing (RNAseq) is a next-generation sequencing technique that is capable of measuring every gene expressed in a cell population.<sup>127</sup> Total RNA is isolated from cells, converted to cDNA, which is then sheered into shorter fragments. Those fragments are separated by gel electrophoresis and 200 base-pair fragments are collected. Paired-end reads are then used to sequence 50 base-pair reads from each end of the fragment. By performing large numbers of reads, it is possible to nearly sequence the entire RNA pool. These reads can then be used to either create a whole new genome *de novo* or can be mapped to an existing reference genome. Using Cufflinks software<sup>128</sup>, the fragments per kilobase of exon per million fragments mapped (FPKMs) can be calculated and provide a quantitative way of comparing all of the genes expressed in the cell population. The FPKMs can then be compared amongst differing cell populations to determine differentially expressed genes.

RNAseq was performed on HL60, HL60/MX2, HL60/MX2/CXL017-6, and HL60/MX2/CXL017/NT cells. The RNA was isolated in triplicate for each cell line, individually sequenced, and the average FPKMs were used to determine differentially expressed genes. In order to identify the genes most likely responsible for resistance observed in HL60/MX2 cells, the common differentially expressed genes in HL60, HL60/MX2/CXL017-6, and HL60/MX2/CXL017/NT cells, compared to HL60/MX2 cells, will be analyzed (Figure 5.6). Only genes with a minimum 2-fold gene change where at least one of two cell lines being compared had an FPKM of 10 were considered. The FPKM cutoff of 10 was set to ensure that any identified genes are reliably expressed.

Using this analysis, 254 genes were identified (137 downregulated and 117 upregulated) as being differentially regulated in HL60 and the two CXL017 treated cell lines when compared to HL60/MX2 (Figure 5.6). In order to evaluate the quality of data from RNAseq, qRT-PCR was run on 12 differentially expressed genes. Fold-changes compared well for the different methods, suggesting that the RNAseq data are reliable (Figure 5.7).

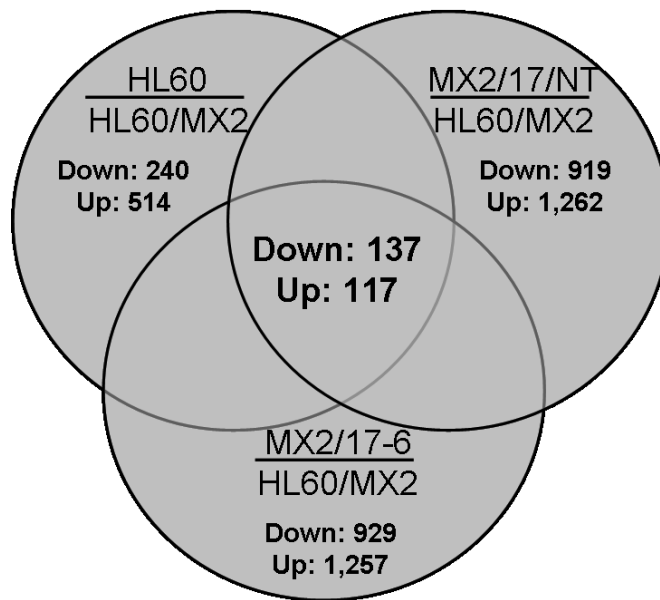


**Figure 5.6** Venn diagram of the number of genes differentially expressed in HL60, HL60/MX2/CXL017-6 and HL60/MX2/CXL017/NT cells compared to HL60/MX2 cells. The overlapping differentially expressed genes in these three populations relative to HL60/MX2 cells are most likely to account of drug resistance/re-sensitization.

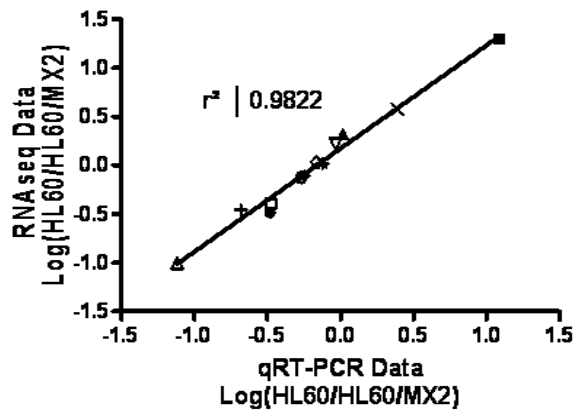


**Figure 5.7** Comparison of gene fold changes between HL60 and HL60/MX2 cells in RNAseq data with qRT-PCR data. 12 genes with varying levels of fold changes were analyzed by qRT-PCR and compared with fold changes in the RNAseq data.

This analysis did not reveal any of the genes that had been previously studied including SERCA2, SERCA3, Bcl-2, Bcl-X<sub>L</sub>, and Mcl-1. However, one gene that was identified during the analysis was *TOP2B*, which corresponds to topoisomerase II  $\beta$  (topo II $\beta$ ). HL60/MX2 cells have extremely low expression of *TOP2B*, which has been previously reported to be responsible for resistance to mitoxantrone.<sup>93</sup> Therefore, the increased expression of *TOP2B* in CXL017 treated cells may account for the observed drug sensitivity in these cells in the case of reported topo II $\beta$  inhibitors. qRT-PCR was also used to measure *TOP2B* levels in these cells, and confirmed the RNAseq data (Figure 5.8). Disappointedly, efforts to Western blot for topo II $\beta$  expression in these cell lines were unsuccessful; however, with a 12 and 28-fold expression change in HL60 and HL60/MX2/CXL017/NT cells, respectively, it is very likely the protein is also overexpressed. Together these data suggest a hypothesis such that the increase in *TOP2B* expression leads to the collateral sensitization observed in HL60/MX2/CXL017/NT cells.

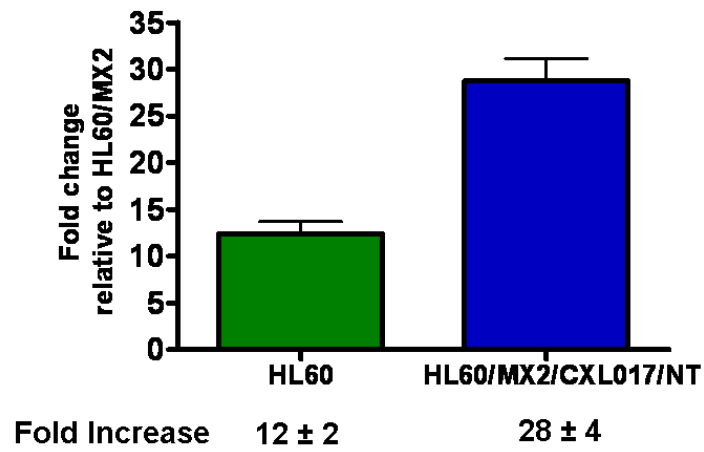


**Figure 5.8** qRT-PCR results for *TOP2B* expression in HL60 and HL60/MX2/CXL017/NT cells compared to HL60/MX2 cells. Total RNA was isolated from HL60, HL60/MX2, and HL60/MX2/CXL017/NT cells. *TOP2B* expression was assessed using qRT-PCR, and the fold expression change was determined. RNA was isolated in triplicate and data represent the average with SD.

### 5.2.6 Topoisomerase II $\beta$ knockdown

In order to evaluate the effect topo II $\beta$  downregulation has in drug resistance, shRNA was used to transduce HL60 and HL60/MX2/CXL017/NT cells and knockdown *TOP2B*. Stable knockdown cell lines were obtained following transduction with lentivirus by selection with puromycin, as with previous shRNA experiments. Evaluation of knockdown efficiency was performed using qRT-PCR (Figure 5.9 A). Levels of *TOP2B* were reduced by 6.1-fold and 3.1-fold in HL60/*TOP2B* and MX2/CXL017/*TOP2B* cells, respectively, when compared to scrambled shRNA control cells. As a control for the specificity of *TOP2B* shRNA, *TOP2A* was also monitored by qRT-PCR with no change in either of the transduced cell lines (Figure 5.9 A). In comparison to HL60/MX2 cells, *TOP2B* expression remained 1.8-fold higher in HL60/*TOP2B* cell line; whereas HL60/Ctrl cells had 10-fold higher levels of *TOP2B* (Figure 5.9 B). Expression of *TOP2B* in MX2/CXL017/*TOP2B* cells remained 6-fold higher than HL60/MX2 cells compared to 19-fold higher in the MX2/CXL017/Ctrl cells. The successful knockdown of *TOP2B* in both cell lines will provide a system for evaluating the effect of reduced topo II $\beta$  protein levels with respect to mitoxantrone drug resistance as well as other topo II inhibitors.

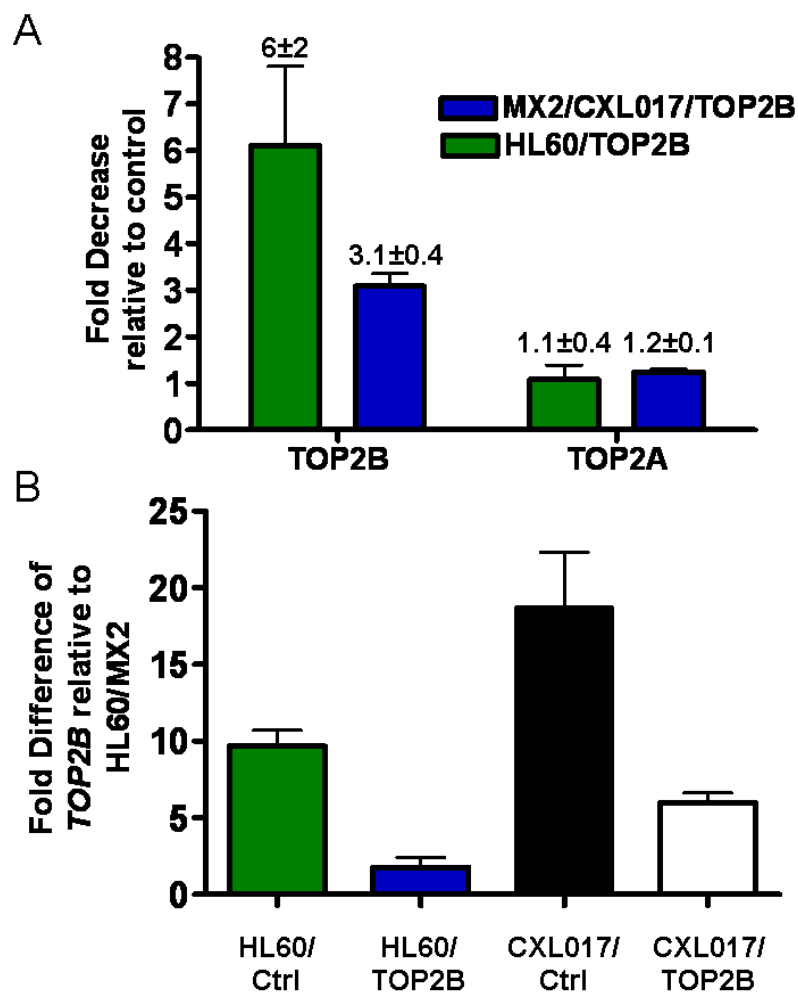


**Figure 5.9 qRT-PCR data of *TOP2B* knockdown cells.** A) Fold decrease of *TOP2B* and *TOP2A* levels in HL60/TOP2B and HL60/MX2/CXL017/NT cells relative to their respective controls. B) *TOP2B* expression in HL60/Ctrl, HL60/TOP2B, HL60/MX2/CXL017/NT/Ctrl, and HL60/MX2/CXL017/NT/TOP2B cells relative to HL60/MX2 cells. Total RNA was isolated from each cell line in duplicate and data are average fold difference between each cell line and HL60/MX2 cells with SD.

Following successful knockdown of *TOP2B*, cytotoxicity was performed on the newly generated cell lines to determine the effect on drug resistance. Compounds evaluated included the topo II inhibitors mitoxantrone, etoposide, and doxorubicin, as well as CXL017 and cytarabine (Ara-C). Based on previous data, knockdown of *TOP2B* was suspected to result in drug resistance against all the topo II inhibitors while no change in cytotoxicity was expected for CXL017 or Ara-C. The reduced expression of *TOP2B* in HL60/*TOP2B* and MX2/CXL017/*TOP2B* cell lines did result in a 3.0-fold and 1.8-fold increase in their respective IC<sub>50</sub>'s to mitoxantrone (Figure 5.10). Less of an effect was observed for the other two topo II inhibitors with less than 1.5-fold resistance observed to either inhibitor in either cell line (Table 5.4). As expected, no change was observed for CXL017 or Ara-C.

These results suggest that reduction in the levels of *TOP2B* does induce drug resistance to mitoxantrone; however, the resistance observed in the knockdown cell lines is far less than that of the naturally occurring HL60/MX2 cell line of 45-fold. This may be because the transduced cell lines still expressed slightly higher levels of *TOP2B* relative to HL60/MX2 cells, but it is more likely that there are other factors contributing to the resistance in HL60/MX2 cells. The current data also suggest that a reduction in the levels of *TOP2B* alone is insufficient to induce drug resistance against doxorubicin or etoposide, further support for the role of other drug resistance mechanisms in HL60/MX2.



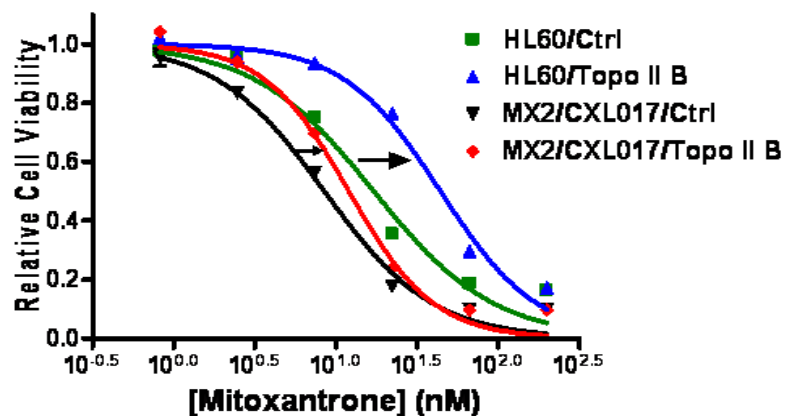


**Figure 5.10** Cytotoxicity of mitoxantrone in *TOP2B* knockdown cell lines. Cells were treated for 48 hours with various concentrations of mitoxantrone and cell viability was determined by cell titer blue.

**Table 5.4** 48 hour  $IC_{50}$  values of various compounds in *TOP2B* knockdown cell lines.

	HL60/Ctrl	HL60/TOP2B	CXL017/Ctrl	CXL017/TOP2B
<b>Mitoxantrone (nM)</b>	<b>14 ± 3</b>	<b>43.6 ± 0.8</b>	<b>6.7 ± 0.5</b>	<b>10.7 ± 0.2</b>
CXL017 (μM)	10.2 ± 0.9	10.0 ± 0.1	3.50 ± 0.05	3.5 ± 0.1
Etoposide (μM)	1.7 ± 0.4	2.5 ± 0.2	0.234 ± 0.04	0.274 ± 0.009
Doxorubicin (μM)	0.147 ± .05	0.182 ± 0.03	0.036 ± 0.003	0.042 ± 0.006
Cytarabine (μM)	5.6 ± 0.5	3.81 ± 0.08	0.034 ± 0.006	0.044 ± 0.006
Vincristine (nM)	2.8 ± 0.2	2.5 ± 0.5	0.600 ± 0.01	0.652 ± 0.05

Data are averages of two independent experiments with SD.

### **5.2.7 Evaluating Mcl-1 for its contribution to mitoxantrone induced drug resistance**

Data suggesting reduction of topo II $\beta$  is insufficient to induce the levels of drug resistance found in HL60/MX2 cells combined with Mcl-1's established role in drug resistance<sup>129</sup>, led to the hypothesis that overexpression of Mcl-1 in HL60/MX2 cells played a significant role in the observed drug resistance. Earlier efforts made to knockdown Mcl-1 in HL60/MX2 cells via shRNA were unsuccessful, due to cell viability being negatively affected in the Mcl-1 shRNA treated cell lines. Therefore, transient knockdown of Mcl-1 using small interfering RNA (siRNA) was performed. It was thought that transient knockdown would be more tunable to the level of knockdown because it does not require incorporation of shRNA into the genome or a selection step allowing for faster evaluation of knockdown efficacy. This method also allows for the quantification of cell death due to the siRNA transfection because the protein levels will start to be reduced almost immediately after the transfection, due to the short half-life of Mcl-1, without the time delay associated with shRNA. HL60/MX2 cells were transfected via electroporation with 12.5 nM siRNA against Mcl-1 or scrambled siRNA as a control, and cells were analyzed for protein expression at 3 and 6 hours post transfection by Western blot. This method proved to be effective in down regulating Mcl-1 in cells; however, cell viability was greatly reduced in cells transfected with Mcl-1 siRNA compared to control siRNA cells (Figure 5.11 A). Within 24 hours of transfection, Mcl-1 knockdown cells remained only 40% viable compared to controls. Despite several attempts to reduce the loading level of siRNA, conditions leading to effective knockdown

of Mcl-1 without greatly reducing the viability of cells were not achieved. This made it unfeasible to attempt to perform cytotoxicity experiments using mitoxantrone to evaluate Mcl-1's role in drug resistance.

In order to determine if Mcl-1 was as crucial in HL60 cells as HL60/MX2 cells, both cell lines were transfected using Mcl-1 siRNA and cell viability was monitored over the course of 48 hours at various time points (Figure 5.11 B). It was observed that HL60/MX2 cells were much more dependent on Mcl-1 expression compared to HL60 cells. Reduced cell viability was observed within 4 hours post-transfection in HL60/MX2 cells, with 80% cell death at 48 hours. The remaining cells probably represent unsuccessfully transfected cells as the transfection efficiency is approximately 80%. In Mcl-1 transfected HL60 cells, no cell death was observed in the first 6 hours and cell viability remained at 70% through 48 hours. These results suggest that HL60/MX2 cells rely on the overexpression of Mcl-1 for cell survival; therefore, targeting Mcl-1 would be a useful strategy in eliminating drug resistant cells.

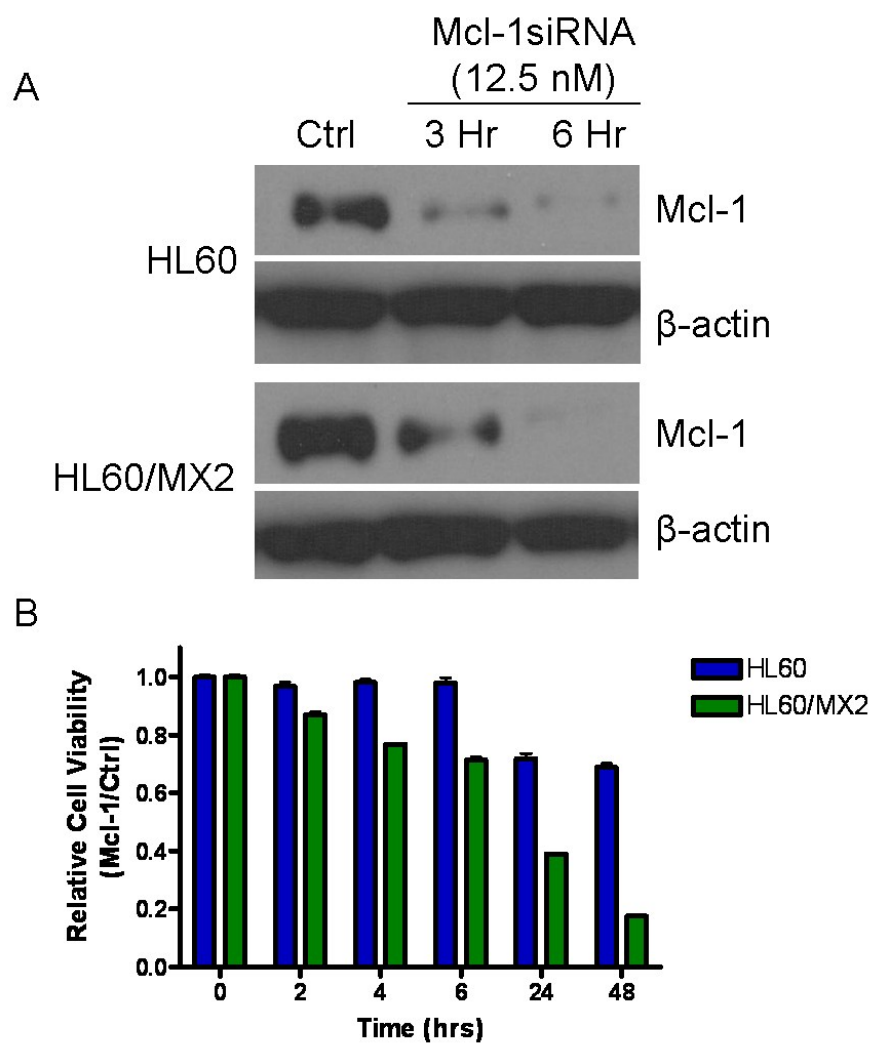


**Figure 5.11 Mcl-1 transient knockdown in HL60 and HL60/MX2 cells.** A) Western blot of Mcl-1 levels following electroporation of HL60 and HL60/MX2 cells with 12.5 nM siRNA targeted against Mcl-1. Control cells were treated with scrambled siRNA. Cells were collected 3 and 6 hours post transfection. Data is representative of two experiments. B) Relative cell viability of HL60 and HL60/MX2 cells post transfection with 12.5 nM siRNA targeting Mcl-1. Cells were electroporated and cell viability was determined at the given time points.

Encouraged by the results from knockdown studies of Mcl-1 suggesting the protein plays a role in drug resistance, Mcl-1 was transiently overexpressed in HL60 cells. Plasmid DNA coding for the open reading frame (ORF) of Mcl-1 was transfected via electroporation into HL60 cells. After 48 hours, cells were harvested and analyzed by Western blot for successful overexpression of Mcl-1 (Figure 5.12 A). Once the conditions were optimized, 24 hour cytotoxicity of mitoxantrone, CXL017, and ABT-737 was performed on Mcl-1 overexpressing HL60 cells (Figure 5.13 B-D). ABT-737 was used as a positive control as it is reported to suffer from drug resistance when Mcl-1 is overexpressed.<sup>130</sup> Mcl-1 transfected cells displayed 24-fold resistance to ABT-737, 8-fold drug resistance to mitoxantrone, and only 2-fold resistance to CXL017. This data implies that Mcl-1 is likely a key contributing factor in the drug resistance observed in HL60/MX2 cells, and the 45-fold resistance to mitoxantrone is not solely due to topo II $\beta$  down regulation.

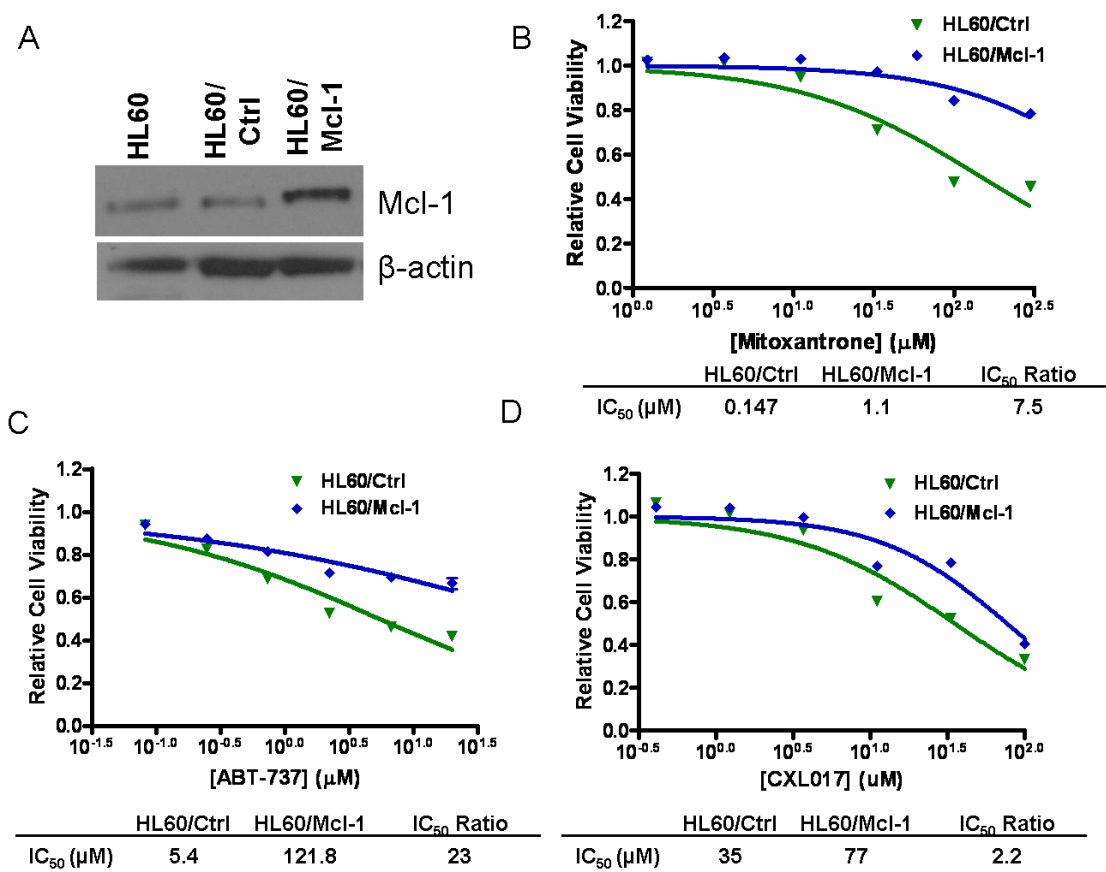


**Figure 5.12 Overexpression of Mcl-1 in HL60 cells.** Cells were transfected via electroporation with 5 $\mu$ g of plasmid DNA encoded with the Mcl-1 open reading frame. A) Western blot analysis of Mcl-1 expression 48 hours post-transfection. B-D) 24 hour cytotoxicity of B) mitoxantrone, C) ABT-737, and D) CXL017. Data are representative of two independent experiments.

### 5.3 Conclusion

In this chapter several key findings were made. It was discovered that cells exposed chronically to sub-lethal doses of CXL017 for a period of 6 months failed to acquire stable drug resistance to the compound, while cells exposed to Ara-C acquired >250-fold resistance. In addition, cells exposed to CXL017 also became re-sensitized to several standard therapies including mitoxantrone, etoposide, doxorubicin, and Ara-C after 4 months of exposure. Several protein changes were also observed to have taken place at 4 months of treatment. SERCA2, SERCA3, and Bcl-X<sub>L</sub> were all shown to increase in expression, while Mcl-1 decreased. It was then discovered that the decrease in Mcl-1 expression is at least partially due to a shortened protein half-life in HL60/MX2/CXL017/NT cells compared to HL60/MX2 cells and not due to a decrease in gene expression. RNA sequencing revealed that *TOP2B* expression was significantly higher in CXL017 treated cells as well as endogenous levels in HL60 cells. Knockdown of *TOP2B* in HL60 or CXL017 treated cells resulted in slight resistance to mitoxantrone, indicating the increased expression of *TOP2B* is likely one reason for the observed re-sensitization. Lastly, it was established that HL60/MX2 cells are dependent on Mcl-1 overexpression for cell survival and that overexpression Mcl-1 in HL60 cells leads to drug resistance to mitoxantrone. Taken together these results suggest Mcl-1 is a previously unidentified protein that is key to the drug resistance observed in HL60/MX2 cells.

## **5.4 Experimental Procedures**

### **5.4.1 Cell Cultures**

HL60 and HL60/MX2 were purchased from ATCC. The HL-60 cell line was grown in IMDM Glutamax media supplemented with 20% FBS, while HL60/MX2 cells were grown in RPMI 1640 purchased from ATCC, supplemented with 10% FBS at 37°C with 5% CO<sub>2</sub> in air atmosphere.

### **5.4.2 Development of Drug Resistant cell lines (Performed by Dr. Sonia Das)**

HL60 and HL60/MX2 cell lines were exposed to increasing concentration of CXL017 and Ara-C respectively *in vitro*, starting at the IC<sub>20</sub> value for a period of 6 months with gradual increase of drug concentration while maintaining the survival of most cells. Cell medium was changed twice a week. The sensitivity of these cells to the corresponding drugs was monitored once a month, in which the cells were grown in the absence of drug for a period of 7 days and then evaluated for the sensitivity with a cell viability assay. To determine if the cell lines exposed to drug for 6 months demonstrate stable resistance, they were cultured in the absence of drug for a period of 2 months and then re-evaluated for their drug sensitivity. For additional comparison, HL60/MX2 cells were exposed to ABT-737 (a known Bcl-2 inhibitor) and TG (a known SERCA inhibitor) for a period of 3 months, using the same protocol described earlier.

### **5.4.3 Evaluation of Cytotoxicity**

The *in vitro* cytotoxicity was determined by the compounds' ability to inhibit the growth of tumor cells. Measurements were performed with the CellTiter-Blue Cell Viability Assay kit from Promega (Madison, Wisconsin). In brief, the tumor cells were



plated in a 96-well plate at a density of  $1 \times 10^4$  cells/well. The cells were treated with a series of 3-fold dilutions of test compounds with final concentrations of 1% DMSO in the final volume. Cells treated with 1% DMSO served as controls. Cells were incubated for 48 hours at 37 °C, and the relative viability was measured using CellTiter-Blue. IC<sub>50</sub> values were determined by plotting the relative viability by the log of drug concentration and fitting to a sigmoidal dose-response (variable slope) model in GraphPad Prism software (San Diego, CA).

#### **5.4.4 Western Blotting**

Cells were lysed in RIPA buffer (10mM Tris-HCl pH=8.0, 150mM NaCl, 1mM EDTA, 1% Igebal, 0.5% Sodium deoxycholate, and 0.1% Sodium Dodecyl Sulfate) containing 1% protease inhibitor from Sigma (St. Louis, MO). Cells were kept on ice for 20 minutes in lysis buffer after vortexing, and then centrifuged at 17 x g for 15 minutes. The supernatant was collected, and protein concentration was determined by bicinchoninic acid (BCA) assay (Pierce, ThermoScientific, Rockford, IL). Following quantification, 40 µg of total protein was mixed with loading dye and sample reducing agent (NuPAGE, Invitrogen, Carlsbad, CA), boiled for 5 minutes, and separated by gel electrophoresis at 150 V on a NuPAGE 4-12% Bis-Tris Gel (Invitrogen, Carlsbad, CA). Proteins were then transferred at 40 V to a polyvinylidene difluoride (PVDF) membrane from Millipore (Billerica, MA). Membranes were blocked in 5% milk in tris buffered saline TWEEN20 (TBST) for 1 hour at room temperature followed by incubation with primary antibody overnight at 4 °C. Membranes were washed 3 times in TBST for 5 minutes and then incubated in the appropriate HRP conjugated antibody (1:3000) for 3

hours at room temperature. Detection was performed using supersignal chemiluminescence system from Pierce (Rockford, IL). The SERCA2 IID8 (1:200), SERCA3 XL-6 (1:300), Mcl-1 S-19 (1:400), Bcl-X<sub>s/L</sub> S-18 (1:750), antibodies were from Santa Cruz Biotechnology, Inc. (Santa Cruz, CA) and used at the specified dilution. The anti-Bcl-2 B3170 antibody (1:10,000), the anti-β-actin (1:40,000) antibody, and secondary antibodies were from Sigma–Aldrich (St. Louis, MO).

#### **5.4.5 RNA isolation and qRT-PCR**

Total RNA was isolated from cells using TRIzol Reagent from Invitrogen (Grand Island, NY) followed by PureLink RNA Mini kit from Life Technologies (Grand Island, NY) following manufactures protocols. Briefly,  $1 \times 10^7$  cells were collected by centrifugation and homogenized in 1 mL TRIzol Reagent. After incubating for 5 minutes at room temperature, 0.2 mL chloroform was added. Samples were shaken for 15 seconds, incubated for 3 minutes, and centrifuged at  $12,000 \times g$  at  $4^\circ\text{C}$ . The colorless aqueous phase was collected and RNA was purified using the PureLink kit. An equal volume of 70% ethanol was added to the aqueous phase, vortexed, and transferred to a spin column. Samples were centrifuged and the flow-through was discarded. After washing the RNA several times, it was eluted from the column using RNase-free water. The RNA was quantified by measuring absorbance at 260 nm and an extinction coefficient of 40. Purity was assessed using A260/A280 nm. Samples were then submitted to the BioMedical Genomics Center at the University of Minnesota (Minneapolis, MN) for qRT-PCR analysis. Data was then compared using the  $2^{-\Delta\Delta C_T}$  method as described.<sup>131</sup>

#### **5.4.6 RNA sequencing**

Total RNA was isolated as described in **5.4.5** and submitted to the BioMedical Genomics Center at the University of Minnesota (Minneapolis, MN) for Next Generation Sequencing, generating ~10 million 50 base pair paired end reads. Data was processed in Galaxy/UMN. Initially FASTQ Groomer was run on the data,<sup>132</sup> followed by Tophat, assigning reads to the hg-19 human reference genome with a mean inner distance between mate pairs of 80 base pairs.<sup>133</sup> Transcripts were then assembled and their abundance determined using Cufflinks<sup>128</sup> with data generated from Tophat. Cuffcompare and Cuffdiff are part of Cufflinks and were used to determine differential gene expression.

#### **5.4.7 Knockdown of topoisomerase II $\beta$**

$1 \times 10^5$  cells in 1 mL of complete media containing 5  $\mu\text{g}/\text{mL}$  polybrene (Santa Cruz Biotechnology, Santa Cruz, CA) were plated in a 12-well tissue culture plate. Cells were transduced with lentivirus containing either scrambled shRNA or shRNA targeting the gene of interest from Santa Cruz Biotechnology, Inc (Santa Cruz, CA) at a multiplicity of infection (MOI) of 3. After 8 hours, the cells were centrifuged and re-suspended in 1 mL of fresh media. 48 hours after transduction, cells were selected with 3  $\mu\text{g}/\text{mL}$  puromycin for a period of 72 hours. Cells were analyzed via Western blot 1-2 weeks after transduction to evaluate protein knockdown.

#### **5.4.8 Transient transfection of HL60 and HL60/MX2 cells**

Cells were transfected using the Neon electroporation system from Life Technologies (Grand Island, NY). Briefly,  $1 \times 10^6$  cells were re-suspended in 100  $\mu$ L phosphate buffered saline (PBS) from Life Technologies. Cells were electroporated using the 100  $\mu$ L tip and pulse voltage of 1350 V, pulse width of 35 ms, and 1 pulse, and re-suspended in 2.5 mL media in a 6-well plate. Cells were either transfected with 12.5 nM siRNA (based on 2.5 mL re-suspension volume) from Life Technologies or 5  $\mu$ g of plasmid containing the Mcl-1 open reading frame (SC315538) from OriGene (Rockville, MD). Successful knockdown was assessed after 6 hours and Mcl-1 expression was assessed after 48 hours via Western blotting.

## 6. References

1. Hanahan, D.; Weinberg, R. A. Hallmarks of cancer: the next generation. *Cell* **2011**, 144, 646-74.
2. Kumar, C. C. Genetic abnormalities and challenges in the treatment of acute myeloid leukemia. *Genes Cancer* **2011**, 2, 95-107.
3. Tallman, M. S.; Gilliland, D. G.; Rowe, J. M. Drug therapy for acute myeloid leukemia. *Blood* **2005**, 106, 1154-63.
4. Shipley, J. L.; Butera, J. N. Acute myelogenous leukemia. *Exp Hematol* **2009**, 37, 649-58.
5. Reed, J. C. Bcl-2 family proteins. *Oncogene* **1998**, 17, 3225-36.
6. Tsujimoto, Y.; Gorham, J.; Cossman, J.; Jaffe, E.; Croce, C. M. The t(14;18) chromosome translocations involved in B-cell neoplasms result from mistakes in VDJ joining. *Science* **1985**, 229, 1390-3.
7. Reed, J. C.; Pellecchia, M. Apoptosis-based therapies for hematologic malignancies. *Blood* **2005**, 106, 408-18.
8. Youle, R. J.; Strasser, A. The BCL-2 protein family: opposing activities that mediate cell death. *Nat Rev Mol Cell Biol* **2008**, 9, 47-59.
9. Krajewski, S.; Tanaka, S.; Takayama, S.; Schibler, M. J.; Fenton, W.; Reed, J. C. Investigation of the subcellular distribution of the bcl-2 oncoprotein: residence in the nuclear envelope, endoplasmic reticulum, and outer mitochondrial membranes. *Cancer Res* **1993**, 53, 4701-14.

10. Lithgow, T.; van Driel, R.; Bertram, J. F.; Strasser, A. The protein product of the oncogene bcl-2 is a component of the nuclear envelope, the endoplasmic reticulum, and the outer mitochondrial membrane. *Cell Growth Differ* **1994**, *5*, 411-7.
11. Yang, T.; Kozopas, K. M.; Craig, R. W. The intracellular distribution and pattern of expression of Mcl-1 overlap with, but are not identical to, those of Bcl-2. *J Cell Biol* **1995**, *128*, 1173-84.
12. Zha, H.; Fisk, H. A.; Yaffe, M. P.; Mahajan, N.; Herman, B.; Reed, J. C. Structure-function comparisons of the proapoptotic protein Bax in yeast and mammalian cells. *Mol Cell Biol* **1996**, *16*, 6494-508.
13. Kelekar, A.; Thompson, C. B. Bcl-2-family proteins: the role of the BH3 domain in apoptosis. *Trends Cell Biol* **1998**, *8*, 324-30.
14. Cheng, E. H.; Kirsch, D. G.; Clem, R. J.; Ravi, R.; Kastan, M. B.; Bedi, A.; Ueno, K.; Hardwick, J. M. Conversion of Bcl-2 to a Bax-like death effector by caspases. *Science* **1997**, *278*, 1966-8.
15. Hunter, J. J.; Bond, B. L.; Parslow, T. G. Functional dissection of the human Bcl-2 protein: sequence requirements for inhibition of apoptosis. *Mol Cell Biol* **1996**, *16*, 877-83.
16. Leber, B.; Lin, J.; Andrews, D. W. Embedded together: the life and death consequences of interaction of the Bcl-2 family with membranes. *Apoptosis* **2007**, *12*, 897-911.

17. Goldstein, J. C.; Munoz-Pinedo, C.; Ricci, J. E.; Adams, S. R.; Kelekar, A.; Schuler, M.; Tsien, R. Y.; Green, D. R. Cytochrome c is released in a single step during apoptosis. *Cell Death Differ* **2005**, 12, 453-62.
18. Rong, Y.; Distelhorst, C. W. Bcl-2 protein family members: versatile regulators of calcium signaling in cell survival and apoptosis. *Annu Rev Physiol* **2008**, 70, 73-91.
19. Scorrano, L.; Oakes, S. A.; Opferman, J. T.; Cheng, E. H.; Sorcinelli, M. D.; Pozzan, T.; Korsmeyer, S. J. BAX and BAK regulation of endoplasmic reticulum Ca<sup>2+</sup>: a control point for apoptosis. *Science* **2003**, 300, 135-9.
20. Pinton, P.; Rizzuto, R. Bcl-2 and Ca<sup>2+</sup> homeostasis in the endoplasmic reticulum. *Cell Death Differ* **2006**, 13, 1409-18.
21. Chen, R.; Valencia, I.; Zhong, F.; McColl, K. S.; Roderick, H. L.; Bootman, M. D.; Berridge, M. J.; Conway, S. J.; Holmes, A. B.; Mignery, G. A.; Velez, P.; Distelhorst, C. W. Bcl-2 functionally interacts with inositol 1,4,5-trisphosphate receptors to regulate calcium release from the ER in response to inositol 1,4,5-trisphosphate. *J Cell Biol* **2004**, 166, 193-203.
22. Hanson, C. J.; Bootman, M. D.; Distelhorst, C. W.; Wojcikiewicz, R. J.; Roderick, H. L. Bcl-2 suppresses Ca<sup>2+</sup> release through inositol 1,4,5-trisphosphate receptors and inhibits Ca<sup>2+</sup> uptake by mitochondria without affecting ER calcium store content. *Cell Calcium* **2008**, 44, 324-38.
23. Dremina, E. S.; Sharov, V. S.; Kumar, K.; Zaidi, A.; Michaelis, E. K.; Schoneich, C. Anti-apoptotic protein Bcl-2 interacts with and destabilizes the

- sarcoplasmic/endoplasmic reticulum Ca<sup>2+</sup>-ATPase (SERCA). *Biochem J* **2004**, 383, 361-70.
24. Kuo, T. H.; Kim, H. R.; Zhu, L.; Yu, Y.; Lin, H. M.; Tsang, W. Modulation of endoplasmic reticulum calcium pump by Bcl-2. *Oncogene* **1998**, 17, 1903-10.
25. Berridge, M. J.; Lipp, P.; Bootman, M. D. The versatility and universality of calcium signalling. *Nat Rev Mol Cell Biol* **2000**, 1, 11-21.
26. Orrenius, S.; Zhivotovsky, B.; Nicotera, P. Regulation of cell death: the calcium-apoptosis link. *Nat Rev Mol Cell Biol* **2003**, 4, 552-65.
27. Pinton, P.; Giorgi, C.; Siviero, R.; Zecchini, E.; Rizzuto, R. Calcium and apoptosis: ER-mitochondria Ca<sup>2+</sup> transfer in the control of apoptosis. *Oncogene* **2008**, 27, 6407-6418.
28. Periasamy, M.; Kalyanasundaram, A. SERCA pump isoforms: Their role in calcium transport and disease. *Muscle & Nerve* **2007**, 35, 430-442.
29. Lytton, J.; Westlin, M.; Burk, S. E.; Shull, G. E.; MacLennan, D. H. Functional comparisons between isoforms of the sarcoplasmic or endoplasmic reticulum family of calcium pumps. *Journal of Biological Chemistry* **1992**, 267, 14483-14489.
30. Lytton, J.; Westlin, M.; Hanley, M. R. Thapsigargin inhibits the sarcoplasmic or endoplasmic reticulum Ca-ATPase family of calcium pumps. *Journal of Biological Chemistry* **1991**, 266, 17067-17071.
31. Treiman, M.; Caspersen, C.; Christensen, S. B. A tool coming of age: thapsigargin as an inhibitor of sarco-endoplasmic reticulum Ca<sup>2+</sup>-ATPases. *Trends in Pharmacological Sciences* **1998**, 19, 131-135.



32. Denmeade, S. R.; Jakobsen, C. M.; Janssen, S.; Khan, S. R.; Garrett, E. S.; Lilja, H.; Christensen, S. B.; Isaacs, J. T. Prostate-specific antigen-activated thapsigargin prodrug as targeted therapy for prostate cancer. *J Natl Cancer Inst* **2003**, *95*, 990-1000.
33. Jakobsen, C. M.; Denmeade, S. R.; Isaacs, J. T.; Gady, A.; Olsen, C. E.; Christensen, S. B. Design, synthesis, and pharmacological evaluation of thapsigargin analogues for targeting apoptosis to prostatic cancer cells. *J Med Chem* **2001**, *44*, 4696-703.
34. Vander Griend, D. J.; Antony, L.; Dalrymple, S. L.; Xu, Y.; Christensen, S. B.; Denmeade, S. R.; Isaacs, J. T. Amino acid containing thapsigargin analogues deplete androgen receptor protein via synthesis inhibition and induce the death of prostate cancer cells. *Mol Cancer Ther* **2009**, *8*, 1340-9.
35. Zhao, L.; Ackerman, S. L. Endoplasmic reticulum stress in health and disease. *Current Opinion in Cell Biology* **2006**, *18*, 444-452.
36. Shore, G. C.; Papa, F. R.; Oakes, S. A. Signaling cell death from the endoplasmic reticulum stress response. *Curr Opin Cell Biol* **2010**, *23*, 143-9.
37. McCullough, K. D.; Martindale, J. L.; Klotz, L. O.; Aw, T. Y.; Holbrook, N. J. Gadd153 sensitizes cells to endoplasmic reticulum stress by down-regulating Bcl2 and perturbing the cellular redox state. *Mol Cell Biol* **2001**, *21*, 1249-59.
38. Yan, W.; Frank, C. L.; Korth, M. J.; Sopher, B. L.; Novoa, I.; Ron, D.; Katze, M. G. Control of PERK eIF2alpha kinase activity by the endoplasmic reticulum stress-induced molecular chaperone P58IPK. *Proc Natl Acad Sci U S A* **2002**, *99*, 15920-5.

39. Reed, J. C. Bcl-2: prevention of apoptosis as a mechanism of drug resistance. *Hematol Oncol Clin North Am* **1995**, 9, 451-73.
40. Tzifi, F.; Economopoulou, C.; Gourgiotis, D.; Ardavanis, A.; Papageorgiou, S.; Scorilas, A. The Role of BCL2 Family of Apoptosis Regulator Proteins in Acute and Chronic Leukemias. *Adv Hematol* **2011**, 2012, 524308.
41. Campos, L.; Rouault, J. P.; Sabido, O.; Oriol, P.; Roubi, N.; Vasselon, C.; Archimbaud, E.; Magaud, J. P.; Guyotat, D. High expression of bcl-2 protein in acute myeloid leukemia cells is associated with poor response to chemotherapy. *Blood* **1993**, 81, 3091-6.
42. Lauria, F.; Raspadori, D.; Rondelli, D.; Ventura, M. A.; Fiacchini, M.; Visani, G.; Forconi, F.; Tura, S. High bcl-2 expression in acute myeloid leukemia cells correlates with CD34 positivity and complete remission rate. *Leukemia* **1997**, 11, 2075-8.
43. Ong, Y. L.; McMullin, M. F.; Bailie, K. E.; Lappin, T. R.; Jones, F. G.; Irvine, A. E. High bax expression is a good prognostic indicator in acute myeloid leukaemia. *Br J Haematol* **2000**, 111, 182-9.
44. Del Poeta, G.; Venditti, A.; Del Principe, M. I.; Maurillo, L.; Buccisano, F.; Tamburini, A.; Cox, M. C.; Franchi, A.; Bruno, A.; Mazzone, C.; Panetta, P.; Suppo, G.; Masi, M.; Amadori, S. Amount of spontaneous apoptosis detected by Bax/Bcl-2 ratio predicts outcome in acute myeloid leukemia (AML). *Blood* **2003**, 101, 2125-31.
45. Glaser, S. P.; Lee, E. F.; Trounson, E.; Bouillet, P.; Wei, A.; Fairlie, W. D.; Izon, D. J.; Zuber, J.; Rappaport, A. R.; Herold, M. J.; Alexander, W. S.; Lowe, S. W.; Robb,

- L.; Strasser, A. Anti-apoptotic Mcl-1 is essential for the development and sustained growth of acute myeloid leukemia. *Genes Dev* **2012**, 26, 120-5.
46. Gores, G. J.; Kaufmann, S. H. Selectively targeting Mcl-1 for the treatment of acute myelogenous leukemia and solid tumors. *Genes Dev* **2012**, 26, 305-11.
47. Opferman, J. T. Unraveling MCL-1 degradation. *Cell Death Differ* **2006**, 13, 1260-2.
48. Zhong, Q.; Gao, W.; Du, F.; Wang, X. Mule/ARF-BP1, a BH3-Only E3 Ubiquitin Ligase, Catalyzes the Polyubiquitination of Mcl-1 and Regulates Apoptosis. *Cell* **2005**, 121, 1085-1095.
49. Ding, Q.; He, X.; Hsu, J. M.; Xia, W.; Chen, C. T.; Li, L. Y.; Lee, D. F.; Liu, J. C.; Zhong, Q.; Wang, X.; Hung, M. C. Degradation of Mcl-1 by beta-TrCP mediates glycogen synthase kinase 3-induced tumor suppression and chemosensitization. *Mol Cell Biol* **2007**, 27, 4006-17.
50. Wertz, I. E.; Kusam, S.; Lam, C.; Okamoto, T.; Sandoval, W.; Anderson, D. J.; Helgason, E.; Ernst, J. A.; Eby, M.; Liu, J.; Belmont, L. D.; Kaminker, J. S.; O'Rourke, K. M.; Pujara, K.; Kohli, P. B.; Johnson, A. R.; Chiu, M. L.; Lill, J. R.; Jackson, P. K.; Fairbrother, W. J.; Seshagiri, S.; Ludlam, M. J.; Leong, K. G.; Dueber, E. C.; Maecker, H.; Huang, D. C.; Dixit, V. M. Sensitivity to antitubulin chemotherapeutics is regulated by MCL1 and FBW7. *Nature* **2011**, 471, 110-4.
51. Schwickart, M.; Huang, X.; Lill, J. R.; Liu, J.; Ferrando, R.; French, D. M.; Maecker, H.; O'Rourke, K.; Bazan, F.; Eastham-Anderson, J.; Yue, P.; Dornan, D.;

Huang, D. C.; Dixit, V. M. Deubiquitinase USP9X stabilizes MCL1 and promotes tumour cell survival. *Nature* **2009**, 463, 103-7.

52. Maurer, U.; Charvet, C.; Wagman, A. S.; Dejardin, E.; Green, D. R. Glycogen synthase kinase-3 regulates mitochondrial outer membrane permeabilization and apoptosis by destabilization of MCL-1. *Mol Cell* **2006**, 21, 749-60.

53. Kobayashi, S.; Lee, S. H.; Meng, X. W.; Mott, J. L.; Bronk, S. F.; Werneburg, N. W.; Craig, R. W.; Kaufmann, S. H.; Gores, G. J. Serine 64 phosphorylation enhances the antiapoptotic function of Mcl-1. *J Biol Chem* **2007**, 282, 18407-17.

54. Reed, J. C.; Stein, C.; Subasinghe, C.; Haldar, S.; Croce, C. M.; Yum, S.; Cohen, J. Antisense-mediated inhibition of BCL2 protooncogene expression and leukemic cell growth and survival: comparisons of phosphodiester and phosphorothioate oligodeoxynucleotides. *Cancer Res* **1990**, 50, 6565-70.

55. Campos, L.; Sabido, O.; Rouault, J. P.; Guyotat, D. Effects of BCL-2 antisense oligodeoxynucleotides on in vitro proliferation and survival of normal marrow progenitors and leukemic cells. *Blood* **1994**, 84, 595-600.

56. Tauchi, T.; Sumi, M.; Nakajima, A.; Sashida, G.; Shimamoto, T.; Ohyashiki, K. BCL-2 antisense oligonucleotide genasense is active against imatinib-resistant BCR-ABL-positive cells. *Clin Cancer Res* **2003**, 9, 4267-73.

57. Makin, G.; Dive, C.; Saha, V.; Kearns, P. Targeting Bcl-2 Family Proteins in Childhood Leukemia

New Agents for the Treatment of Acute Lymphoblastic Leukemia. In Springer New York: 2011; pp 117-141.

58. Piche, A.; Grim, J.; Rancourt, C.; Gomez-Navarro, J.; Reed, J. C.; Curiel, D. T. Modulation of Bcl-2 protein levels by an intracellular anti-Bcl-2 single-chain antibody increases drug-induced cytotoxicity in the breast cancer cell line MCF-7. *Cancer Res* **1998**, *58*, 2134-40.
59. Holinger, E. P.; Chittenden, T.; Lutz, R. J. Bak BH3 peptides antagonize Bcl-xL function and induce apoptosis through cytochrome c-independent activation of caspases. *J Biol Chem* **1999**, *274*, 13298-304.
60. Sattler, M.; Liang, H.; Nettlesheim, D.; Meadows, R. P.; Harlan, J. E.; Eberstadt, M.; Yoon, H. S.; Shuker, S. B.; Chang, B. S.; Minn, A. J.; Thompson, C. B.; Fesik, S. W. Structure of Bcl-xL-Bak peptide complex: recognition between regulators of apoptosis. *Science* **1997**, *275*, 983-6.
61. Stewart, M. L.; Fire, E.; Keating, A. E.; Walensky, L. D. The MCL-1 BH3 helix is an exclusive MCL-1 inhibitor and apoptosis sensitizer. *Nat Chem Biol* **2010**, *6*, 595-601.
62. Wang, J. L.; Zhang, Z. J.; Choksi, S.; Shan, S.; Lu, Z.; Croce, C. M.; Alnemri, E. S.; Korngold, R.; Huang, Z. Cell permeable Bcl-2 binding peptides: a chemical approach to apoptosis induction in tumor cells. *Cancer Res* **2000**, *60*, 1498-502.
63. Wang, J. L.; Liu, D.; Zhang, Z. J.; Shan, S.; Han, X.; Srinivasula, S. M.; Croce, C. M.; Alnemri, E. S.; Huang, Z. Structure-based discovery of an organic compound that binds Bcl-2 protein and induces apoptosis of tumor cells. *Proc Natl Acad Sci U S A* **2000**, *97*, 7124-9.

64. Lickliter, J. D.; Wood, N. J.; Johnson, L.; McHugh, G.; Tan, J.; Wood, F.; Cox, J.; Wickham, N. W. HA14-1 selectively induces apoptosis in Bcl-2-overexpressing leukemia/lymphoma cells, and enhances cytarabine-induced cell death. *Leukemia* **2003**, *17*, 2074-80.
65. Manero, F.; Gautier, F.; Gallenne, T.; Cauquil, N.; Gree, D.; Cartron, P. F.; Geneste, O.; Gree, R.; Vallette, F. M.; Juin, P. The small organic compound HA14-1 prevents Bcl-2 interaction with Bax to sensitize malignant glioma cells to induction of cell death. *Cancer Res* **2006**, *66*, 2757-64.
66. Oliver, L.; Mahe, B.; Gree, R.; Vallette, F. M.; Juin, P. HA14-1, a small molecule inhibitor of Bcl-2, bypasses chemoresistance in leukaemia cells. *Leuk Res* **2007**, *31*, 859-63.
67. Pei, X. Y.; Dai, Y.; Grant, S. The proteasome inhibitor bortezomib promotes mitochondrial injury and apoptosis induced by the small molecule Bcl-2 inhibitor HA14-1 in multiple myeloma cells. *Leukemia* **2003**, *17*, 2036-45.
68. Pei, X. Y.; Dai, Y.; Grant, S. The small-molecule Bcl-2 inhibitor HA14-1 interacts synergistically with flavopiridol to induce mitochondrial injury and apoptosis in human myeloma cells through a free radical-dependent and Jun NH2-terminal kinase-dependent mechanism. *Mol Cancer Ther* **2004**, *3*, 1513-24.
69. Wlodkowic, D.; Skommer, J.; Pelkonen, J. Brefeldin A triggers apoptosis associated with mitochondrial breach and enhances HA14-1- and anti-Fas-mediated cell killing in follicular lymphoma cells. *Leuk Res* **2007**, *31*, 1687-700.

70. Degtarev, A.; Lugovskoy, A.; Cardone, M.; Mulley, B.; Wagner, G.; Mitchison, T.; Yuan, J. Identification of small-molecule inhibitors of interaction between the BH3 domain and Bcl-xL. *Nat Cell Biol* **2001**, *3*, 173-82.
71. Wang, G.; Nikolovska-Coleska, Z.; Yang, C. Y.; Wang, R.; Tang, G.; Guo, J.; Shangary, S.; Qiu, S.; Gao, W.; Yang, D.; Meagher, J.; Stuckey, J.; Krajewski, K.; Jiang, S.; Roller, P. P.; Abaan, H. O.; Tomita, Y.; Wang, S. Structure-based design of potent small-molecule inhibitors of anti-apoptotic Bcl-2 proteins. *J Med Chem* **2006**, *49*, 6139-42.
72. Sun, Y.; Wu, J.; Aboukameel, A.; Banerjee, S.; Arnold, A. A.; Chen, J.; Nikolovska-Coleska, Z.; Lin, Y.; Ling, X.; Yang, D.; Wang, S.; Al-Katib, A.; Mohammad, R. M. Apogossypolone, a nonpeptidic small molecule inhibitor targeting Bcl-2 family proteins, effectively inhibits growth of diffuse large cell lymphoma cells in vitro and in vivo. *Cancer Biol Ther* **2008**, *7*, 1418-26.
73. Wei, J.; Stebbins, J. L.; Kitada, S.; Dash, R.; Placzek, W.; Rega, M. F.; Wu, B.; Cellitti, J.; Zhai, D.; Yang, L.; Dahl, R.; Fisher, P. B.; Reed, J. C.; Pellecchia, M. BI-97C1, an optically pure Apogossypol derivative as pan-active inhibitor of antiapoptotic B-cell lymphoma/leukemia-2 (Bcl-2) family proteins. *J Med Chem* **2010**, *53*, 4166-76.
74. Al-Katib, A. M.; Sun, Y.; Goustin, A. S.; Azmi, A. S.; Chen, B.; Aboukameel, A.; Mohammad, R. M. SMI of Bcl-2 TW-37 is active across a spectrum of B-cell tumors irrespective of their proliferative and differentiation status. *J Hematol Oncol* **2009**, *2*, 8.
75. Arnold, A. A.; Aboukameel, A.; Chen, J.; Yang, D.; Wang, S.; Al-Katib, A.; Mohammad, R. M. Preclinical studies of Apogossypolone: a new nonpeptidic pan small-

molecule inhibitor of Bcl-2, Bcl-XL and Mcl-1 proteins in Follicular Small Cleaved Cell Lymphoma model. *Mol Cancer* **2008**, 7, 20.

76. Dash, R.; Azab, B.; Quinn, B. A.; Shen, X.; Wang, X. Y.; Das, S. K.; Rahmani, M.; Wei, J.; Hedvat, M.; Dent, P.; Dmitriev, I. P.; Curiel, D. T.; Grant, S.; Wu, B.; Stebbins, J. L.; Pellecchia, M.; Reed, J. C.; Sarkar, D.; Fisher, P. B. Apogossypol derivative BI-97C1 (Sabutoclax) targeting Mcl-1 sensitizes prostate cancer cells to mda-7/IL-24-mediated toxicity. *Proc Natl Acad Sci U S A* **2011**, 108, 8785-90.

77. Konopleva, M.; Watt, J.; Contractor, R.; Tsao, T.; Harris, D.; Estrov, Z.; Bornmann, W.; Kantarjian, H.; Viallet, J.; Samudio, I.; Andreeff, M. Mechanisms of antileukemic activity of the novel Bcl-2 homology domain-3 mimetic GX15-070 (obatoclax). *Cancer Res* **2008**, 68, 3413-20.

78. O'Brien, S. M.; Claxton, D. F.; Crump, M.; Faderl, S.; Kipps, T.; Keating, M. J.; Viallet, J.; Cheson, B. D. Phase I study of obatoclax mesylate (GX15-070), a small molecule pan-Bcl-2 family antagonist, in patients with advanced chronic lymphocytic leukemia. *Blood* **2009**, 113, 299-305.

79. Oltersdorf, T.; Elmore, S. W.; Shoemaker, A. R.; Armstrong, R. C.; Augeri, D. J.; Belli, B. A.; Bruncko, M.; Deckwerth, T. L.; Dinges, J.; Hajduk, P. J.; Joseph, M. K.; Kitada, S.; Korsmeyer, S. J.; Kunzer, A. R.; Letai, A.; Li, C.; Mitten, M. J.; Nettlesheim, D. G.; Ng, S.; Nimmer, P. M.; O'Connor, J. M.; Oleksijew, A.; Petros, A. M.; Reed, J. C.; Shen, W.; Tahir, S. K.; Thompson, C. B.; Tomaselli, K. J.; Wang, B.; Wendt, M. D.; Zhang, H.; Fesik, S. W.; Rosenberg, S. H. An inhibitor of Bcl-2 family proteins induces regression of solid tumours. *Nature* **2005**, 435, 677-681.



80. van Delft, M. F.; Huang, D. C. How the Bcl-2 family of proteins interact to regulate apoptosis. *Cell Res* **2006**, 16, 203-13.
81. Doshi, J. M.; Tian, D.; Xing, C. Structure-activity relationship studies of ethyl 2-amino-6-bromo-4-(1-cyano-2-ethoxy-2-oxoethyl)-4H-chromene-3-carboxylate (HA 14-1), an antagonist for antiapoptotic Bcl-2 proteins to overcome drug resistance in cancer. *J Med Chem* **2006**, 49, 7731-9.
82. Doshi, J. M.; Tian, D.; Xing, C. Ethyl-2-amino-6-bromo-4-(1-cyano-2-ethoxy-2-oxoethyl)-4H-chromene-3-carboxylate (HA 14-1), a prototype small-molecule antagonist against antiapoptotic Bcl-2 proteins, decomposes to generate reactive oxygen species that induce apoptosis. *Mol Pharm* **2007**, 4, 919-28.
83. Tian, D.; Das, S. G.; Doshi, J. M.; Peng, J.; Lin, J.; Xing, C. sHA 14-1, a stable and ROS-free antagonist against anti-apoptotic Bcl-2 proteins, bypasses drug resistances and synergizes cancer therapies in human leukemia cell. *Cancer Lett* **2008**, 259, 198-208.
84. Grynkiewicz, G.; Poenie, M.; Tsien, R. Y. A new generation of Ca<sup>2+</sup> indicators with greatly improved fluorescence properties. *J Biol Chem* **1985**, 260, 3440-50.
85. Monteith, G. R.; McAndrew, D.; Faddy, H. M.; Roberts-Thomson, S. J. Calcium and cancer: targeting Ca<sup>2+</sup> transport. *Nat Rev Cancer* **2007**, 7, 519-530.
86. Yoshida, I.; Monji, A.; Tashiro, K.-i.; Nakamura, K.-i.; Inoue, R.; Kanba, S. Depletion of intracellular Ca<sup>2+</sup> store itself may be a major factor in thapsigargin-induced ER stress and apoptosis in PC12 cells. *Neurochemistry International* **2006**, 48, 696-702.

87. Harding, H. P.; Novoa, I.; Zhang, Y.; Zeng, H.; Wek, R.; Schapira, M.; Ron, D. Regulated Translation Initiation Controls Stress-Induced Gene Expression in Mammalian Cells. *Molecular Cell* **2000**, *6*, 1099-1108.
88. Bilmen, J. G.; Michelangeli, F. Inhibition of the type 1 inositol 1,4,5-trisphosphate receptor by 2-aminoethoxydiphenylborate. *Cellular Signalling* **2002**, *14*, 955-960.
89. Wootton, L. L.; Michelangeli, F. The Effects of the Phenylalanine 256 to Valine Mutation on the Sensitivity of Sarcoplasmic/Endoplasmic Reticulum Ca<sup>2+</sup> ATPase (SERCA) Ca<sup>2+</sup> Pump Isoforms 1, 2, and 3 to Thapsigargin and Other Inhibitors. *Journal of Biological Chemistry* **2006**, *281*, 6970-6976.
90. Shah, N.; Asch, R. J.; Lysholm, A. S.; LeBien, T. W. Enhancement of stress-induced apoptosis in B-lineage cells by caspase-9 inhibitor. *Blood* **2004**, *104*, 2873-2878.
91. Tian, D.; Das, S. G.; Doshi, J. M.; Peng, J.; Lin, J.; Xing, C. sHA 14-1, a stable and ROS-free antagonist against anti-apoptotic Bcl-2 proteins, bypasses drug resistances and synergizes cancer therapies in human leukemia cell. *Cancer Letters* **2008**, *259*, 198-208.
92. Harker, W. G.; Slade, D. L.; Dalton, W. S.; Meltzer, P. S.; Trent, J. M. Multidrug resistance in mitoxantrone-selected HL-60 leukemia cells in the absence of P-glycoprotein overexpression. *Cancer Res* **1989**, *49*, 4542-9.
93. Harker, W. G.; Slade, D. L.; Drake, F. H.; Parr, R. L. Mitoxantrone resistance in HL-60 leukemia cells: reduced nuclear topoisomerase II catalytic activity and drug-

induced DNA cleavage in association with reduced expression of the topoisomerase II beta isoform. *Biochemistry* **1991**, 30, 9953-61.

94. Fujimori, A.; Harker, W. G.; Kohlhagen, G.; Hoki, Y.; Pommier, Y. Mutation at the catalytic site of topoisomerase I in CEM/C2, a human leukemia cell line resistant to camptothecin. *Cancer Res* **1995**, 55, 1339-46.

95. Fujimori, A.; Hoki, Y.; Popescu, N. C.; Pommier, Y. Silencing and selective methylation of the normal topoisomerase I gene in camptothecin-resistant CEM/C2 human leukemia cells. *Oncol Res* **1996**, 8, 295-301.

96. Kaufmann, S. H.; Karp, J. E.; Svingen, P. A.; Krajewski, S.; Burke, P. J.; Gore, S. D.; Reed, J. C. Elevated Expression of the Apoptotic Regulator Mcl-1 at the Time of Leukemic Relapse. *Blood* **1998**, 91, 991-1000.

97. Holleman, A.; Cheok, M. H.; den Boer, M. L.; Yang, W.; Veerman, A. J. P.; Kazemier, K. M.; Pei, D.; Cheng, C.; Pui, C.-H.; Relling, M. V.; Janka-Schaub, G. E.; Pieters, R.; Evans, W. E. Gene-Expression Patterns in Drug-Resistant Acute Lymphoblastic Leukemia Cells and Response to Treatment. *New England Journal of Medicine* **2004**, 351, 533-542.

98. Garrido, C.; Galluzzi, L.; Brunet, M.; Puig, P. E.; Didelot, C.; Kroemer, G. Mechanisms of cytochrome c release from mitochondria. *Cell Death Differ* **2006**, 13, 1423-1433.

99. Wuytack, F.; Dode, L.; Baba-Aissa, F.; Raeymaekers, L. The SERCA3-type of organellar Ca<sup>2+</sup> pumps. *Bioscience Reports* **1995**, 15, 299-306.

100. Tang, R.; Cohen, S.; Perrot, J. Y.; Faussat, A. M.; Zuany-Amorim, C.; Marjanovic, Z.; Morjani, H.; Fava, F.; Corre, E.; Legrand, O.; Marie, J. P. P-gp activity is a critical resistance factor against AVE9633 and DM4 cytotoxicity in leukaemia cell lines, but not a major mechanism of chemoresistance in cells from acute myeloid leukaemia patients. *BMC Cancer* **2009**, *9*, 199.
101. Vaziri, S. A.; Grabowski, D. R.; Tabata, M.; Holmes, K. A.; Sterk, J.; Takigawa, N.; Bukowski, R. M.; Ganapathi, M. K.; Ganapathi, R. c-IAP1 is overexpressed in HL-60 cells selected for doxorubicin resistance: effects on etoposide-induced apoptosis. *Anticancer Res* **2003**, *23*, 3657-61.
102. Plasschaert, S. L. A.; Groninger, E.; Boezen, M.; Kema, I.; de Vries, E. G. E.; Uges, D.; Veerman, A. J. P.; Kamps, W. A.; Vellenga, E.; de Graaf, S. S.; de Bont, E. S. J. M. Influence of functional polymorphisms of the MDR1 gene on vincristine pharmacokinetics in childhood acute lymphoblastic Leukemia[ast]. *Clin Pharmacol Ther* **2004**, *76*, 220-229.
103. Chen, M.; Beck, W. T. DNA topoisomerase II expression, stability, and phosphorylation in two VM-26-resistant human leukemic CEM sublines. *Oncol Res* **1995**, *7*, 103-11.
104. Zhou, D.-C.; Ramond, S.; Viguie, F.; Faussat, A.-M.; Zittoun, R.; Marie, J.-P. Sequential emergence of MRP- and MDR1-gene over-expression as well as MDR1-gene translocation in homoharringtonine-selected K562 human leukemia cell lines. *International Journal of Cancer* **1996**, *65*, 365-371.

105. Hall, M. D.; Salam, N. K.; Hellawell, J. L.; Fales, H. M.; Kensler, C. B.; Ludwig, J. A.; Szakacs, G.; Hibbs, D. E.; Gottesman, M. M. Synthesis, activity, and pharmacophore development for isatin-beta-thiosemicarbazones with selective activity toward multidrug-resistant cells. *J Med Chem* **2009**, 52, 3191-204.
106. Shoemaker, R. H. The NCI60 human tumour cell line anticancer drug screen. *Nat Rev Cancer* **2006**, 6, 813-823.
107. Hermanson, D.; Addo, S. N.; Bajer, A. A.; Marchant, J. S.; Das, S. G.; Srinivasan, B.; Al-Mousa, F.; Michelangeli, F.; Thomas, D. D.; Lebien, T. W.; Xing, C. Dual mechanisms of sHA 14-1 in inducing cell death through endoplasmic reticulum and mitochondria. *Mol Pharmacol* **2009**, 76, 667-78.
108. Oliver, C. L.; Miranda, M. B.; Shangary, S.; Land, S.; Wang, S.; Johnson, D. E. (âˆ’)-Gossypol acts directly on the mitochondria to overcome Bcl-2- and Bcl-XL-mediated apoptosis resistance. *Molecular Cancer Therapeutics* **2005**, 4, 23-31.
109. Janssen, K.; Horn, S.; Niemann, M. T.; Daniel, P. T.; Schulze-Osthoff, K.; Fischer, U. Inhibition of the ER Ca<sup>2+</sup> pump forces multidrug-resistant cells deficient in Bak and Bax into necrosis. *J Cell Sci* **2009**, 122, 4481-4491.
110. Vandecaetsbeek, I.; Trekels, M.; De Maeyer, M.; Ceulemans, H.; Lescrinier, E.; Raeymaekers, L.; Wuytack, F.; Vangheluwe, P. Structural basis for the high Ca<sup>2+</sup> affinity of the ubiquitous SERCA2b Ca<sup>2+</sup> pump. *Proceedings of the National Academy of Sciences* **2009**, 106, 18533-18538.
111. Wang, J.-L.; Liu, D.; Zhang, Z.-J.; Shan, S.; Han, X.; Srinivasula, S. M.; Croce, C. M.; Alnemri, E. S.; Huang, Z. Structure-based discovery of an organic compound that

binds Bcl-2 protein and induces apoptosis of tumor cells. *Proceedings of the National Academy of Sciences* **2000**, 97, 7124-7129.

112. Kotzyba-Hibert, F.; Kapfer, I.; Goeldner, M. Recent Trends in Photoaffinity Labeling. *Angewandte Chemie International Edition in English* **1995**, 34, 1296-1312.

113. Kolb, H. C.; Finn, M. G.; Sharpless, K. B. Click Chemistry: Diverse Chemical Function from a Few Good Reactions. *Angewandte Chemie International Edition* **2001**, 40, 2004-2021.

114. Fabiato, A.; Fabiato, F. Calculator programs for computing the composition of the solutions containing multiple metals and ligands used for experiments in skinned muscle cells. *J Physiol (Paris)* **1979**, 75, 463-505.

115. Winters, D. L.; Autry, J. M.; Svensson, B.; Thomas, D. D. Interdomain fluorescence resonance energy transfer in SERCA probed by cyan-fluorescent protein fused to the actuator domain. *Biochemistry* **2008**, 47, 4246-56.

116. Das, S. G.; Srinivasan, B.; Hermanson, D. L.; Bleeker, N.; Doshi, J. M.; Tang, R.; Beck, W. T.; Xing, C. Structure Activity Relationship and Molecular Mechanisms of Ethyl 2-Amino-6-(3,5-Dimethoxyphenyl)-4-(2-Ethoxy-2-Oxoethyl)-4H-Chromene-3-Carboxylate (CXL017) and Its Analogs. *J Med Chem* **2011**.

117. McCurrach, M. E.; Connor, T. M.; Knudson, C. M.; Korsmeyer, S. J.; Lowe, S. W. bax-deficiency promotes drug resistance and oncogenic transformation by attenuating p53-dependent apoptosis. *Proc Natl Acad Sci U S A* **1997**, 94, 2345-9.

118. Erler, J. T.; Cawthorne, C. J.; Williams, K. J.; Koritzinsky, M.; Wouters, B. G.; Wilson, C.; Miller, C.; Demonacos, C.; Stratford, I. J.; Dive, C. Hypoxia-mediated down-

regulation of Bid and Bax in tumors occurs via hypoxia-inducible factor 1-dependent and -independent mechanisms and contributes to drug resistance. *Mol Cell Biol* **2004**, 24, 2875-89.

119. Day, C. L.; Chen, L.; Richardson, S. J.; Harrison, P. J.; Huang, D. C. S.; Hinds, M. G. Solution Structure of Prosurvival Mcl-1 and Characterization of Its Binding by Proapoptotic BH3-only Ligands. *Journal of Biological Chemistry* **2005**, 280, 4738-4744.

120. Ewings, K. E.; Hadfield-Moorhouse, K.; Wiggins, C. M.; Wickenden, J. A.; Balmanno, K.; Gilley, R.; Degenhardt, K.; White, E.; Cook, S. J. ERK1/2-dependent phosphorylation of BimEL promotes its rapid dissociation from Mcl-1 and Bcl-xL. *EMBO J* **2007**, 26, 2856-67.

121. Inoshita, S.; Takeda, K.; Hatai, T.; Terada, Y.; Sano, M.; Hata, J.; Umezawa, A.; Ichijo, H. Phosphorylation and inactivation of myeloid cell leukemia 1 by JNK in response to oxidative stress. *J Biol Chem* **2002**, 277, 43730-4.

122. Mills, J. R.; Hippo, Y.; Robert, F.; Chen, S. M. H.; Malina, A.; Lin, C.-J.; Trojahn, U.; Wendel, H.-G.; Charest, A.; Bronson, R. T.; Kogan, S. C.; Nadon, R.; Housman, D. E.; Lowe, S. W.; Pelletier, J. mTORC1 promotes survival through translational control of Mcl-1. *Proceedings of the National Academy of Sciences* **2008**, 105, 10853-10858.

123. Obrig, T. G.; Culp, W. J.; McKeehan, W. L.; Hardesty, B. The mechanism by which cycloheximide and related glutarimide antibiotics inhibit peptide synthesis on reticulocyte ribosomes. *J Biol Chem* **1971**, 246, 174-81.

124. Schneider-Poetsch, T.; Ju, J.; Eyler, D. E.; Dang, Y.; Bhat, S.; Merrick, W. C.; Green, R.; Shen, B.; Liu, J. O. Inhibition of eukaryotic translation elongation by cycloheximide and lactimidomycin. *Nat Chem Biol* **6**, 209-217.
125. Stewart, D. P.; Koss, B.; Bathina, M.; Perciavalle, R. M.; Bisanz, K.; Opferman, J. T. Ubiquitin-independent degradation of antiapoptotic MCL-1. *Mol Cell Biol* **2010**, *30*, 3099-110.
126. Crawford, L. J.; Walker, B.; Ovaa, H.; Chauhan, D.; Anderson, K. C.; Morris, T. C.; Irvine, A. E. Comparative selectivity and specificity of the proteasome inhibitors BzLLCOCOCHO, PS-341, and MG-132. *Cancer Res* **2006**, *66*, 6379-86.
127. Wang, Z.; Gerstein, M.; Snyder, M. RNA-Seq: a revolutionary tool for transcriptomics. *Nat Rev Genet* **2009**, *10*, 57-63.
128. Trapnell, C.; Williams, B. A.; Pertea, G.; Mortazavi, A.; Kwan, G.; van Baren, M. J.; Salzberg, S. L.; Wold, B. J.; Pachter, L. Transcript assembly and quantification by RNA-Seq reveals unannotated transcripts and isoform switching during cell differentiation. *Nat Biotechnol* **28**, 511-5.
129. Wulleme-Toumi, S.; Robillard, N.; Gomez, P.; Moreau, P.; Le Gouill, S.; Avet-Loiseau, H.; Harousseau, J. L.; Amiot, M.; Bataille, R. Mcl-1 is overexpressed in multiple myeloma and associated with relapse and shorter survival. *Leukemia* **2005**, *19*, 1248-1252.
130. Konopleva, M.; Contractor, R.; Tsao, T.; Samudio, I.; Ruvolo, P. P.; Kitada, S.; Deng, X.; Zhai, D.; Shi, Y. X.; Sneed, T.; Verhaegen, M.; Soengas, M.; Ruvolo, V. R.; McQueen, T.; Schober, W. D.; Watt, J. C.; Jiffar, T.; Ling, X.; Marini, F. C.; Harris, D.;



Dietrich, M.; Estrov, Z.; McCubrey, J.; May, W. S.; Reed, J. C.; Andreeff, M. Mechanisms of apoptosis sensitivity and resistance to the BH3 mimetic ABT-737 in acute myeloid leukemia. *Cancer Cell* **2006**, *10*, 375-88.

131. Livak, K. J.; Schmittgen, T. D. Analysis of relative gene expression data using real-time quantitative PCR and the  $2^{-\Delta\Delta C(T)}$  Method. *Methods* **2001**, *25*, 402-8.

132. Blankenberg, D.; Gordon, A.; Von Kuster, G.; Coraor, N.; Taylor, J.; Nekrutenko, A. Manipulation of FASTQ data with Galaxy. *Bioinformatics* **2010**, *26*, 1783-5.

133. Trapnell, C.; Pachter, L.; Salzberg, S. L. TopHat: discovering splice junctions with RNA-Seq. *Bioinformatics* **2009**, *25*, 1105-11.